NOTICE

The quality of this microform is heavily dependent upon the quality of the original thesis submitted for microfilming. Every effort has been made to ensure the highest quality of reproduction possible.

If pages are missing, contact the university which granted the degree.

Some pages may have indistinct print especially if the original pages were typed with a poor typewriter ribbon or if the university sent us an inferior photocopy.

Reproduction in full or in part of this microform is governed by the Canadian Copyright Act, R.S.C. 1970, c. C-30, and subsequent amendments.

AVIS

La qualité de cette microforme dépend grandement de la qualité de la thèse soumise au microfilmage. Nous avons tout fait pour assurer une qualité supérieure de reproduction.

S'il manque des pages, veuillez communiquer avec l'université qui a conféré le grade.

La qualité d'impression de certaines pages peut laisser à désirer, surtout si les pages originales ont été dactylographiées à l'aide d'un ruban usé ou si l'université nous a fait parvenir une photocopie de qualité inférieure.

La reproduction, même partielle, de cette microforme est soumise à la Loi canadienne sur le droit d'auteur, SRC 1970, c. C-30, et ses amendements subséquents.

OPTIMAL DESIGN OF FIBRE COMPOSITE PRESSURE VESSELS

by

M.A. TENACE

Thesis presented

to the University of Ottawa

December, 1990

in partial fulfillment of the

requirements for the degree of

MASTER of APPLIED SCIENCE

in

MECHANICAL ENGINEERING

Ottawa-Carleton Institute for

Mechanical and Aeronautical Engineering

ISBN 0-315-67992-1

UNIVERSITÉ D'OTTAWA
UNIVERSITY OF OTTAWA

ABSTRACT

Fibre composite pressure vessels are replacing conventional metallic vessels because of their higher efficiencies (stored energy/unit weight). In this study, multi-layered fibre composite pressure vessels have been designed using a Direct Search method to simultaneously determine the optimal design parameters of layer thickness and wind angle (based upon maximum vessel efficiency according to an interactive failure theory). It was shown that the ability of the fibre composite pressure vessel to resist the internal pressure without failure increased with increasing total wall thickness, up to a certain limit, after which little or no increase in failure pressure was possible. It was also shown that an improved design of a fibre composite pressure vessel can be accomplished by increasing the number of individual equal thickness layers in the vessel wall. Additional improvement in the design can be obtained by allowing the thickness of each individual layer to vary, especially for thicker vessels.

Peak vessel efficiency generally occured at the same wall thickness, implying that efficiency is mostly affected by the type of fibre/matrix combination selected. A slight improvement in efficiency was noticed by increasing the number of individual layers and aalowing their thicknesses to vary. Finally, the manufacturing and testing aspects are described.

ACKNOWLEDGEMENTS

The author would like to express thanks to Professor Munro, for his innumerable suggestions, time and patience and without whom, this study would not have been possible.

It is also wished to express particular thanks to my colleagues, Etienne Bernard, Hans Öhman and Martin Guay who all provided valuable help and suggestions, which were greatly appreciated.

The author would like to thank the National Research Council for providing funding of this study in the form of a Research Assistanceship grant.

Finally, special thanks are given to Lynne Lapensée, for providing much help and encouragement throughout this study.

LIST OF SYMBOLS

ε_{ij}	normal strains
γ_{ij}	shearing strains
σ_{ij}	normal stress
τ_{ij}	shearing stress
ν_{ij}	Poisson's ratio
α	helix angle
θ	angular position, in cylindrical coordinates
r	radial position
b	outside radius of vessel
a	inside radius of vessel
z	axial position
E_{ij}	elastic moduli
G_{ij}	shear moduli
X_T	longitudinal ultimate tensile strength
X_C	longitudinal ultimate compressive strength
Y_T	transverse ultimate tensile strength
Y_C	transverse ultimate compressive strength
S	in-plane shear ultimate strength

$\varepsilon_{1T}(ult)$	longitudinal ultimate tensile strain
$\varepsilon_{1C}(ult)$	longitudinal ultimate compressive strain
$\varepsilon_{2T}(ult)$	transverse ultimate tensile strain
$\varepsilon_{2C}(ult)$	transverse ultimate compressive strain
$\gamma_{12}(ult)$	shear ultimate strain
X_f	volume fraction of fibre
P_b	burst pressure
V_{encl}	enclosed volume of vessel
W	vessel weight
u_r	radial displacement
β	eigenvalue for isotropic cylinder
$\beta^{(i)}$	displacement coefficients
ω	solution vector for displacement coefficients
ε	vessel efficiency
ρ	density of composite material
l	length of cylindrical section of vessel
$\Phi(X)$	maximum value of failure criteria
$\Omega_i(X)$	failure criteria value at each layer

TABLE OF CONTENTS

LIST OF FIGURES

LIST OF TABLES

Chapter 1

INTRODUCTION

1.1 Thesis Perspective

The combination of high-strength fibres with a polymeric resin matrix (Figure 1-1) in a composite results in structural elements and parts which have exceedingly high strength-to-weight and stiffness-to-weight ratios. The weight advantages of a composite are readily apparent in Figure 1-2, which shows the specific strength (tensile strength/density) versus specific modulus (tensile elastic modulus/density) for typical fibre composites and metallic materials. As the behaviour of composites is extremely sensitive to the orientation of the reinforcing fibres, there are two cases that are shown for each composite: unidirectional and biaxial fibre orientation. The unidirectional composite has, by far, the best mechanical properties. The biaxial properties are significantly lower, but are still better than even the strongest metals, on a weight basis. In addition to this, many fibre composites have advantages which depend upon the type of fibre, e.g. extremely low coefficients of thermal expansion

and high internal damping of carbon fibre composites.

Although man-made composites have existed for thousands of years (eg. straw in mud bricks), the technology of high-performance composites has evolved in industry only in the last twenty to thirty years. In the 1960's, pressure vessels and rocket motor casings using glass fibres were the first strength-critical applications for modern composites. Since that time, composites have been used extensively in the aerospace industry for military and commercial aircraft.

Pressure vessels made from fibre composite materials have had an enormous impact on engineering structures where weight savings is an important consideration. They have been used in applications as varied as in pressurized gas tanks used by fire fighters, mountain climbers and scuba divers, in deep submergence vehicles, fuel tanks for helicopters and tanker trucks for the transportation of chemicals, to name a few.

The development of lightweight fibre composite pressure vessels for energy storage has been investigated at the University of Ottawa since 1983 [1-5]. The areas of stress analysis, manufacturing and testing have been addressed. This thesis, which is a continuation of earlier work, is concerned with more advanced concepts for all three areas.

1.2 Fibre Composite Pressure Vessels

1.2.1 General Structure

Fibre composite pressure vessels consist of a liner, shell or bladder, over which high-strength and high-stiffness fibres, bound by a resinous matrix are wound. The liner acts to prevent leakage and is adhesively bonded to the composite material, transferring longitudinal, hoop and radial loads from the liner to the composite by means of shear and normal stresses. The liner is fitted with one or more fill tubes to introduce pressurized fluids.

The most common fibres used for the composite material are glass, aramid and carbon fibres, while the matrix is usually an epoxy, polyester or vinyl-ester resin. The most common liner materials are elastomeric or metallic.

A material with properties that do not vary with orientation are said to be isotropic, which is generally the case for the matrix material. If a single plane exists where properties are invariant to rotation in that plane, then the material is said to be transversely isotropic, as is the case for plane 2-3, shown in Figure 1-1.

The composite material is often layered; each individual layer is called a lamina and the set of laminae are called a laminate (Figure 1-3). The properties of the laminate are dependent on the stacking sequence, fibre orientation in the individual laminae and laminae material properties. The composite material is assumed to behave in a brittle manner (i.e., linear-elastic stress-strain behaviour until failure).

1.2.2 Manufacturing Process

Filament winding is used for the fabrication of fibre composite pressure vessels. The main process of filament winding of fibre-reinforced polymeric composites consists of placing resin-impregnated bands of fibres under controlled tension through a payout (or delivery) eye onto a rotating surface (mandrel) in a pre-determined geometric path (Figure 1-4). The fibre bands may be impregnated with resin during the winding process (termed as "wet winding"), or alternately the fibre may be obtained pre-impregnated by the material supplier with either a thermosetting or thermoplastic resin. For high quality, high performance fibre composite components, precise control of the tension in the fibre bands must be maintained. The placement of the fibre bands on the rotating mandrel requires precise control of the payout eye with respect to the rotating mandrel. The nature of this control depends on the type of filament winder. There are basically two standard types of filament winding machines: polar and helical.

(a) Polar Filament Winding:

The polar winding machines are generally mechanically controlled devices in which the mandrel is stationary and the payout eye rotates around the mandrel, or the mandrel rotates and the payout eye remains stationary (Figure 1-5). These machines are suitable for large production runs typically of closed-end pressure vessels with a low length/diameter ratio. Fibres, in this case are predominantly aligned within 15

degrees of the longitudinal axis of the vessel. The relative motion of the axes is governed by a mechanical transmission typically employing gears, cams and chain components.

b) Helical Filament Winding:

The mechanically-controlled helical-type filament winding machine (Figure 1-6) is particularly well-suited for large production runs of cylindrical components in which the wind angle is constant. Many of the present control systems are micro-processor based in which the positions of the axes are pre-calculated from the input parameters. The large number of possible axes of control (Figure 1-7) result in a very versatile filament winder suitable for fabricating both rotationally symmetric and asymmetric components.

1.3 Problem Definition

Due to their high specific strengths and stiffnesses, composite materials are the appropriate choice for light-weight structures, such as fibre composite pressure vessels. However, the high cost of the base materials is one of the major motivating factors for obtaining an optimal design. This should be the design which has the highest performance yet is capable of withstanding all loading conditions.

The performance of the vessel can be either the maximum internal pressure or the efficiency of the vessel. The efficiency of a pressure vessel is defined as being the product of the burst pressure and the contained volume, divided by the vessel weight:

$$\varepsilon = \frac{P_b V_{encl}}{W} \qquad (1\text{-}1)$$

There are essentially three distinct markets for fibre composite pressure vessels: industrial, military and aerospace (Table 1-1). Each has its own guidelines with regards to design, testing and qualifications procedures. Fibre composite pressure vessels can also be categorized according to their service pressure.

- low service pressure: up to 3.5 MPa (500 psi).
- moderate service pressure: 3.5 to 14 MPa (500-2,000 psi).
- high service pressure: 14 to 70 MPa (2,000-10,000 psi).
- ultra-high service pressure: 70 MPa and up (10,000 psi +).

Low and moderate service pressure vessels generally employ an elastomeric bladder (or liner) to restrict the slow permeation of high-pressure gases to the atmosphere. Vessels in the last two categories, high and ultra-high service pressure, are distinguished by the use of a metallic liner material. The liners are either thin, usually with a well-bonded composite overwrap, or thick, where the liner shares a sizeable percentage of the applied load.

This program was concerned with ultra-high pressure applications. Since the main goal of the overall program was to develop a high performance (i.e. stored energy/unit weight) fibre composite pressure vessel, a thin, rather than thick metallic liner was used. The most successful pressure vessels designed by other researchers have, besides employing thin metallic liners, used an approximate, optimized multiple-layered composite wall in which the wind angle (fibre orientation with respect to longitudinal axis of the vessel) varied for each layer [6,7]. In some cases, the effect of altering the thickness of individual layers was investigated [8,9]. Finally, different composite materials were used in the separate layers [10,11,12]. The design approach for most of these vessels was unsophisticated in that trial-and-error methods, based upon previous results generally prevailed in the selection of the design parameters.

There have been a large number of papers written on the topic of fibre composite pressure vessels; of those found, ones specific with regards to a formal optimization of the general design parameters were few.

T.R. Tauchert [13] discussed reinforced pressure vessels. Tauchert considered the effect of optimum distribution of steel bars in concrete cylinders, where the concrete was assumed to be ineffective in tension. Tsai-Hill failure theory was employed to characterize the failure of the composite. A stress function approach, in conjunction with a modified Rayleigh-Ritz technique, was employed to obtain an approximate solution to the non-linear optimization problem. The criterion of minimum strain energy (or maximum stiffness) was used to obtain the optimum distribution of reinforcing bars in the vessel wall. Tauchert concluded that an optimal fibre distribution, rather than a uniform distribution, would result in a substantial

reduction in the maximum radial displacement and an increase in the failure pressure. Tauchert did not consider the effect of changing the orientation of the reinforcing steel bars.

R.E. Sherrer [14] considered the case where the pressure vessel was comprised of helically and circumferentially-wrapped fibres. The optimum percentage of helical wraps were chosen so that all fibres were equally-stressed. The optimum was obtained by performing trials of 33, 40, 50 and 100% of helical wraps. No failure criteria was used in this case. A helix angle of 55 degrees was chosen for all helical wraps. Sherrer concluded that the resin stresses did not vary much with changes in wind angles. Wind angles were therefore not considered in the optimum design. Sherrer's analysis was interesting, but lacked generality.

A.S. Tooth et al. [15] studied a multi-layered thin-walled E-glass/polyester cylindrical vessel. The layup (or manner in which the laminate was constructed) for these vessels was a combination of continuous uni-directional fibres and discontinuous fibres (chopped strand mat, and woven roving). Three different failure theories were considered: maximum strain, stress and Tsai-Hill theory. The vessels were then compared on the basis of the critical (maximum) value for the failure theory. The effect of transverse shear was ignored in the analysis and all wind angles were in the axial or circumferential direction.

P.M.J.W. Martin's study [16] on filament wound pressure vessels used a numerical method (quadratic approximation of the objective function) to obtain the optimum shape, as described by a B-spline and the thickness distribution of the layer.

Martin used the Tsai-Hill theory to formulate his problem. Stresses in each layer of the laminate were determined using laminate theory. The fibres were assumed to lie along the geodesic of the arbitrary surface of revolution. Martin concluded that significant weight savings could be accomplished by optimization of shape and distribution. Although encouraging, Martin's results showed little detail with regards to the formulation of the actual optimization problem.

Yong-Qiu Jiang [7] reported optimum wind angles for laminated cylindrical shells with fibre-reinforced composites. Jiang considered failure of the vessels by deflection, buckling and vibration. Even-thicknesses were assumed for each layer. The optimization technique used to solve the unconstrained minimization problem was the Variable Metric method and the Golden Section method for solving the one-dimensional minimization problem.

V.T. Tomashevskii et al. [12] performed an optimization for thin-walled composite reinforced cylindrical shells. Their study assumed wind angles of $(0°,90°,\pm\alpha)$ for each elementary layer. The stresses at each layer in the material were obtained using membrane theory. The Tsai-Hill theory was again used to predict the strength of the composite. As the paper was translated from Russian, the presentation, many of the details of the method and results were sketchy and/or confusing.

Of the preceding papers, few are directly relevant to the present study. Tauchert's paper was applicable only to concrete cylinders, reinforced with steel bars. Sherrer's study imposed strict constraints on the possible wind angles, as did the studies conducted by Tooth and Tomashevskii. Martin's paper modelled a non-

cylindrical vessel, with a geodesic as the basic winding pattern. The work by Jiang assumed evenly-distributed laminae and considered failure by deflection, buckling and vibration.

Finally, the work done by Roy and Tsai [6] was the most pertinent to the present study. They presented a design method for thick-walled composite cylinders. Their analysis considered open-ended and closed-ended cylinders subject to internal and external pressures and axial loads. The failure of the cylinder was predicted using a quadratic failure theory (Tsai-Wu theory) and a degradation model was used to calculate burst pressures. Roy and Tsai did predict optimized wind angles for their vessels, though; even thickness of all layers were assumed for all vessels. The optimal design for their cylindrical vessels, which were subject to internal pressure only, was found by changing the wind angles of the individual laminae. No details about the actual optimization method were given. The authors themselves suggested that further analysis be done where the thickness of each layer, rather than being assumed as in their study, is optimized simultaneously with wind angle. This will, in fact, be one of the main goals for this study.

With the recent advances in microcomputers, the solution of numerical problems has become a far more practical approach than was previously possible. With an appropriate mathematical model of the problem, a suitable numerical method can often be applied to solve for the optimal design parameters, in a reasonable length of computation time. A standard optimization technique will be applied in this study to achieve the previously described main goal.

As in the previous studies [1-5], the vessel will be cylindrical; neither the end attachments nor the liner will be optimized but will be merely adequate to test the cylindrical section. The composite material selected will be the E/X-AS carbon fibre/epoxy. A thin as opposed to thick metallic liner will be used in order to further benefit from the load-carrying capability of the carbon fibres. A hybrid laminate was not considered, as radial stress compatibility was desired to be maintained throughout the laminate thickness. Finally, experimental verification will be carried out. The pressure-deformation characteristics of the actual vessel will then be compared to that of the mathematical model.

1.4 Thesis Overview

In Chapter 1, the general concepts of composite materials are introduced. Applications of filament wound pressure vessels are outlined, followed by a summary of the current design methods for fibre composite shells or vessels, found in the literature. Chapter 2 outlines the mathematical modelling of the cylinder, which includes the description of currently-used failure theories. The approach of the Hooke & Jeeves Direct Search method is done in Chapter 3. The results from the optimization of multiple-layer, equal and unequal thickness vessels are interpreted in Chapter 4. In Chapter 5, the vessel manufacturing techniques and testing procedures as well as equipment upgrade and maintenace are described. Finally, the conclusions and recommendations are discussed in Chapter 6.

Table 1-1 Composite Pressure Vessel End Uses [5]

Service Pressure MPa (psi)	Industrial Market	Military Market	Aerospace/Aeronautical Market	Remaining Challenges
Low	E glass/polyester		S glass, Kevlar, Carbon/Epoxy	manufacturing economics
0 – 3.5 (0 – 500)	– compressor tanks – chemical storage/ processing – filtration tanks		– rocket fuel/oxidizer storage	
Moderate	E glass, S glass/epoxy		S glass,Kevlar, Carbon/Epoxy	manufacturing economics
3.5 – 14 (500 – 2000)	– chemical storage/ processing – salt water desalination		– rocket fuel/oxidizer storage – nitrogen storage for spacecraft	
High	S glass,Kevlar/epoxy	S glass, Kevlar, Carbon/epoxy	Kevlar/epoxy	– liner buckling – liner weight – manufacturing variability
14 – 70 (2000 – 10000)	– compressed natural gas – compressed air back pack	– rocket launching tubes	– compressed air (Boeing 747) – compressed helium (shuttle) – air tanks/space suits – hydrogen storage (Venus probe)	
Ultra-High	Metals	S glass/Kevlar/ Carbon Hybrids	S glass,Kevlar, Carbon hybrids	– composite material properties – liner problems
70 + (10000 +)	– high pressure processing – material research – detonation tanks	– compressed helium/missile systems	– compressed helium/spacecraft	

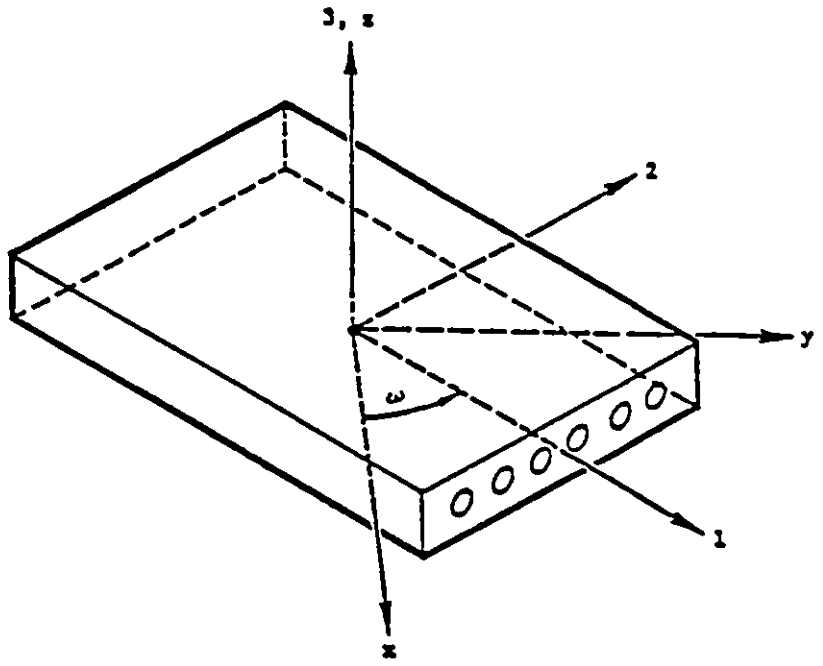

Figure 1-1 Fibre Reinforced Composite Material

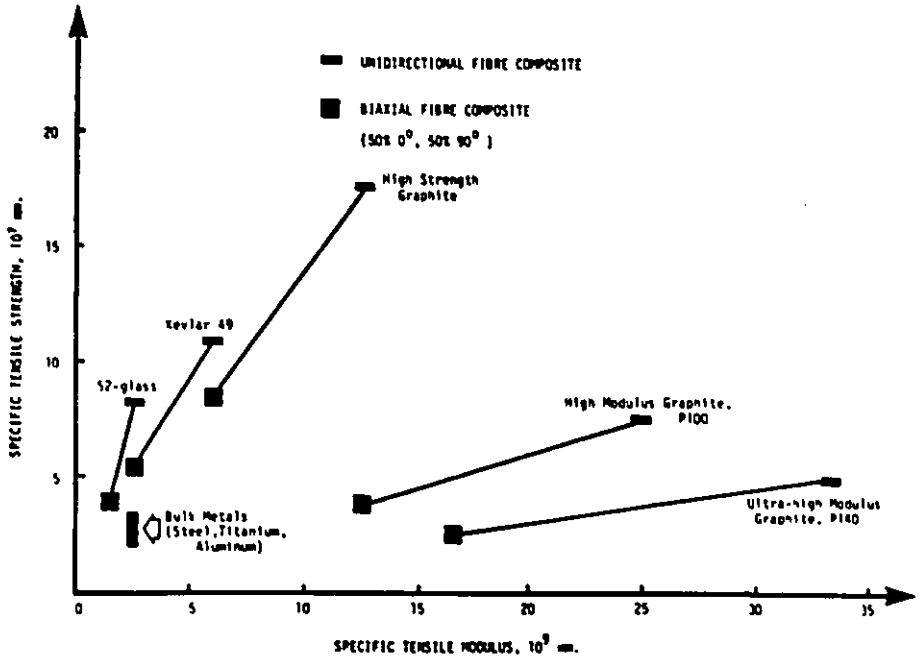

Figure 1-2 Specific Strength Versus Specific Modulus for Typical Fibre Composite and Metallic Materials [40]

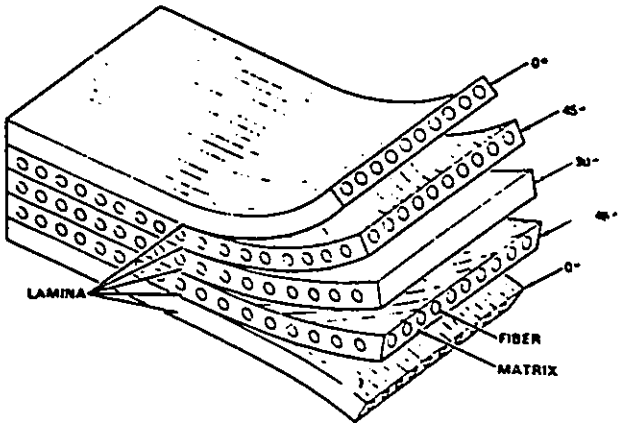

Figure 1-3 Composite Laminate [19]

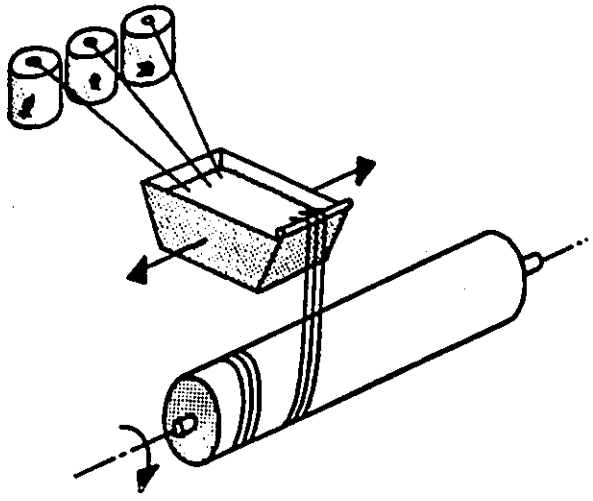

Figure 1-4 Basic Process of Filament Winding [28]

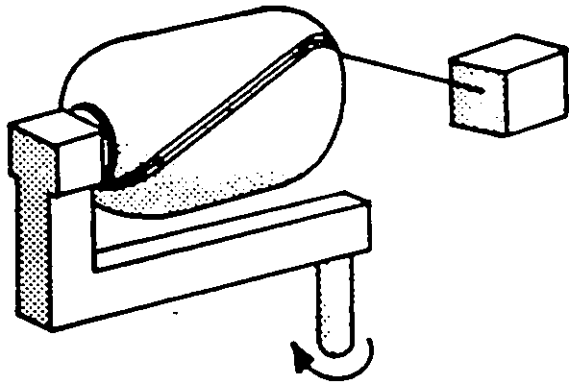

Figure 1-5 Polar Filament Winding [28]

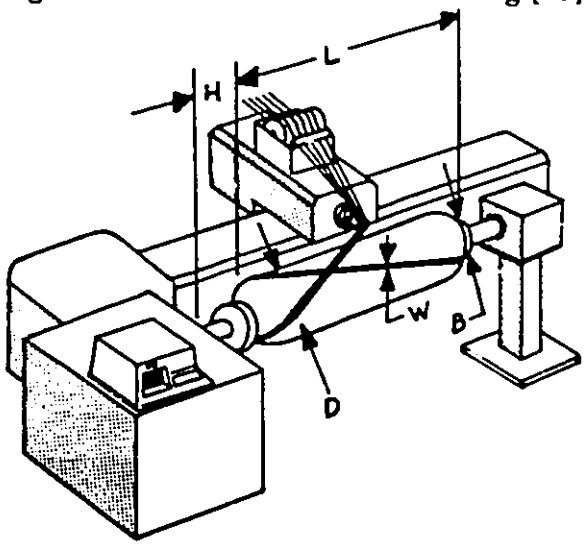

Figure 1-6 Helical Filament Winding [28]

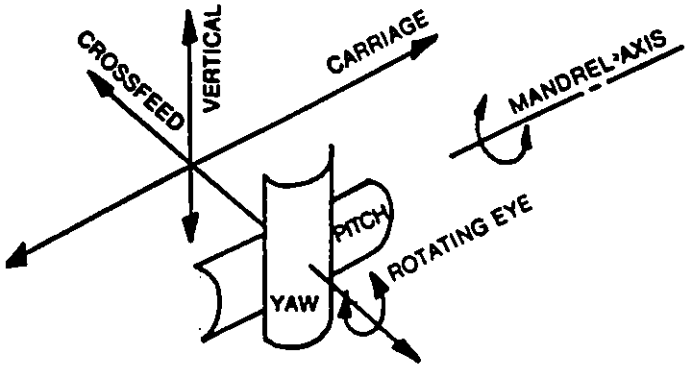

Figure 1-7 Typical Axes of Control For a Computer-Controlled Helical Filament Winder (modified from [28])

Chapter 2

MODELLING OF PROBLEM

2.1 Chapter Overview

In this chapter, three important introductory aspects are presented. First of all, in order to predict the failure pressure of a multi-layered laminated pressure vessel, the stresses and strains throughout the laminate must be determined using an appropriate method. These stresses and strains are then used in an appropriate failure theory to predict the overall laminate strength. Finally, by the use of a suitable optimization technique, the optimal design parameters of the vessel can be determined to maximize the performance of the vessel.

2.2 Stress Analysis

The exact solution for a multi-layered orthotropic cylinder (or pressure vessel) of infinite length has been calculated using elasticity methods by Sherrer [11]. Douglas Lindstrom developed a set of Fortran-based subroutines (called "EXACT"), formulated using Sherrer's analysis, which predicted the stresses and strains in a multi-layered fibre composite pressure vessel [1]. Lindstrom also formulated and devised a series solution approach to solve the elasticity equations [5], which was in good agreement [1] with Sherrer's results as well as those of Roy and Tsai [6].

Lindstrom's formulation of Sherrer's analysis was used in this study to predict the stresses and strains in the laminate (or multi-layered composite wall). The method will be briefly outlined. It was assumed that the laminate consists of perfectly bonded layers, where the bond is not shear deformable. Each layer is considered to be orthotropic and homogeneous. Three dimensional plane strain is assumed for the orthotropic laminate.

The strain-deformation equations can be written as

$$e_{zz} = e_{zz}^{(0)} \tag{2-1}$$

$$e_{\theta\theta} = \frac{u_r}{r} \tag{2-2}$$

$$e_{rr} = \frac{du_r}{dr} \tag{2-3}$$

$$\gamma_{\theta z} = \gamma_{\theta z}^{(1)} r \tag{2-4}$$

where all other shear terms are null.

Substituting these into the stress equilibrium equation (equation 3-10 in [5]) gives the following second order differential equation

$$u_r'' + \frac{u_r'}{r} - \alpha^2 \frac{u_r}{r} = \beta_1 \frac{e_{zz}^{(0)}}{r} + \beta_2 \gamma_{\theta z}^{(1)} \tag{2-5}$$

the general exact solution to this differential equation is

$$u_r^{(i)} = A_i r^{\alpha_i} + B_i r^{-\alpha_i} + \beta_1^{(i)} \frac{e_{zz}^{(0)}}{1 - \omega_i^2} r + \beta_2^{(i)} \frac{\gamma_{\theta z}^{(1)}}{4 - \omega_i^2} r^2 \tag{2-6}$$

where A and B are deformation coefficients.

The set of equations (5-16 through 5-20 in [5]) are expressed in terms of u_r, resulting in a system of equations which, when solved by a Gauss-Jordan Elimination Technique with iteration, gives u_r and the constant strain values $\varepsilon_{zz}^{(0)}$ and $\gamma_{\theta z}^{(1)}$.

The stresses and strains are then obtained in the load axes directions at the inner, mid-plane and outer sections of each lamina in the laminate (Figure 2-1). To apply the appropriate failure criteria, these stresses and strains must first be rotated to the material directions by performing the following transformations, for each individual lamina:

$$e_1 = e_x\cos^2\alpha + e_y\sin^2\alpha + \gamma_{xy}\sin\alpha\cos\alpha \tag{2-7}$$

$$e_2 = e_x\sin^2\alpha + e_y\cos^2\alpha - \gamma_{xy}\sin\alpha\cos\alpha \tag{2-8}$$

$$\frac{\gamma_{12}}{2} = -e_x\sin\alpha\cos\alpha + e_y\sin\alpha\cos\alpha + \frac{\gamma_{xy}}{2}(\cos^2\alpha - \sin^2\alpha) \tag{2-9}$$

and

$$\sigma_1 = \sigma_x\cos^2\alpha + \sigma_y\sin^2\alpha + 2\tau_{xy}\sin\alpha\cos\alpha \tag{2-10}$$

$$\sigma_2 = \sigma_x\sin^2\alpha + \sigma_y\cos^2\alpha - 2\tau_{xy}\sin\alpha\cos\alpha \tag{2-11}$$

$$\tau_{12} = -\sigma_x\sin\alpha\cos\alpha + \sigma_y\sin\alpha\cos\alpha + \tau_{xy}(\cos^2\alpha - \sin^2\alpha) \tag{2-12}$$

These stresses and strains can now be applied to the failure theories in order to predict failure of the individual layers.

2.3 Failure Theories

In a fibre-reinforced composite, failure is a difficult phenomena to accurately predict. There are many possible failure modes (fibre failure, de-bonding, matrix cracking, etc.) operating interactively, concurrently as well as sequentially. In addition to this, it is unreasonable to experimentally establish the strength characteristics of materials for every complex stress state; the concept of a failure theory has been introduced to predict the strengths of materials under multi-axial loading conditions, using the strength data obtained from uniaxial tests. The failure theory defines a surface or "failure envelope" which encloses the stress state that the material can sustain without failure. Because of their anisotropy and the greater complexity of their composition, composites demand a much more complex structural evaluation than isotropic materials, such as metals. There is very little agreement on what constitutes a so-called failure and how to predict its occurrence. For these reasons, an appropriate failure theory can only serve as a guide to design.

Five of the more popular failure theories were considered: maximum strain, maximum stress, Tsai-Hill, Hoffman and Tsai-Wu. There are many more; Nahas [17] outlined 32 different failure theories, many of which are variations of the five theories considered in this study. The following is a short description of five failure theories, which all assume plane stress. Plane strain-based theories will be discussed later.

2.3.1 Maximum Strain Theory

Failure of a layer as defined by this theory, occurs when any one of the strains in the principal material axes ($\varepsilon_1,\varepsilon_2,\gamma_{12}$) reaches its corresponding ultimate value as determined from the unidirectional loading conditions.

$$\varepsilon_1 = \varepsilon_{1\ T,C}\ (ult) \tag{2-13}$$

$$\varepsilon_2 = \varepsilon_{2\ T,C}\ (ult) \tag{2-14}$$

$$\gamma_{12} = \gamma_{12}\ (ult) \tag{2-15}$$

2.3.2 Maximum Stress Theory

As in the preceding case, failure occurs when any one of the stresses in the principal material axes ($\sigma_1,\sigma_2,\tau_{12}$) reaches its corresponding ultimate value.

$$\sigma_1 = X_T \quad \text{or} \quad X_C \tag{2-16}$$

$$\sigma_2 = Y_T \quad \text{or} \quad Y_C \tag{2-17}$$

$$\tau_{12} = S \tag{2-18}$$

2.3.3 Tsai-Hill (Azzi-Tsai) Theory

Unlike the two previous theories, where failures in different modes are presumed to occur independently, this theory [18] considers "interaction" between the failure strengths. This results in a smooth envelope rather than the intersecting straight lines obtained with maximum strain or stress theories (see Figure 2-2).

$$\frac{\sigma_1^2}{X^2} - \frac{\sigma_1\sigma_2}{X^2} + \frac{\sigma^2}{Y^2} + \frac{\tau_{12}^2}{S^2} = 1 \qquad (2\text{-}19)$$

Failure occurs when the left-hand-side of the equation is greater than unity. It should be mentioned that no distinction between tensile or compressive strength is made for this failure theory. For a carbon fibre composite, the transverse strength is different in tension and compression, hence some generality is lost for this failure theory.

2.3.4 Hoffman Theory

Hoffman [16] has generalized the Hill theory to account for different strengths in tension and compression.

$$\frac{\sigma_1^2-\sigma_1\sigma_2}{X_T X_C} + \frac{\sigma_2^2}{Y_T Y_C} + \frac{X_C-X_T}{X_C X_T}\sigma_1 + \frac{Y_C-Y_T}{Y_C Y_T}\sigma_2 + \frac{\tau_{12}^2}{S^2} = 1 \qquad (2\text{-}20)$$

Again, failure occurs when the left-hand-side of equation 2-20 becomes greater than unity.

2.3.5 Tsai-Wu Theory

The basic assumption for the Tsai-Wu theory [19] is that there exists a failure surface in the stress space which may be expressed in terms of a stress tensor polynomial equation. It is analogous to maximum distortional energy and is considered to be the most general theory of strength for anisotropic materials. Wu [20] has shown that most of the existing failure theories in use are degenerated cases of the Tsai-Wu theory.

$$F_i\sigma_i + F_{ij}\sigma_i\sigma_j = 1 \qquad i,j=1,2,...6 \tag{2-21}$$

For the transversely isotropic case

$$F_1\sigma_1 + F_2\sigma_2 + F_{11}\sigma_1^2 + F_{22}\sigma_2^2 + 2F_{12}\sigma_1\sigma_2 + F_{66}\sigma_6^2 = 1 \tag{2-22}$$

where

$$F_{11} = -\frac{1}{X_T X_C} \qquad F_{22} = -\frac{1}{Y_T Y_C} \qquad F_{66} = \frac{1}{S^2}$$

$$F_1 = \frac{1}{X_T} + \frac{1}{X_C} \qquad F_2 = \frac{1}{Y_T} + \frac{1}{Y_C}$$

F_{12} is constrained by the following condition

$$F_{11}F_{22} - F_{12}^2 \geq 0 \tag{2-23}$$

This condition ensures that the failure envelope is closed; i.e., the shape remains ellipsoidal and that the material has finite strength in all directions. A point inside this envelope shows a state of stress where failure has not occured.

As mentioned earlier, the five failure theories previously outlined were selected on the basis that they were the most often used in practice by designers. In a study by Burk [21] in 1983, the selected theories were, in order of preference, maximum strain, maximum stress, Tsai-Hill and Tsai-Wu theory (Figure 2-3). One of the advantages to using maximum strain theory is that the mode of failure of the failed lamina is determined, which physically predicts the onset of detectable failure.

2.4 Selection Of Optimization Technique

An optimization technique was selected to determine the optimal input parameters to obtain maximum vessel performance (defined in section 1.3). The input parameters, or design constraints for this problem consisted of the various wind angles

(α_1,α_2,..) and thicknesses (t_1,t_2,..) of the individual layers within the laminate. Figure 2-4 shows a cylindrical section from the vessel. The normalized thickness, or b/a ratio is defined as the outer radius of the wall, divided by the inner radius. A section of the laminate is shown in Figure 2-5. This defines the individual laminae orientations and thicknesses for a given laminate configuration.

This problem can be considered as a special case of the general (or constrained) non-linear problem. The special characteristic of this problem is that the solution vector

$$\boldsymbol{X} = \begin{pmatrix} x_1 \\ x_2 \\ : \\ x_n \end{pmatrix} \tag{2-24}$$

need not satisfy any constraint. The optimization technique will minimize the objective function

$$f(X) = f(x_1, x_2, \ldots x_n) \tag{2-25}$$

The objective function surface, also known as the hypersurface, is defined as

the locus of all points satisfying the objective function, f(X). The hypersurface is an (n+1) dimensional space where n is the number of design or search variables.

Specifically, the objective function for this problem is defined as

$$\textit{Minimize } \Phi(X) \tag{2-26}$$

where

$$X = (\alpha_1, \alpha_2, \ldots \alpha_n, t_1, t_2, \ldots t_n) \tag{2-27}$$

$$\Phi(X) = \textit{Maximum } [\Omega^n ; \Omega^n = F_i \sigma_i^n + F_{ij} \sigma_i^n \sigma_j^n - 1] \tag{2-28}$$

and

$$\sigma_i^n = \xi(\alpha_n, t_n) \tag{2-29}$$

where n is the number of individual layers in the laminate

The numerical methods available for solving an unconstrained optimization problem can be classified into two broad categories: direct search methods and gradient methods.

Gradient methods require that the objective function be differentiable, which is

clearly difficult for the particular problem being studied. A non-differentiable objective function problem is well suited to a direct search approach. In this fashion, only the ability to evaluate the objective function at specified points, together with the function being continuous are necessary criteria.

Although these methods have been developed heuristically and no proofs of convergence have been derived for them, in practice they have generally proved to be robust and reliable, in that only rarely do they fail to locate at least a local minimum of a given function (although the rate of convergence can sometimes be very slow [22]). In addition to this, the relative simplicity of the direct search approach compared with the gradient techniques can prove to be advantageous; generally the methods are computationally compact and make only modest demands on storage, which is an important consideration in solution to practical optimization problems.

Of the direct search methods, there are the following methods:

(1) Random search

(2) Univariate methods

(3) Pattern search methods:

    a) Powell's method

    b) Hooke & Jeeves method

(4) Rosenbrock's rotating coordinate method

(5) Simplex method

All the unconstrained minimization methods are iterative in nature; they start

from an initial trial solution and proceed towards the minimum in a sequential manner. Unconstrained minimization methods differ from one another in the manner in which they generate a new point X_{i+1} from X_i and in testing the point X_{i+1} for optimality.

The direct search methods assume that the objective function is unimodal. A unimodal function is one where there is only one overall minimum value (i.e. a global minimum). As can be expected, the ability of a search method to locate a global minimum is highly dependent on the initial trial solution of the objective function. In order to lessen the probability of finding only a local minimum, an initial trial solution is randomly generated for each optimization where the entire procedure is looped a number of times.

Of the first two direct search methods, random and univariate are not appropriate for this problem. The random search method, where the objective function is evaluated at many uniformly distributed points in the hyperspace is too inefficient; the univariate method, where only one variable is changed at a time is not appropriate, for the same reason. Of the remaining methods, Powell's, Hooke & Jeeves, Rosenbrock's and Simplex, all will likely perform reasonably well, as they are similar in that they all use an exploratory move to determine the most promising search direction. The Hooke & Jeeves method was selected as it is straightforward, widely used and relatively efficient.

2.4.1 Hooke & Jeeves Method

The pattern search method of Hooke & Jeeves is a sequential technique, where each step consists of two kinds of moves, one called the "exploratory" move and the other called the "pattern" move. The first type of move is used to explore the local behaviour of the objective function; the second type of move is used to take advantage of the best search direction. The general procedure can be described by the following steps [23]:

1. Start with an arbitrarily chosen point, (called the starting base point) and prescribe a step length Δx_i in each of the coordinate directions $\mathbf{u}_i$, i=1,2...n.. Set k=1.

2. Compute $f_k=f(X_k)$. Set i=1, $Y_{k0}=X_k$ and start the exploratory move. The point Y_{kj} indicates the temporary base point obtained from the base point X_k by perturbing the j^{th} component of X_k.

3. The variable x_i is perturbed about the current temporary base point, $Y_{k,i-1}$ to obtain the new temporary base point as:

$$Y_{k,i} = \begin{cases} Y_{k,i-1} + \Delta x_i \mathbf{u}_i & \text{if } f^+ = f(Y_{k,i-1} + \Delta x_i \mathbf{u}_i) < f = f(Y_{k,i-1}) \\ Y_{k,i-1} - \Delta x_i \mathbf{u}_i & \text{if } f^- = f(Y_{k,i-1} - \Delta x_i \mathbf{u}_i) < f = f(Y_{k,i-1}) \text{ and} \\ & \text{if } < f^+ = f(Y_{k,i-1} + \Delta x_i \mathbf{u}_i) \end{cases}$$

$Y_{k,i-1}$ if $f = f(Y_{k,i-1}) < \min(f^+, f^-)$

This process of finding the new temporary base point is continued for i=1,2,.. until x_n is perturbed to find $Y_{k,n}$.

4. If the point $Y_{k,n}$ remains the same as X_k, reduce the step length Δx_i. Set i=1 and go to step 3. If $Y_{k,n}$ is different from X_k, obtain the new base point as $X_{k+1} = Y_{k,n}$ and go to step 5.

5. With the help of the base points X_k and X_{k+1}, establish a pattern direction S as

$$S = X_{k+1} + X_k$$

and find a point $Y_{k+1,0}$ as

$$Y_{k+1,0} = X_{k+1} + \lambda S$$

where λ is the step length.

6. Set k=k+1, $f_k = f(Y_{k0})$, i=1 and repeat step 3. If at the end of step 3, $f(Y_{k,n}) < f(X_k)$, take the new base point as $X_{k+1} = Y_{k,n}$ and go to step 5. On the other hand, if $f(Y_{k,n}) > f(X_k)$, set $X_{k+1} \equiv X_k$, reduce the step length Δx_i, set k=k+1 and go to step 2.

7. The process is assumed to have converged whenever the step lengths fall below a small quantity ε. The process is terminated if

$$\max(\Delta x_i) < \varepsilon$$

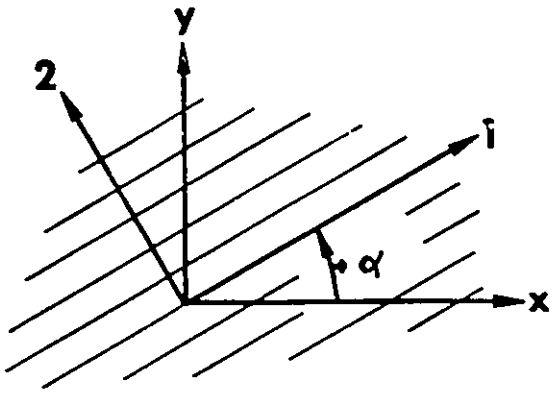

Figure 2-1 Load and Material Coordinate Directions

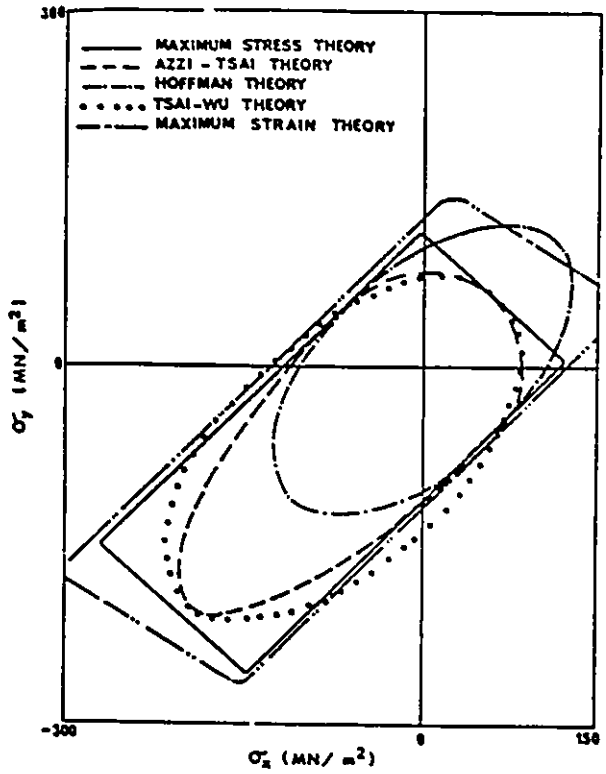

Figure 2-2 Comparison of the Most Common Failure Theories [17]

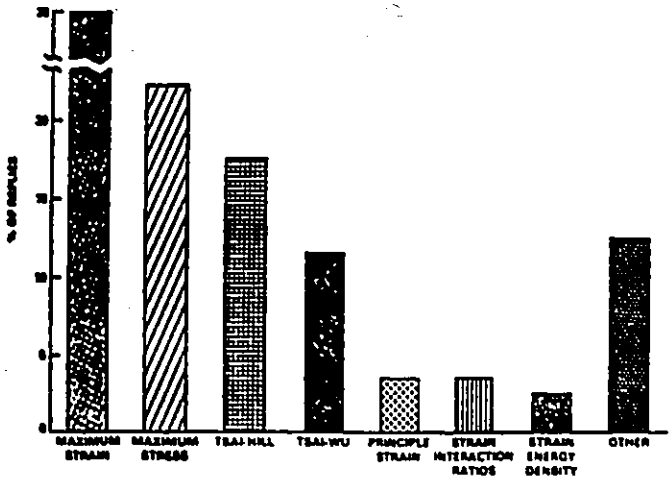

Figure 2-3 Failure Criteria Currently Used [21]

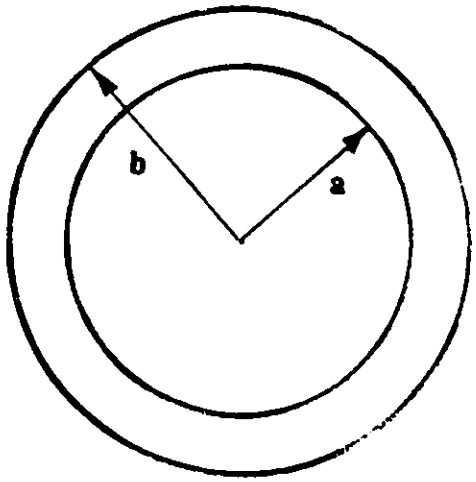

Figure 2-4 Cylindrical Cross Section of Vessel

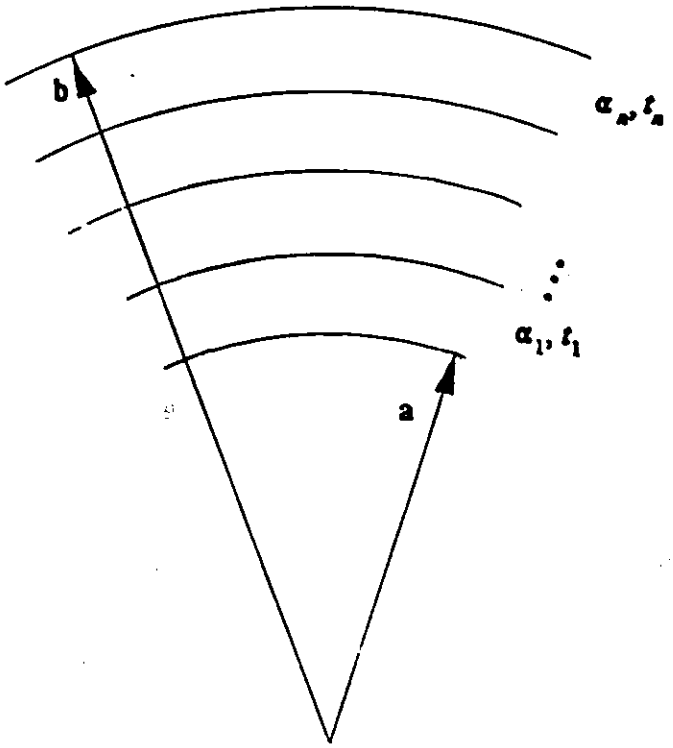

Figure 2-5 Composite Laminate of Vessel

Chapter 3

DEVELOPMENT OF THE OBJECTIVE FUNCTION

3.1 Outline Of Model

For this study, the objective was to devise a mathematical algorithm that will individually or simultaneously optimize the wind angles and the thicknesses of the individual layers of the reinforcing wall of a fibre composite pressure vessel. The general outline is as follows:

- The closed-end cylinder was subjected to internal pressure only.

- The cylinder was assumed to be infinitely long, so that end effects could be neglected.

- A comparison and selection of an appropriate failure theory was done.

- The effects of equal and unequal thicknesses of the individual layers were compared.

- A simultaneous optimization of wind angle and thickness was performed for each layer.

- The layers were assumed to have adjacent ($\pm\alpha$) laminae and were referred to as one single layer of angle α.

- All lamina were assumed to behave in a linear-elastic manner up to their respective failure point.

Normally, a multi-layered laminate (representing the vessel wall) undergoes layer by layer failure as the loading (caused by internal pressure, in this case) is increased. It is very difficult to experimentally determine the point of failure of one of the individual layers. One method to model failure is to design a multi-layered laminate that experiences simultaneous failure of all layers in the laminate. This approach enables easier experimental verification; however, it was found that this design was not the one that possessed the highest performance. It was therefore not considered to be an optimum design.

As mentioned previously, the normal approach is to assume that the entire laminate will not fail because of an individual layer failing. These methods of modelling the laminate failure are considered to be "degradation" approaches, where the mechanical properties of the laminate are systematically reduced to account for the

failed layers. What characterizes these "degradation methods" is the manner in which the failed layers are dealt with. Some methods consider the failed layer to have zero mechanical properties, as the method outlined by Jones [30] (Appendix B) shows, whereas others systematically reduce the properties by a preselected factor [17].

Jones' method can be described in the following manner: Loading of the laminate causes the first lamina failure. The mechanical properties of the failed lamina are set to zero and the loading of the laminate continues until the next lamina fails. Once the final lamina has failed, the ultimate load-carrying capability of the laminate has been reached.

Roy and Tsai employed a method, used for their study of pressure vessels [6], where the degraded lamina properties were not zero, but a certain percentage of the original properties, in order to have agreement between the predicted and experimental results. This method essentially employs "curve fitting" and will not be used for this study. There is, however, no generally accepted degradation method and none will be used for this study.

The design approach used for this study will be one where the laminate experiences failure when any of the laminae reach their respective loading limit, as defined by the failure theory. This idealized approach to design is usually termed as "first-ply-failure" (FPF). Of course, this "idealized" failure mode does not always result in total vessel failure.

3.2 Selection Of Mechanical Properties

In order to properly model the reinforced cylinder, a careful selection of material properties of the composite are required for the stress analysis model, to be later used by the failure theory. The majority of the mechanical properties were determined by earlier testing done at the University of Ottawa for the identical composite material, i.e. Grafil E/XA-S carbon fibre and a polymeric matrix of Shell Epon 825 epoxy resin with Pacific Anchor Ancamine 1482 hardener (at 19 parts, by weight per 100 parts epoxy resin). Fibre volume fraction was approximately 60%. The mechanical properties are shown in Tables [3-1 to 3-4].

3.2.1 Elastic Moduli Values

It is assumed that all elastic properties of the composite normal to the fibre direction are the same, or as being transversely isotropic. The following material properties must be specified for the composite:

$$E_{11} \quad G_{12} \quad \nu_{12}$$
$$E_{22} \quad G_{13} \quad \nu_{13}$$
$$E_{33} \quad G_{23} \quad \nu_{23}$$

where $E_{22} = E_{33}$, $G_{12} = G_{13}$ and $\nu_{12} = \nu_{13}$.

The value for E_{11} was determined by uniaxial tensile tests on flat bar specimens [24] as were the values for E_{22} [25] and the assumed value for E_{33}.

The shear moduli values for the composite were estimated using different methods. The G_{12} shear term was obtained using the method proposed by Munro and Lee [26], which relates the shear modulus of the composite to the shear modulus and volume fraction of the matrix material.

$$G_{12} = \frac{G_m^2}{V_m} \tag{3-1}$$

Since the matrix material is considered to be isotropic, the shear modulus of the matrix can be found, knowing the tensile modulus, which has been determined experimentally.

$$G_m = \frac{E_m}{2(1 + \nu_m)} \tag{3-2}$$

Where E_m=2.65x10^9 and ν_m=0.35. The G_{13} term is the same, by transverse isotropy.

The G_{23} term is estimated, using the Chamis formula [27]:

$$G_{23} = \frac{G_m}{1 - \sqrt{x_f}(1 - \frac{G_m}{G_{f_{23}}})} \qquad (3\text{-}3)$$

G_{f23}, the transverse shear modulus of the fibre, was found in [25].

3.2.2 Poisson's Ratio

The ν_{12} and assumed values for the ν_{13} Poisson's ratios were determined experimentally at the University of Ottawa, again from flat bar tests [25]. The ν_{23} term was estimated, using equation 3-4 (from Chamis [27]).

$$\nu_{23} = \frac{E_{22}}{2\,G_{23}} - 1 \qquad (3\text{-}4)$$

3.2.3 Failure Strains

The longitudinal tensile and the transverse tensile and compressive strains, were determined using flat bar specimens ([24],[25] and [3], respectively). The shearing failure strain, γ_{12}, was based on Iosipescu tests performed for the T300/5208 composite, which possesses similar mechanical properties to the E/X-AS/epoxy composite [26].

3.2.4 Failure Strengths

The longitudinal tensile and transverse tensile and compressive strengths were again determined using flat bar specimens. The value for the longitudinal strength was determined in [24] and the value for the transverse tensile and compressive strengths were determined in [25] and [3], respectively. The value for the shear strength was estimated similarly to the shearing strain.

3.3 Failure Theories

Of the five failure theories being considered, only three can be considered to be true failure theories: They are Tsai-Hill, Hoffman and Tsai-Wu theory. Maximum stress and maximum strain are only limit theories, where no interaction (other than that due to Poisson's ratio) between failures modes is possible. Tsai-Hill, Hoffman and Tsai-Wu theories are quadratic failure theories. They are all defined by a scalar equation of the form:

$$F_i\sigma_i + F_{ij}\sigma_i\sigma_j = 1 \qquad i,j=1,2,...6 \tag{3-5}$$

The failure condition is represented by an ellipsoidal-shaped surface. Any stress point within the surface represents a stress-state whose magnitude is less than that required for failure. Any stress point lying on the surface represents a stress point causing failure and finally, any point lying outside the surface is not admissible. The

failure theories will be based on a plane-stress condition.

This failure condition will be applied throughout the vessel wall to all inner and outer points of each layer in the laminate, since the stress state is also changing throughout the wall thickness. The wind angles of each layer in the laminate will be chosen so that the magnitude of the maximum failure condition of all points are minimized. A failure is assumed to have occurred when the failure condition (FPF) has been met at any point in the laminate.

3.3.1 Comparison of Failure Theories

As was stated earlier, the optimal design for a pressure vessel will be one where the performance is highest. For a pressure vessel of a given volume, length and internal pressure, maximum performance can be assumed to occur at the internal pressure causing first-ply-failure.

Although a three-dimensional (plane-strain) stress analysis has been employed to obtain the stresses throughout the laminate, two-dimensional (plane stress) failure criteria were chosen. This is partly due to the fact that not all the failure theories were formulated for plane strain conditions.

However, trial calculations were performed to obtain the FPF pressure, using a three-dimensional Tsai-Wu quadratic failure theory (equation 2-21). The results from

this experiment showed the radial stress term (σ_{33}) to be the dominant term at the inner layer of the laminate; this is the point where the radial compressive stress term is identical to the internal pressure. Consequently, FPF occurred as soon as the internal pressure reached the radial ultimate strength, (which is low compared to the axial strength) giving lower failure pressure predictions than expected.

From past work on composite pressure vessels, the controlling failure mode(s) were typically not by radial compression. For this reason, it was concluded that two-dimensional failure theories were more appropriate to predict FPF pressure for all the cases being considered. The question of two-dimensional versus three-dimensional models will again be addressed once experimental results are obtained.

The failure pressure (as predicted by FPF) was determined as a function of laminate thickness (b/a) for a one-layer laminate. All points were found by searching for the optimum wind angle(s) for each laminate, then by iterating a number of times to determine the highest possible pressure. This procedure was difficult in that no relation between the scalar quantity representing a point inside the failure surface and burst pressure existed. Referring to Table 3-5, for a single-layer laminate, it was also noticed that the optimum wind angle tended to increase as the thickness of the laminate increased. In addition, all of the five failure theories predicted essentially the same optimum wind angles (within a range of two degrees) for all values of laminate thickness investigated.

Figure 3-1, which graphically depicts the variation of FPF pressure with laminate thickness for a single-layered vessel, for all five failure theories, shows

similar trends for all cases.

Below b/a=1.25, all theories predicted similar failure pressures. As well, a nearly linear relation between thickness and failure pressure was also noticed in this range, which is the same type of behaviour predicted by thin-walled cylinder theory.

Above b/a=2.00, an increase in thickness did not result in any significant increase in failure pressure. Tsai-Hill and Tsai-Wu theories predicted the lowest (and nearly identical) results, whereas Hoffman theory showed slightly higher predicted failure pressures for thicker laminates (i.e. b/a>1.25).

Maximum strain and stress theories showed similar failure pressures for lower values of b/a. However, at higher values (b/a>1.25), the predictions were quite different.

This difference can perhaps be explained by the nature of maximum strain and stress theories, which make no distinction between any of the failure modes; all are equally weighed. For this reason, if maximum strain theory was employed, the controlling failure modes were not necessarily the same as those for maximum stress theory. The failure mode as predicted by maximum strain theory, is transverse tensile failure, while the failure mode predicted from maximum stress theory, at higher values of b/a (>1.75) was simultaneous transverse and longitudinal tensile failure. Since the ultimate strengths and failure strains of the fibre composite in the transverse and shear direction are far inferior to the properties in the longitudinal direction, the higher predictions using maximum stress theory were understandable.

Seeing as the vessel is assumed to have a leak-proof liner, cracks that are easily produced in the transverse direction to the fibre would likely not produce failure of the vessel. The failure mode for maximum strain and stress theories were thus changed to be longitudinal tensile failure of the fibre composite by increasing the internal pressure. The results are shown in Figure 3-2. As expected, by setting the failure mode to be longitudinal tensile failure, the FPF predictions of maximum strain and stress theories were more similar for all ranges of b/a.

3.3.2 Selection Of Failure Theory

The best choice of a failure theory will be one which is general for any type of laminate. It will also be one where interaction (or coupling) can occur between the many different failure modes. For this reason, an interactive, rather than limit-type (maximum stress or strain) failure theory was selected.

With regards to the quadratic failure theories, Tsai-Wu theory is the most general, while Hoffman and Tsai-Hill theories are both specific cases of Tsai-Wu theory. It should be noted that Tsai-Wu theory predicted the lowest failure pressures of all types considered, giving the most conservative estimate of the laminate strength of the quadratic failure theories. For these reasons, Tsai-Wu theory was judged as being

the most appropriate failure theory for all subsequent analysis in this study.

Table 3-1 Moduli Values for Grafil E/X-AS - Shell Epon 825 Epoxy

Term	Modulus (GPa)
E_{11}	17.00
E_{22}	8.50
E_{33}	8.50
G_{12}	2.40
G_{13}	2.40
G_{23}	2.63

Table 3-2 Poisson's Ratio for Grafil E/X-AS - Shell Epon 825 Epoxy

Term	Poisson's ratio
ν_{12}	0.30
ν_{13}	0.30
ν_{23}	0.62

Table 3-3 Failure Strains for Grafil E/X-AS - Shell Epon 825 Epoxy

Term	Failure Strain
$\varepsilon_{1T,C}$	0.0133
ε_{2T}	0.0048
ε_{2C}	0.0235
γ_{12}	0.0188

Table 3-4 Failure Stresses for Grafil E/X-AS - Shell Epon 825 Epoxy

Term	Failure Strength (MPa)
$X_{T,C}$	1960.0
Y_T	38.6
Y_C	200.0
S	42.2

Table 3-5 Optimal Wind Angles and FPF Pressures for Five Failure Theories (Assuming Longitudinal Failure for Maximum Strain and Stress Theories)

b/a	Failure Theory	Optimum Wind Angle (degrees)	FPF Pressure (MPa)
1.15	Max. Strain	54	95.0
	Max. Stress	54	90.0
	Tsai-Hill	54	87.0
	Hoffman	54	80.0
	Tsai-Wu	54	85.0
1.35	Max. Strain	54	190.0
	Max. Stress	54	290.0
	Tsai-Hill	55	220.0
	Hoffman	54	220.0
	Tsai-Wu	55	235.0
1.55	Max. Strain	56	240.0
	Max. Stress	56	400.0
	Tsai-Hill	57	300.0
	Hoffman	56	365.0
	Tsai-Wu	57	320.0
1.75	Max. Strain	57	260.0
	Max. Stress	57	500.0
	Tsai-Hill	58	340.0
	Hoffman	57	405.0
	Tsai-Wu	58	340.0
2.00	Max. Strain	57	290.0
	Max. Stress	57	520.0
	Tsai-Hill	58	340.0
	Hoffman	57	410.0
	Tsai-Wu	58	340.0
2.50	Max. Strain	61	320.0
	Max. Stress	61	520.0
	Tsai-Hill	63	355.0
	Hoffman	62	425.0
	Tsai-Wu	63	350.0

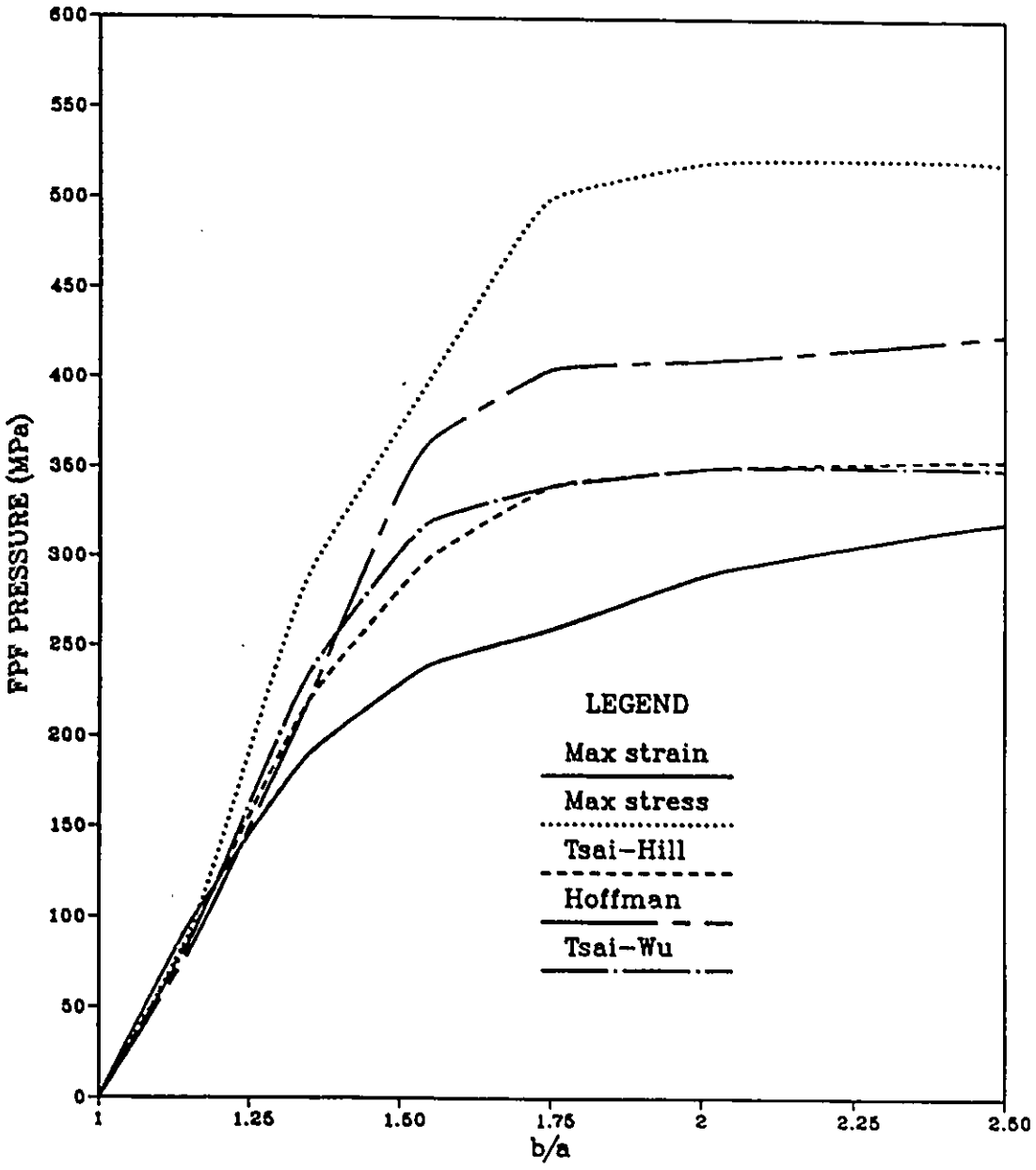

Figure 3-1 **FPF Pressure Versus b/a for a Single-Layer Vessel, using Five Failure Theories (Assuming Longitudinal, Transverse or Shear Failure for Maximum Strain and Stress Theories)**

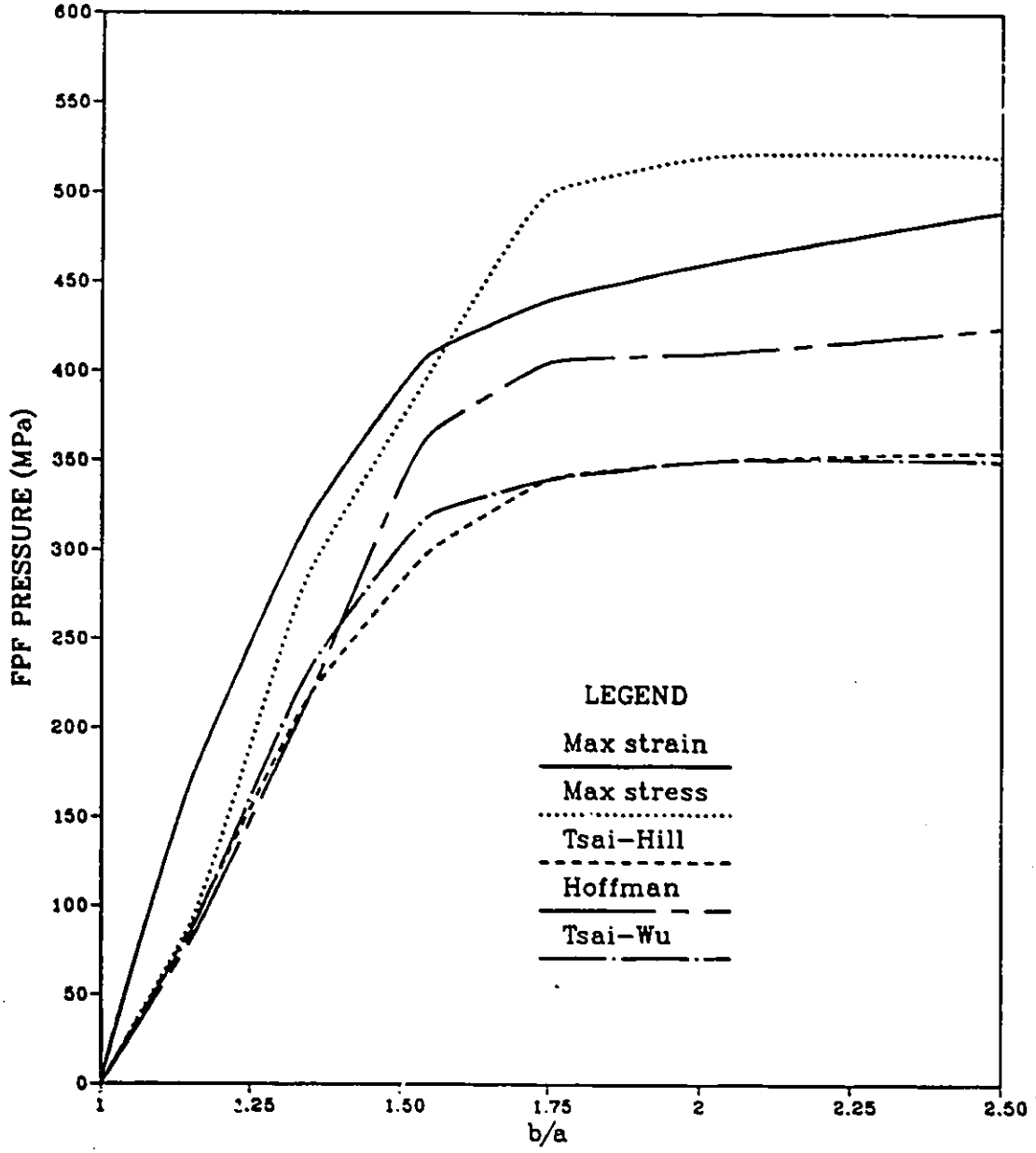

Figure 3-2 FPF Pressure Versus b/a for Single-Layer Vessel for Five Failure Theories (Assuming Longitudinal Failure for Maximum Strain and Stress Theories)

Chapter 4

OPTIMIZATION AND RESULTS

4.1 Chapter Overview

In this chapter, the effects of the individual layers in an equal and unequal thickness laminate in addition to wind angle of layers will be investigated.

4.2 Multi-Layered Vessel with Equal Thickness Layers

The previous chapter presented the results for a single layer vessel with a single wind angle. The next step in the analysis consisted of determining the effect of sub-dividing the laminate into a number of equal thickness individual layers of specific orientations on the performance of the vessel.

It was expected that the effect of increasing the number of individual layers, each with their respective wind angles, would enable the vessel to better resist the applied loads. By increasing the number of individual layers in the laminate, the high strength properties of the composite material could be better placed to match areas of high stress. This trend was also noted by other researchers, [6-12]

Typically, all layers in a laminate were of equal thickness, usually for reasons of simplicity and ease of manufacturing. The effect on first ply failure of constructing the laminate with equal thickness layers was determined for a range of wall thicknesses (Table 4-1).

For the single layer case, it was noticed that the optimum set of wind angles changed as the wall thickness changed. This demonstrated that optimization of wind angles was dependent on the loading conditions (internal pressure in this case) as well as the geometrical conditions (wall thickness) in addition to the type of reinforcing material selected.

The optimum wind angle combinations for one to four equal thickness layers are also shown in Table 4-1. It was noticed, in general, that as the laminate thickness was increased, the inner layers in the laminate tended to be oriented towards the axial direction, while the angles near the outer layers progressively oriented themselves towards the hoop direction.

The relation between FPF pressure and laminate thickness was shown in Figure 4-1, for one to four equal thickness layers. For thin laminates ($b/a<1.35$), there was

not a significant improvement in failure pressure from a single-layer to a four-layer vessel. For thicker vessels, a significant increase was seen.

It should be mentioned that, although the following graphs are for a specific inner radius (a), the results can be considered to be non-dimensional in b/a (normalized thickness), as no dependence on inner radius was found.

The maximum failure (or FPF) pressure was attained at b/a of approximately 1.75. Further increasing the laminate thickness beyond that point did not result in any improvement in FPF pressure for any of the four cases. It was also noticed that the FPF pressure decreased for the 2-layer laminate between b/a =1.75 and 2.50. This is unusual in that a thicker laminate would seem to be able to resist the applied load more effectively than a thinner one. The actual cause of this can likely be attributed to the effect of constraining the layers to fixed equal thickness layers, thereby causing the inner layer to be quite thick, the vessel performance was not improved much beyond that of a single layer vessel. This suggested that equal thickness layers was not necessarily the optimum distribution for all types of vessel configurations.

4.2.1 Optimization Path

In Chapter 2, the Direct Search Method of Hooke & Jeeves was described using a set of algebraic equations. It is of assistance to visualize the steps in an actual optimization problem. The general surface of the objective function is always a

surface of n+1 dimensions, where n is the dimension of the solution vector (or number of parameters). Since a hypersurface of higher dimensions than three is impossible to represent graphically, an example of the hypersurface for two variables (θ_1=wind angle of layer 1, θ_2=wind angle of layer 2) is shown in Figures 4-2 and 4-3.

The hypersurface for a two-layer, even thickness vessel of b/a=1.25 and internal pressure of 165 MPa was previously shown (Figure 4-2). Here, the optimization path that the routine followed was shown graphically for the same vessel, to demonstrate the ability of the Hooke & Jeeves pattern search method to locate the optimum.

The surface (using contours) represented the maximum value of the objective function, $\Omega(X)$, in both layers for a given laminate configuration. It was noticed that the surface was fairly well-behaved in that no sudden peaks or valleys occurred, which might cause the search to terminate prematurely. Also, the minimum region of the graph, which was the region of interest. showed a relatively flat profile, suggesting that the optimum wind angle was insensitive to small changes in wind angle. Although being useful, these results did not necessarily prove that all hypersurfaces are as well behaved and that the global minimum can easily be found, but only suggested that a search method could certainly be effectively used for some cases.

Referring to Figure 4-3, which is a magnification of the surface contour shown before in Figure 4-2, the optimization started at the initial point x_0=(80.0,85.0) or (a). The initial step length was set at 4.00 degrees. The result of the first exploration yielded point (b). Next, there was an accelerated move to point (c). A test of this

point showed that it was better than point (b); this improved point was designated x_1=(72.0,77.0) and a local search was then initiated about that point. Subsequently, point (d) was found; the accelerated move to (e) followed. An exploration about point (e) showed promise in the same direction, but the accelerated move to (g) failed (a higher value of the objective function was found). As a result, the entire accelerated move was then abandoned, the initial step length reduced by a pre-selected amount and the search continued from the last optimal point, (f). The search proceeded in a similar way and the optimum of $\{\alpha_1,\alpha_2\}$=(51.5,58.0) was soon found.

This representation clearly shows the advantages of using a search method with the ability to accelerate, given that a promising search direction is found. There exists more sophisticated search methods, but the Hooke & Jeeves method located the optimal points quite effectively for the searches performed up to now. Another search method will not be considered, unless new developments occur that would suggest a more appropriate method should be considered.

4.2.2 Vessel Efficiency

As stated earlier, it was desired to obtain the vessel design that yielded the highest possible vessel performance. The efficiency was defined as

$$\varepsilon = \frac{P_b V_{encl}}{w} \tag{4-1}$$

where P_b=pressure at FPF.

or alternately, can be expressed in terms of b/a as

$$\varepsilon = \frac{P_b \pi r_i^2 l}{\rho V g} \tag{4-2}$$

$$\varepsilon = \frac{P_b \pi r_i^2 l}{\rho g \pi l(r_o^2 - r_i^2)} \tag{4-3}$$

$$\varepsilon = \frac{P_b}{\rho g (b/a^2 - 1)} \tag{4-4}$$

where ρ =1430 kg/m^3 for the E/X-AS/epoxy composites of this study.

Figure 4-4 depicts the composite efficiency (in units of metres), versus increasing vessel thickness for one to four layered equal thickness vessels. The results are also in Table 4-2. Since the reinforcing effect of the low-strength liner compared to the high-strength fibre composite was only a few percent of the total reinforcing capability of the vessel, its effect was neglected in the analysis.

The efficiency increased quite rapidly up to the peak efficiency (which occured near b/a=1.25, for all cases), then decreased. The curves had moderately higher values

of composite efficiency for increasing number of layers, for all b/a ratios.

4.3 Multi-Layered Vessels with Unequal Thickness Layers

The next step in this study investigated the effect of altering the fixed thicknesses of the individual layers on vessel performance. The procedure involved a simultaneous optimization of wind angles and layer thickness. In this fashion, it was expected to obtain some improvement in FPF pressure over vessels with equal thickness layers, especially for the thicker, less efficient vessels.

The results from the optimization are shown in Figures 4-5 to 4-9 and Tables 4-3 and 4-4. For the 2-layer case (Figure 4-6), an increase in failure pressure was noticed for all values of b/a above 1.25, with a substantial improvement for the thickest laminate (b/a=2.50). The FPF pressure for the case of equal thickness layers decreased from 400 MPa at b/a=1.75 to 355 MPa for b/a=2.50 (Table 4-1). The results from Table 4-3 indicated that the reasons previously suggested were correct, as the resulting increase in FPF pressure resulting from changing the layer thicknesses from $\{t_1,t_2\}$=(23.7,23.7) to (10.2,37.3) was significant. At b/a ratios less than 1.25, there was very little improvement in FPF pressure.

Similar results were seen for the 3 and 4-layer cases. A slight increase in FPF pressure was noted by changing the thickness of the layers for all cases, although the effective increase was greater at higher b/a values.

Finally, the vessel efficiency versus b/a for vessels with unequal thickness layers is shown in Figure 4-9 and Table 4-4. For all vessels (2,3 and 4-layers), the peak efficiency occurred near b/a=1.25, as was the case for the vessels with equal thickness layers. The efficiency of the unequal thickness layers (Table 4-4) were all higher than those of the equal thickness layers, as could be expected. The same trend of increasing efficiency with increasing number of optimized layers was again noticed for this case, albeit the improvement was slight.

For design purposes, should very high FPF pressure be desired, a multi-layer, unequal thickness vessel would be the appropriate choice. If high efficiency were desired, the same configuration would again be chosen. For this case, there would be only a slight improvement in efficiency, as compared to a vessel with equal thickness layers.

4.4 Sensitivity of Optimum Design

For the cases where only two variables, such as two wind angles for a two-layered, equal thickness vessel are being selected, it is possible to represent the hypersurface graphically. This has been done for the five selected failure theories, shown in Figures 4-10 to 4-14, which represent the maximum failure criteria, $\Phi(X)$, plotted for the above case. These figures are very useful for studying the sensitivity of the solution near the optimal point. The lowest point on the graph was the optimal point (i.e., when the function value was equal to unity; all other points were greater

than unity, indicating that at least one layer in the laminate had failed).

The sensitivity to changes in wind angle near the optimum was relatively low, from the two fairly flat plateaus of the surfaces that spread out from these optimal points. The results for the interactive failure theories (Tsai-Hill, Hoffman, Tsai-Wu), are quite similar; however, they all have relatively smoother contours near the optimum point than the limit theories (max. stress and strain). This insensitivity to small changes in wind angle (for these particular examples) could be important from a design perspective, since it allows the designer to be more flexible in selecting the wind angles for the manufactured vessel.

To quantify the extent of the sensitivity of the optimal set of parameters for cases where there are three or more variables, a graphical approach was no longer possible. For the case of a four layer vessel with unequal thickness layers, the sensitivity calculations were performed for a selected set of design variables where α_i=(50/47/55/87), t_i=(3.6mm,3.3mm,2.0mm,2.2mm) and b/a=1.35. This was, in fact, the optimized vessel that was fabricated (Chapter 5).

The effect of small changes in wind angle were first considered. Figure 4-15 shows the maximum Tsai-Wu criteria, $\Phi(X)$, versus small variations in wind angle about the optimal design angles (50/47/55/87) for each of the four wind angles. The relative increase in $\Phi(X)$ due to a small increase in wind angle was seen to be more acute for the inner layers (near the internal surface of the vessel wall). At positions further from the inner wall, the effect became less significant.

Variations in thickness were also investigated. Figure 4-16 shows the results for the maximum Tsai-Wu criterion, $\Phi(X)$ versus small variations in thickness (in steps of 0.1 mm) about the optimum design thicknesses (3.3mm,3.6mm,2.0mm,2.2mm) for each pair of thickness values. These results are interesting in that it was expected that the general effect of variations of design parameters at points close to the inner surface would have a greater effect than at points further away, mostly due to the overall higher state of stress at these inner layers in the laminate.

It should be noted that these results are for a specific case, i.e. the fabricated vessel in Chapter 5 and are intended to only give indications of parameter sensitivity.

Table 4-1 Optimal Wind Angles and FPF Pressures for Multi-Layer, Equal Thickness Vessels, Using Tsai-Wu Theory

b/a	Number of Layers	Optimum Wind Angles (inside to outside)	FPF Pressure (MPa)
1.15	1	54	85.0
	2	48/61	90.0
	3	48/48/68	95.0
	4	45/48/52/76	100.0
1.35	1	55	235.0
	2	51/60	240.0
	3	49/51/70	255.0
	4	47/56/40/77	260.0
1.55	1	57	320.0
	2	50/60	325.0
	3	39/59/77	370.0
	4	51/60/44/81	375.0
1.75	1	58	340.0
	2	26/90	400.0
	3	31/66/85	420.0
	4	31/75/72/74	440.0
2.00	1	60	350.0
	2	5/86	400.0
	3	28/85/86	445.0
	4	30/66/84/87	450.0
2.50	1	63	350.0
	2	70/56	355.0
	3	22/89/90	445.0
	4	28/86/85/88	455.0

Table 4-2 Vessel Efficiency Versus b/a for Multi-Layer, Equal Thickness Vessels, Using Tsai-Wu Theory

b/a	1 Layer (x 1000m)	2 Layers (x 1000m)	3 Layers (x 1000 m)	4 Layers (x 1000 m)
1.15	18.79	19.89	21.00	22.10
1.35	20.37	20.80	22.10	22.53
1.55	16.26	17.28	18.81	19.06
1.75	11.75	11.92	14.52	15.21
2.00	8.32	9.51	10.57	10.69
2.50	4.75	4.75	6.04	6.17

Table 4-3 Optimal Wind Angles and FPF Pressures for Equal Thickness Vessels, Using Tsai-Wu Theory

b/a	No. of Layers	Optimum Wind Angles (inside to outside)	FPF Pressure (MPa)	Layer Thickness (mm) (inside to outside)
1.15	2 3 4	50/70 48/49/73 48/47/55/85	97.0 98.0 102.0	3.5/1.3 2.2/1.2/1.4 1.4/1.5/0.87/0.96
1.35	2 3 4	51/71 50/49/73 50/47/55/87	260.0 262.0 265.0	8.1/3.0 4.6/3.3/3.2 3.3/3.6/2.0/2.2
1.55	2 3 4	35/64 31/44/78 32/36/69/73	360.0 380.0 382.0	4.9/12.5 3.9/5.8/7.6 1.5/6.1/5.4/4.4
1.75	2 3 4	30/79 25/40/88 27/41/74/79	420.0 450.0 450.0	6.2/17.6 5.8/6.1/11.9 5.5/4.2/6.4/7.7
2.00	2 3 4	30/79 17/63/90 27/39/78/89	450.0 455.0 475.0	9.2/22.4 14.7/1.1/15.8 5.3/5.4/20.4/0.65
2.50	2 3 4	29/83 30/81/57 21/41/84/64	455.0 460.0 500.0	10.2/37.3 9.6/38.1/0.0 9.9/6.3/31.4/0.0

Table 4-4 Vessel Efficiency for Multi-Layer, Equal Thickness Vessels, Using Tsai-Wu Theory

b/a	2 Layer (x 1000m)	3 Layers (x 1000m)	4 Layers (x 1000m)
1.15	21.44	21.66	22.55
1.35	22.53	22.71	22.97
1.55	18.30	19.31	19.42
1.75	14.52	15.55	15.55
2.00	10.69	10.81	11.29
2.50	6.18	6.25	6.79

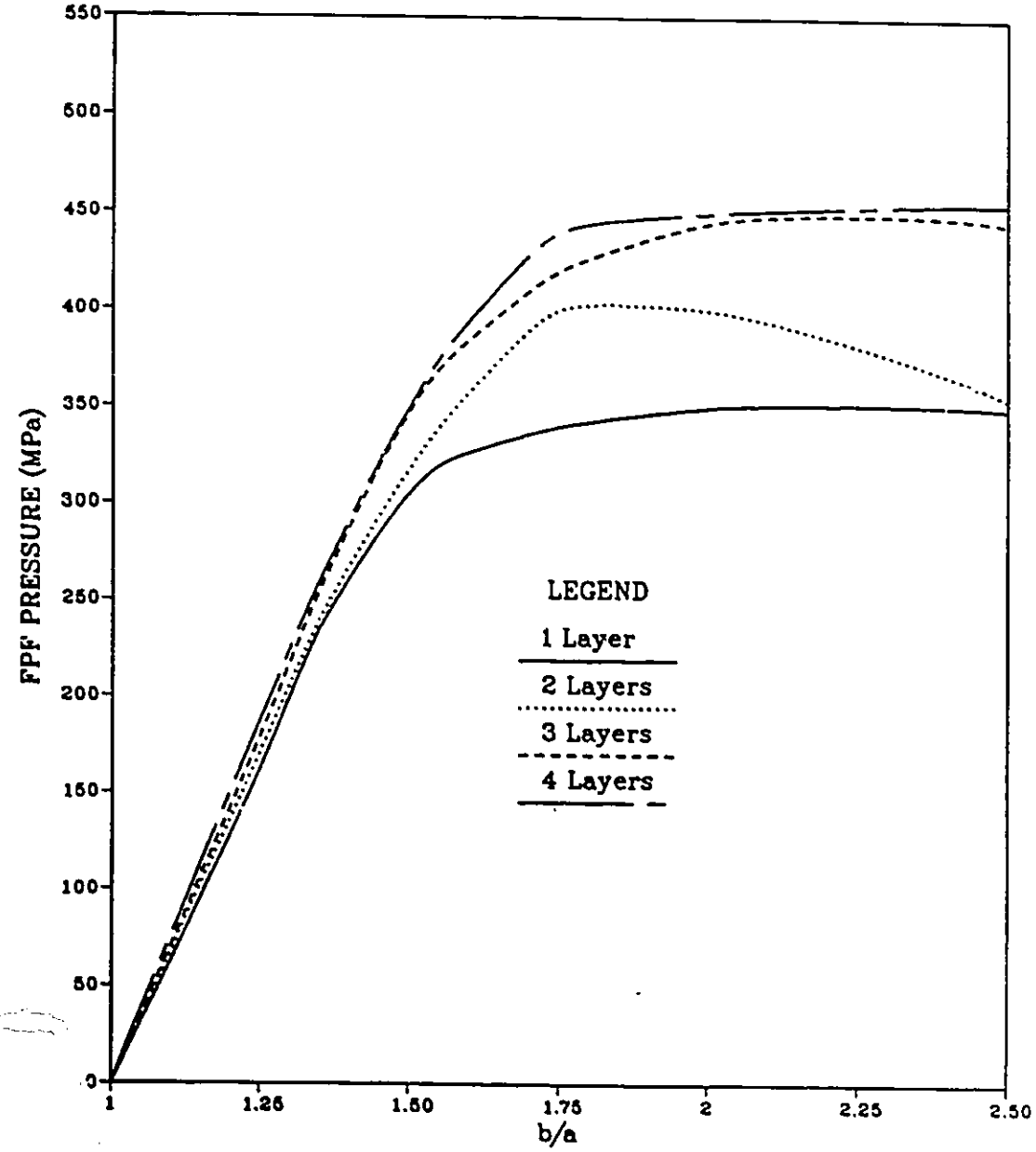

Figure 4-1 FPF Pressure Versus b/a for Multi-Layer, Equal Thickness Vessels, Using Tsai-Wu Theory

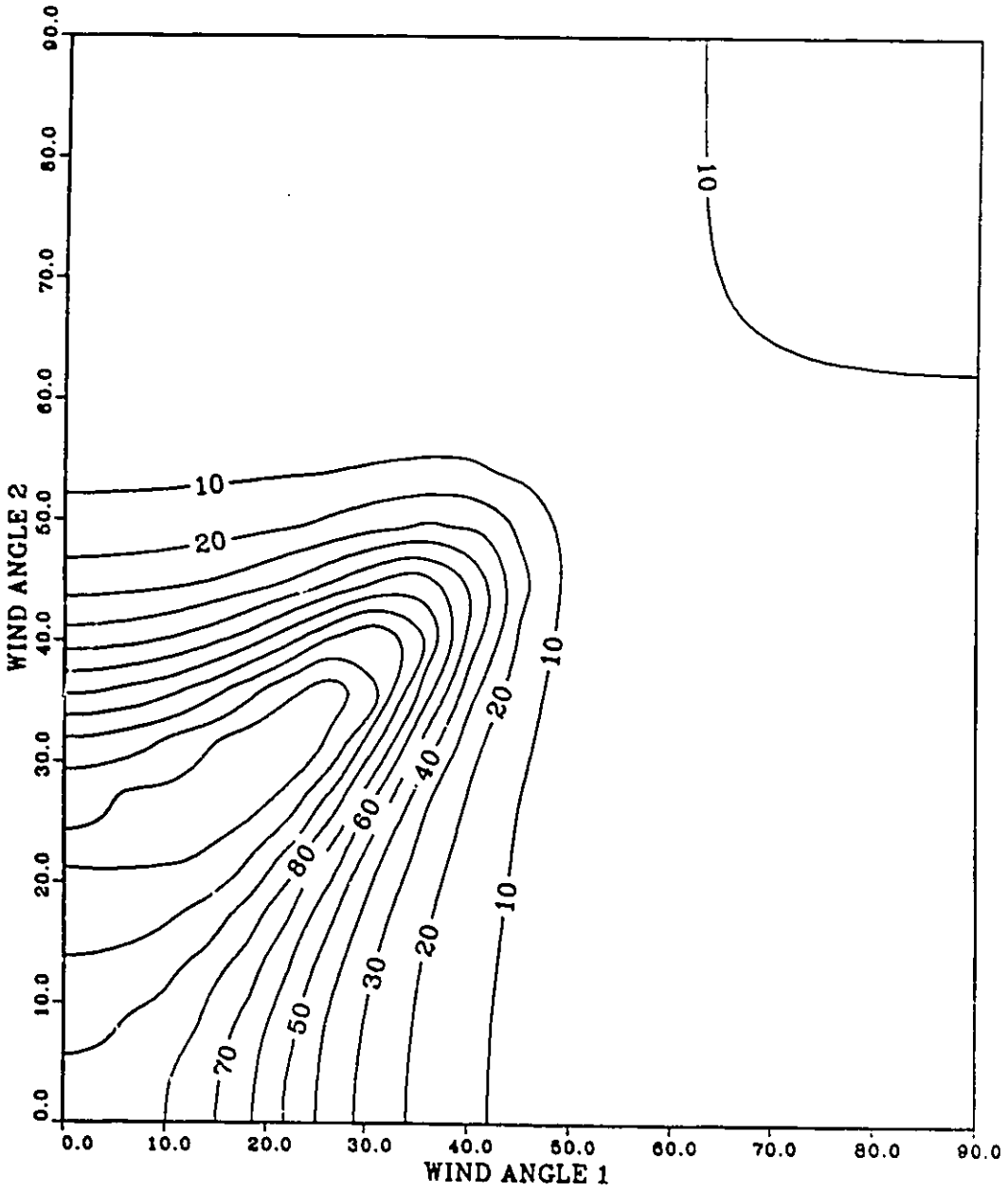

Figure 4-2 Surface Contour of Objective Function, $\Phi(X)$, for a 2 Layer, Equal Thickness Vessel, Using Tsai-Wu Theory (b/a=1.25, p=165 MPa)

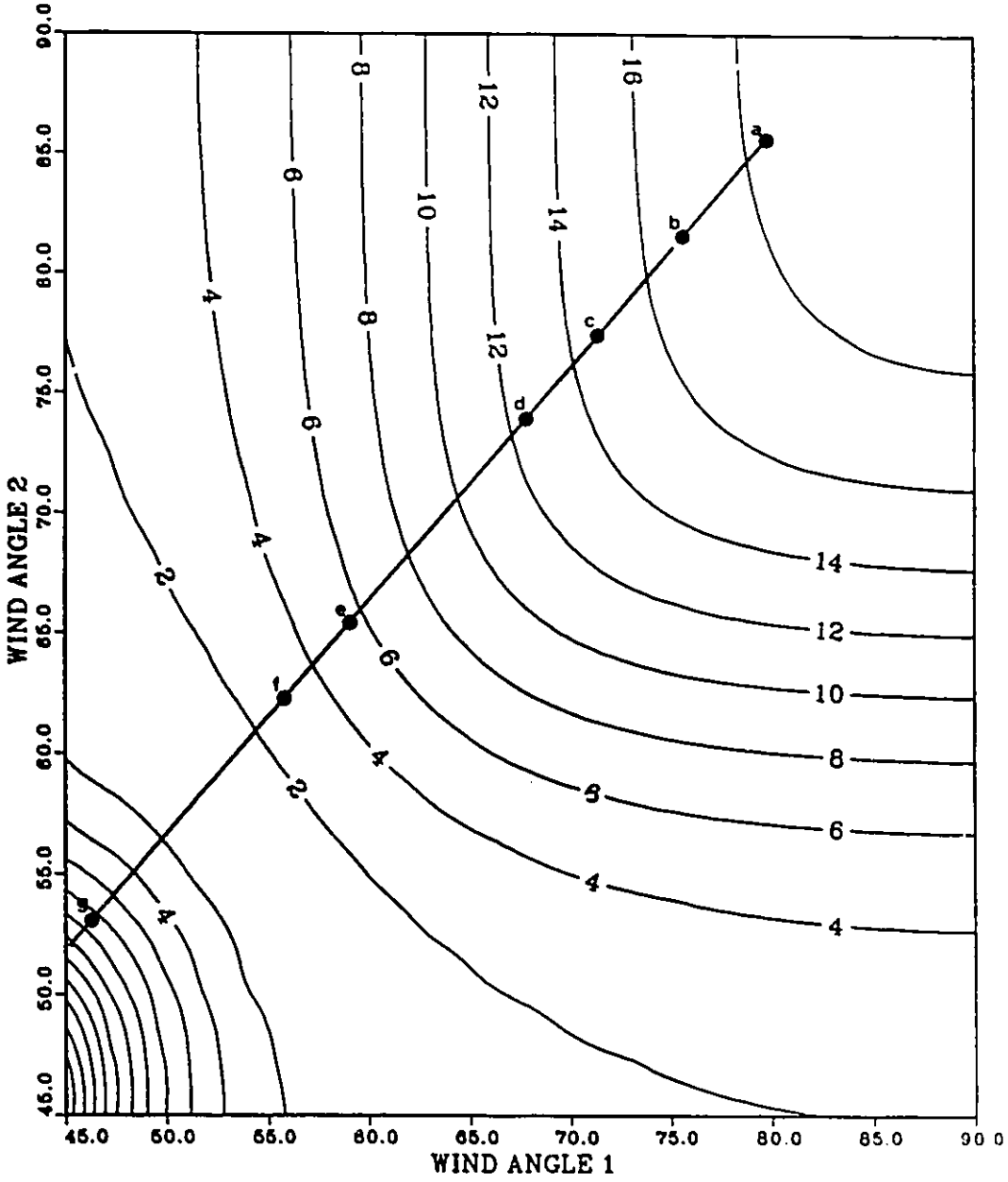

Figure 4-3 Magnified Surface Contour of 2 Layer, Equal Thickness Vessel, Using Tsai-Wu Theory (b/a=1.25, p=165 MPa)

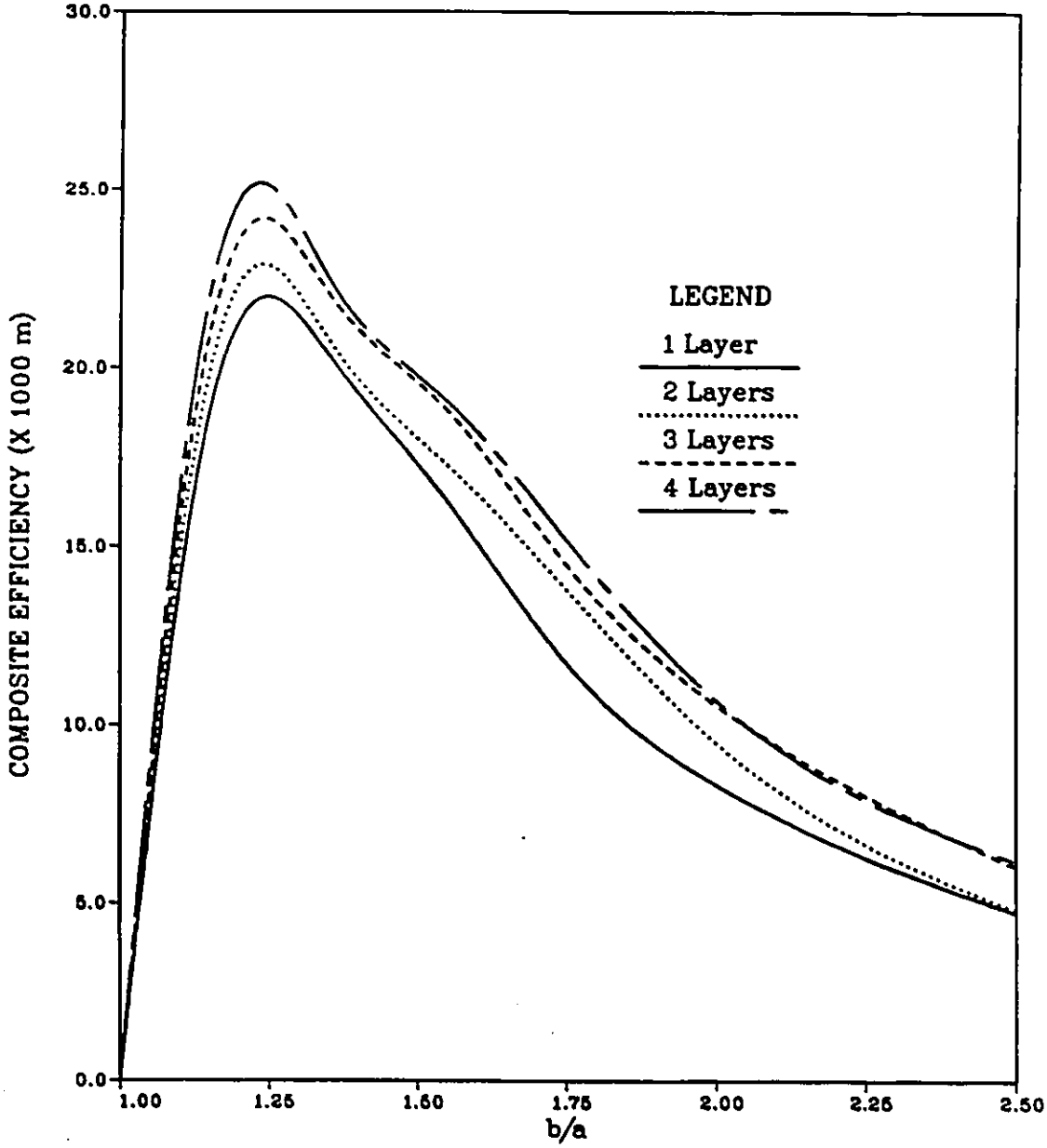

Figure 4-4 Vessel Efficiency Versus b/a for Multi-Layer, Equal Thickness Vessels, Using Tsai-Wu Theory

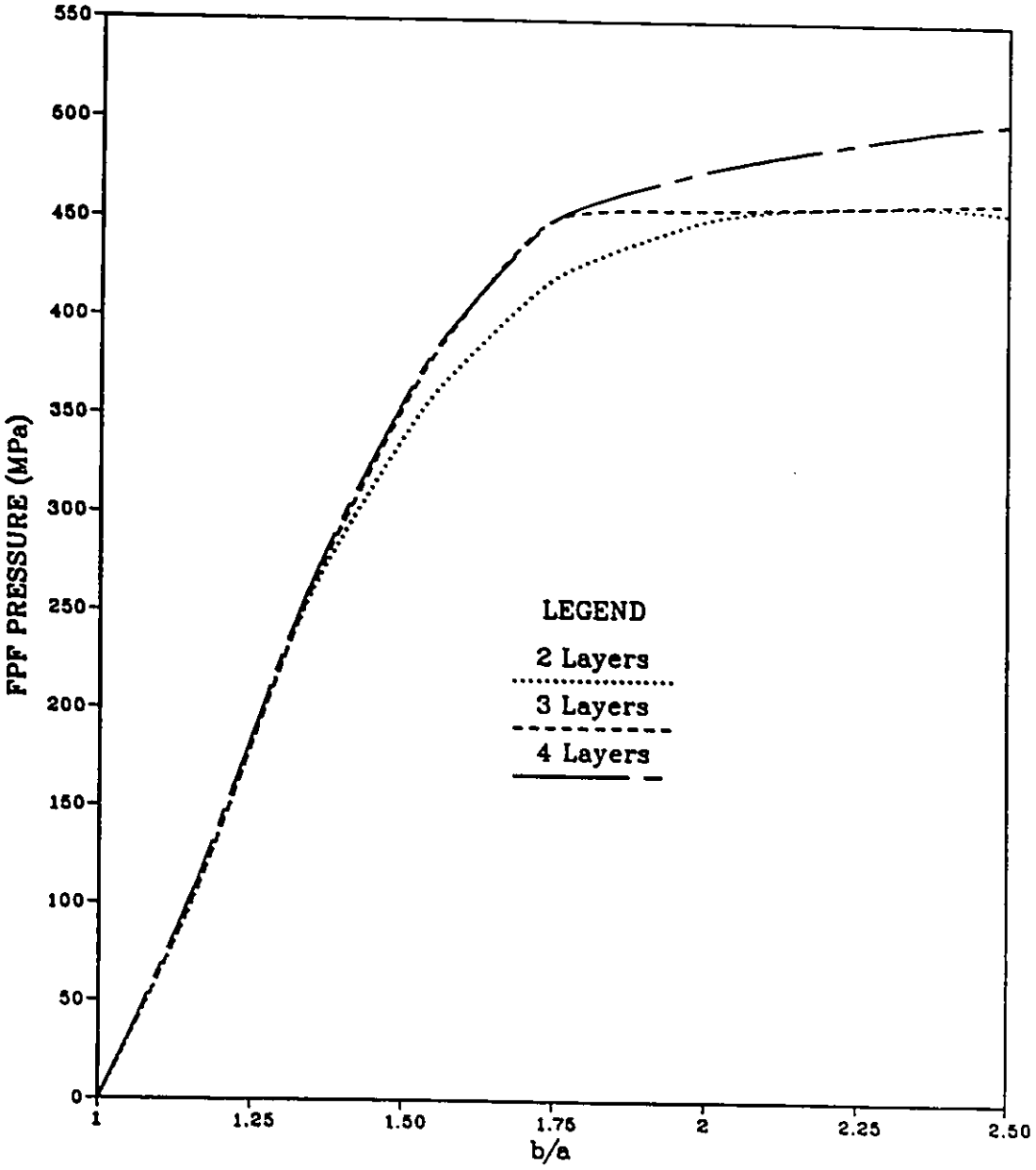

Figure 4-5 FPF Pressure Versus b/a for Multi-Layer, Unequal Thickness Vessels, Using Tsai-Wu Theory

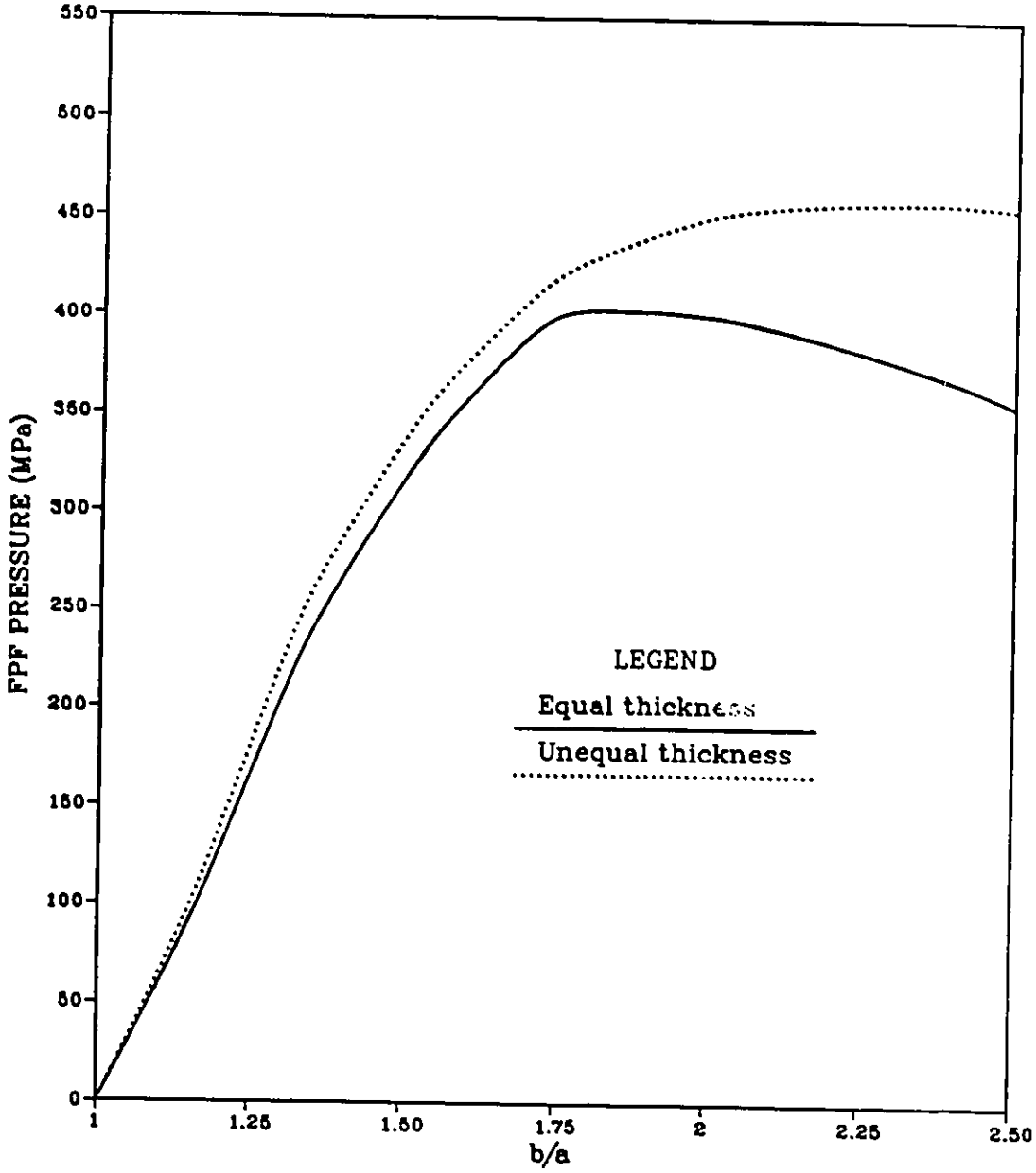

Figure 4-6 FPF Pressure Versus b/a for 2 Layer Vessels, Using Tsai-Wu Theory

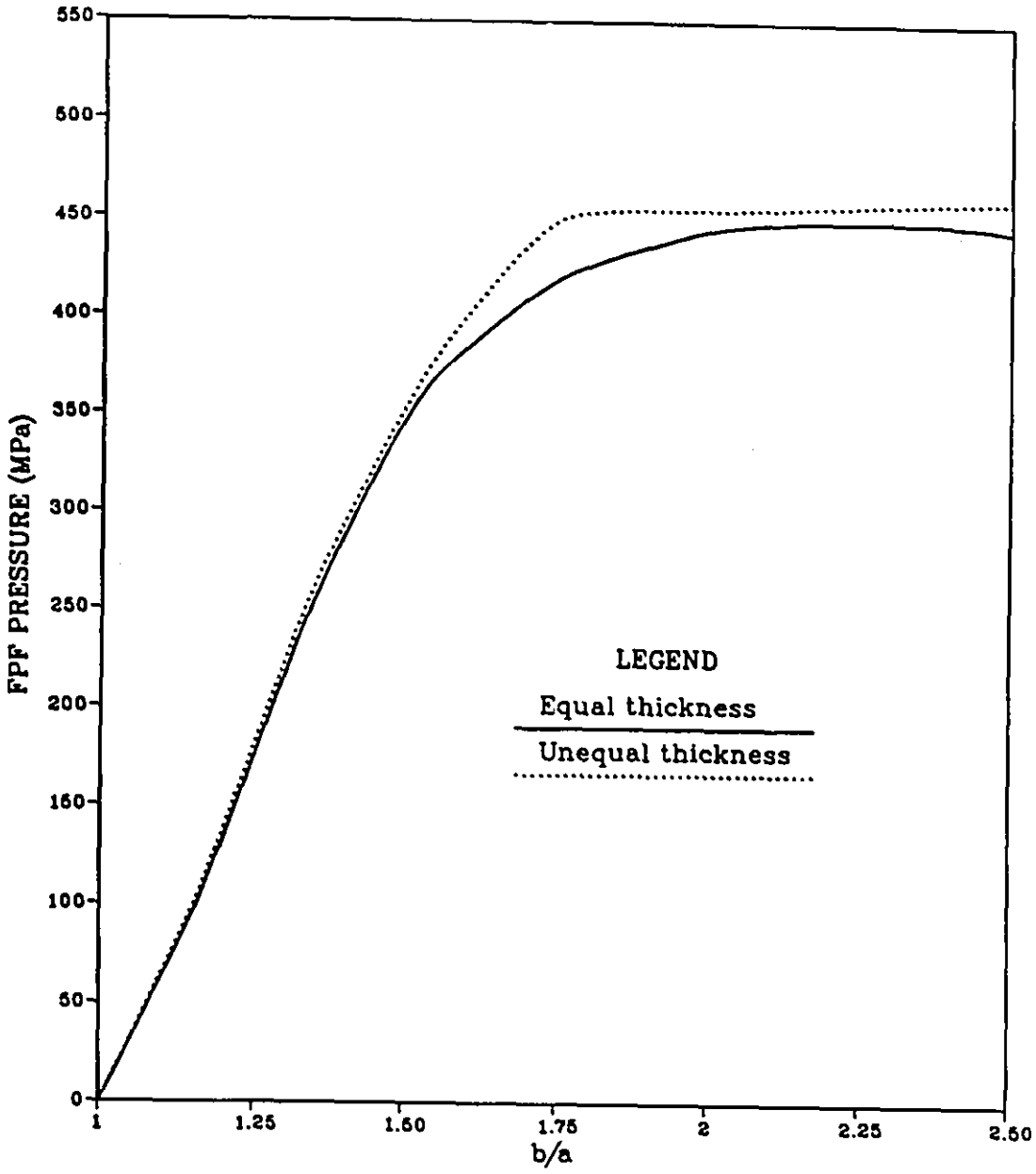

Figure 4-7 FPF Pressure Versus b/a for 3 Layer Vessels, Using Tsai-Wu Theory

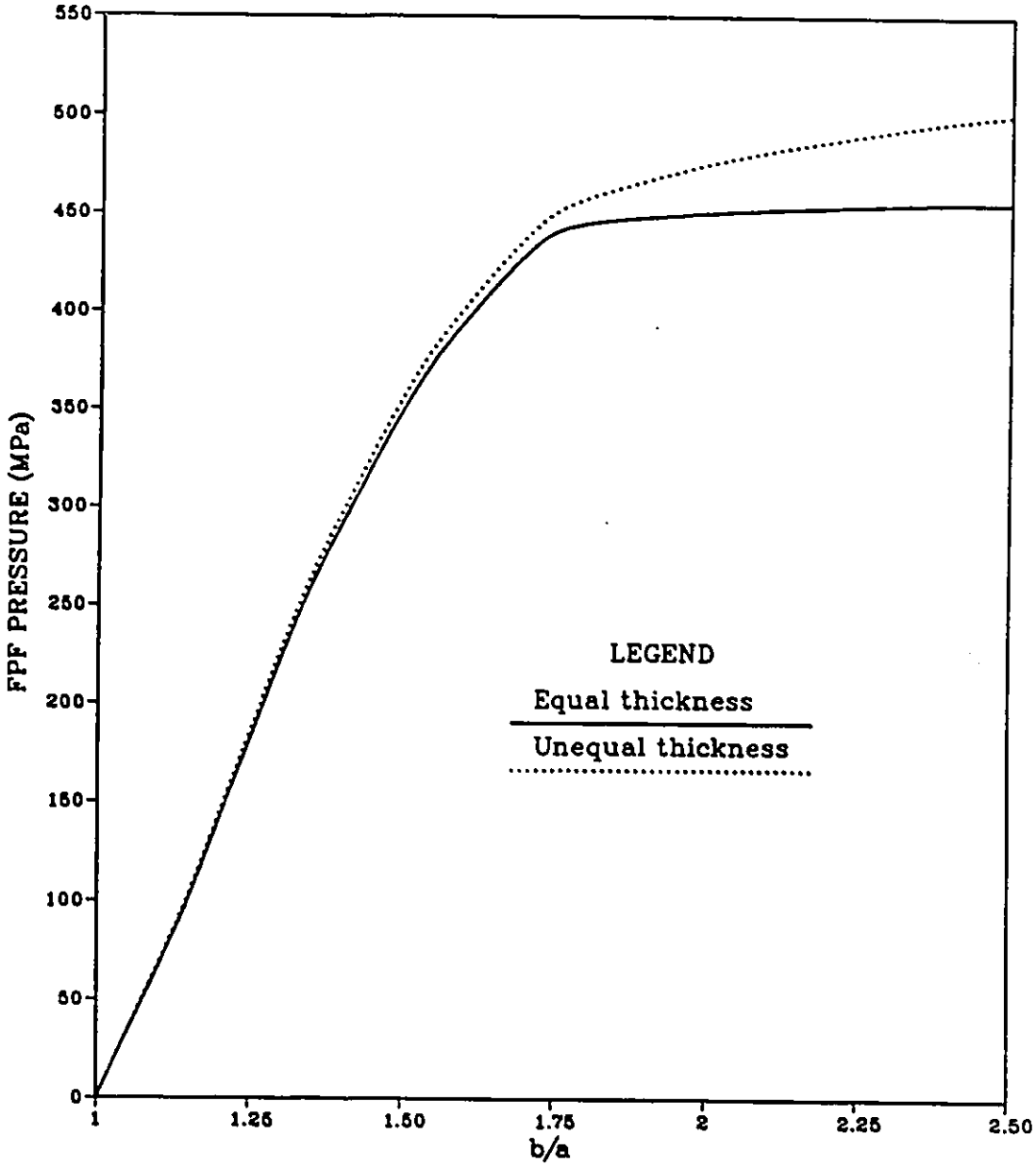

Figure 4-8 FPF Pressure Versus b/a for 4 Layer Vessels, Using Tsai-Wu Theory

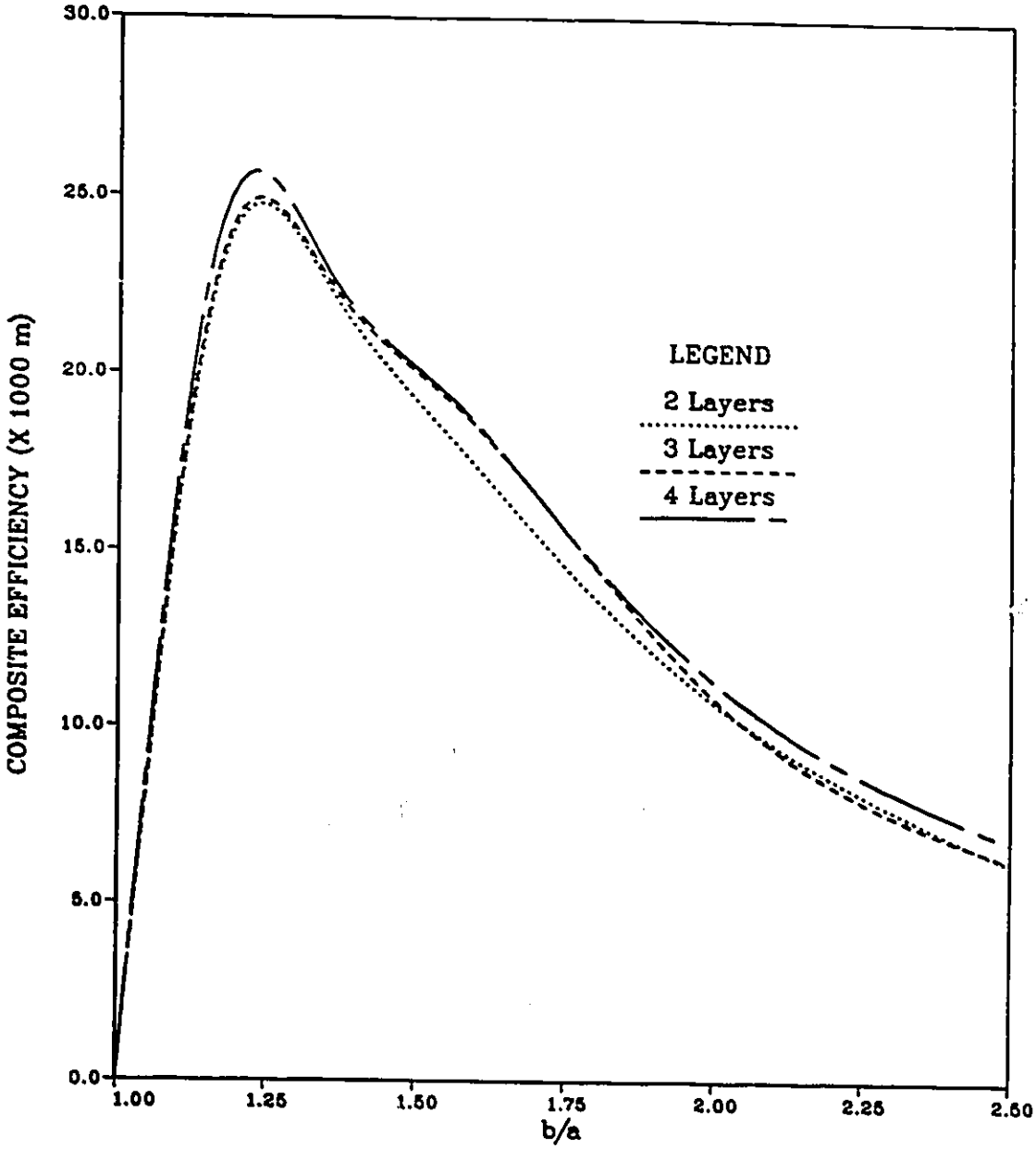

Figure 4-9 Vessel Efficiency for Multi-Layer, Equal Thickness Vessels, Using Tsai-Wu Theory

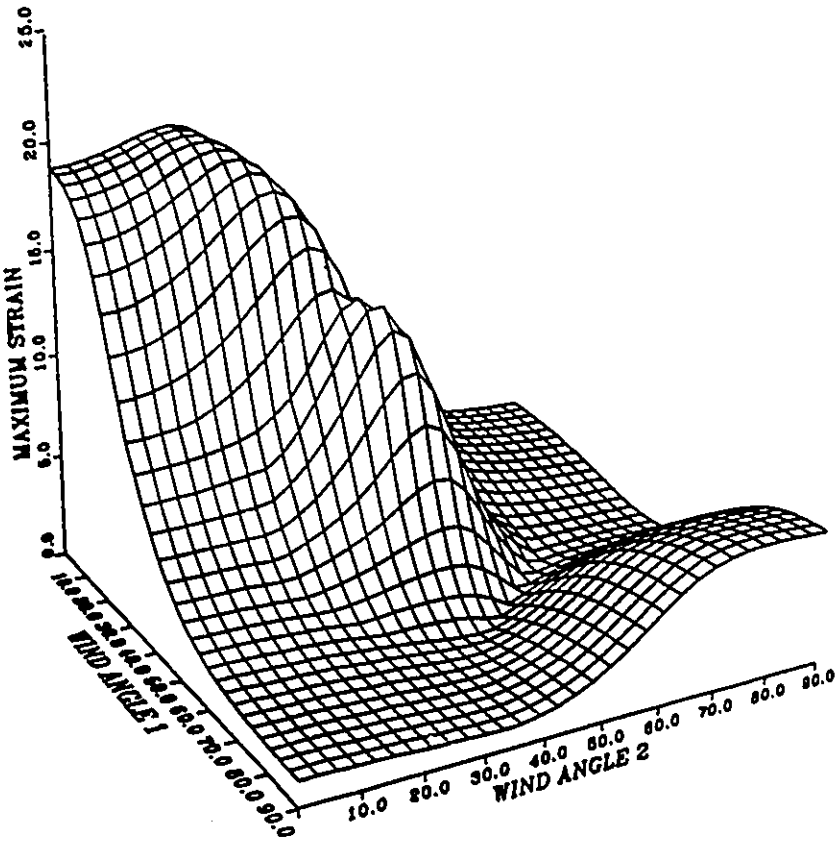

Figure 4-10 Maximum Function Value, $\Phi(X)$, for a 2 Layer, Equal Thickness Vessel, Using Maximum Strain Theory (b/a=1.35, p=190 MPa)

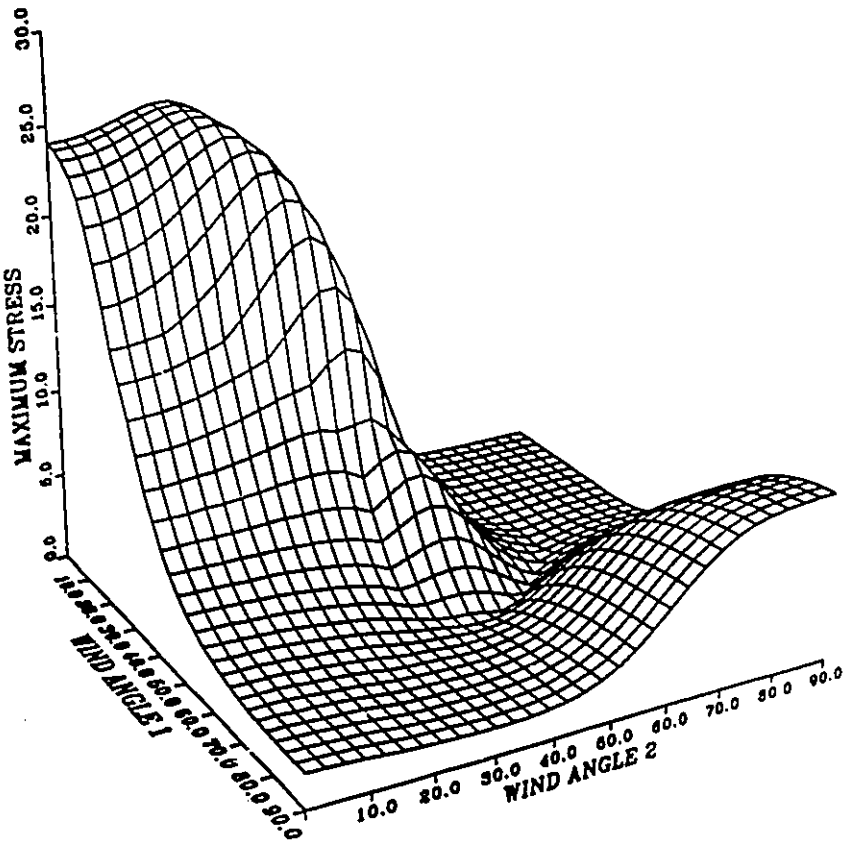

Figure 4-11 Maximum Function Value, $\Phi(X)$, for a 2 Layer, Equal Thickness Vessel, Using Maximum Stress Theory (b/a=1.35, p=270 MPa)

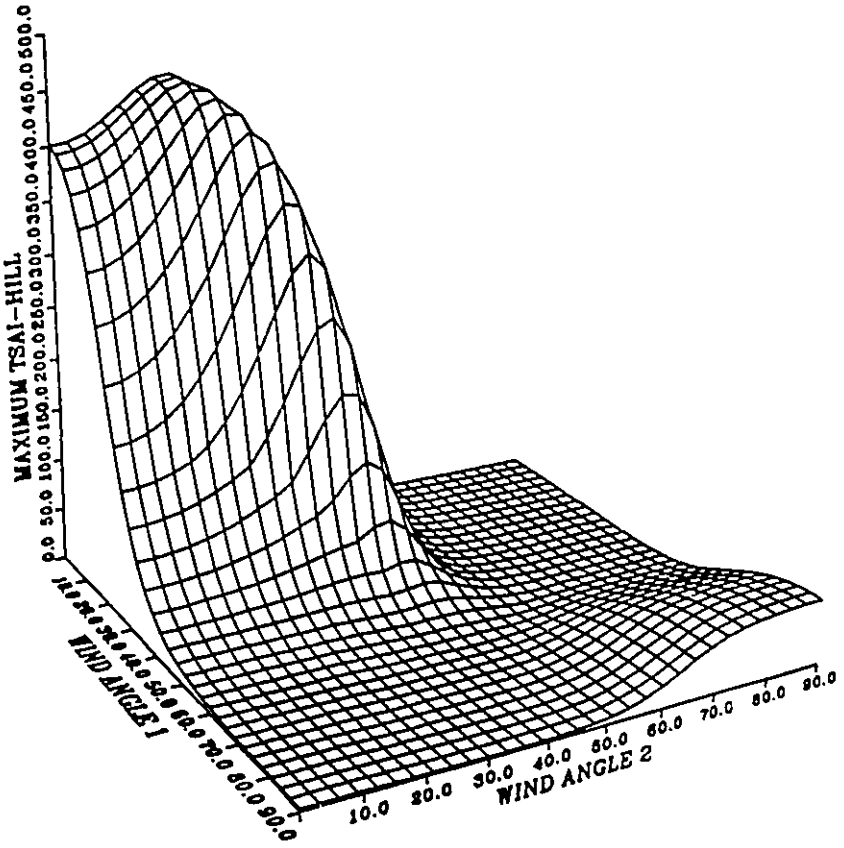

Figure 4-12 Maximum Function Value, $\Phi(X)$, for a 2 Layer, Equal Thickness Vessel, Using Tsai-Hill Theory (b/a=1.35, p=235 MPa)

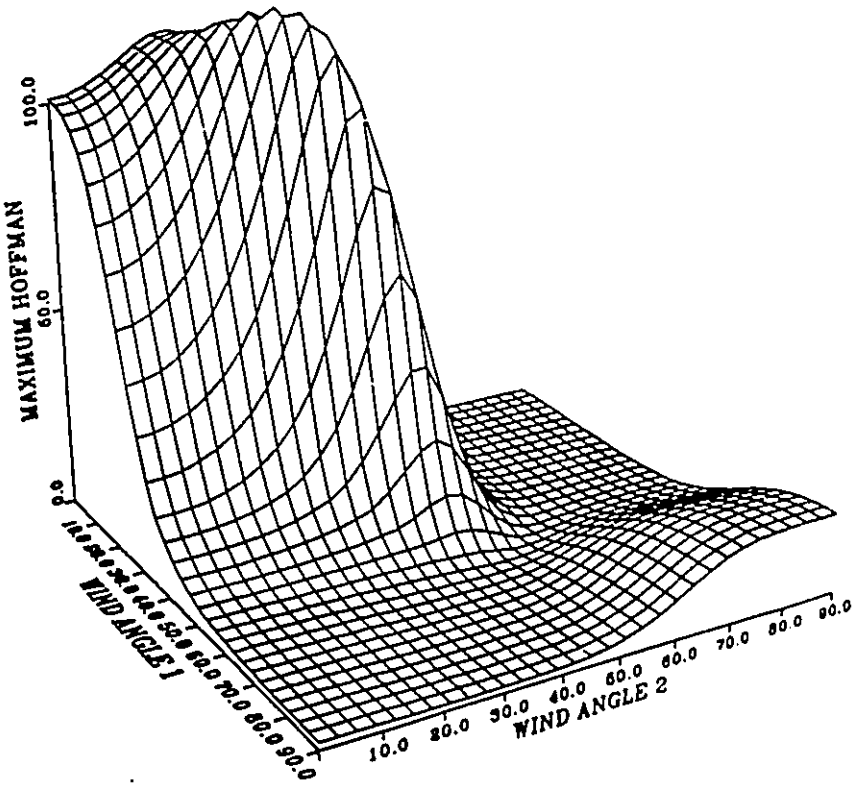

Figure 4-13 Maximum Function Value, $\Phi(X)$, for a 2 Layer, Equal Thickness Vessel, Using Hoffman Theory (b/a=1.35, p=235 MPa)

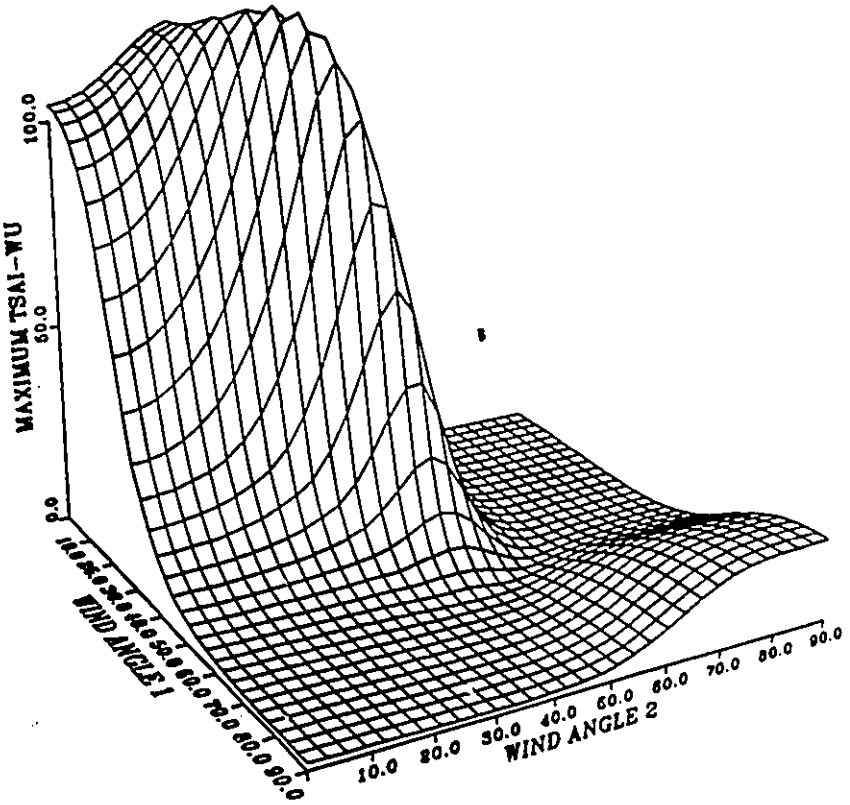

Figure 4-14 Maximum Function Value, Φ(X), for a 2 Layer, Equal Thickness Vessel, Using Hoffman Theory (b/a=1.35, p=235 MPa)

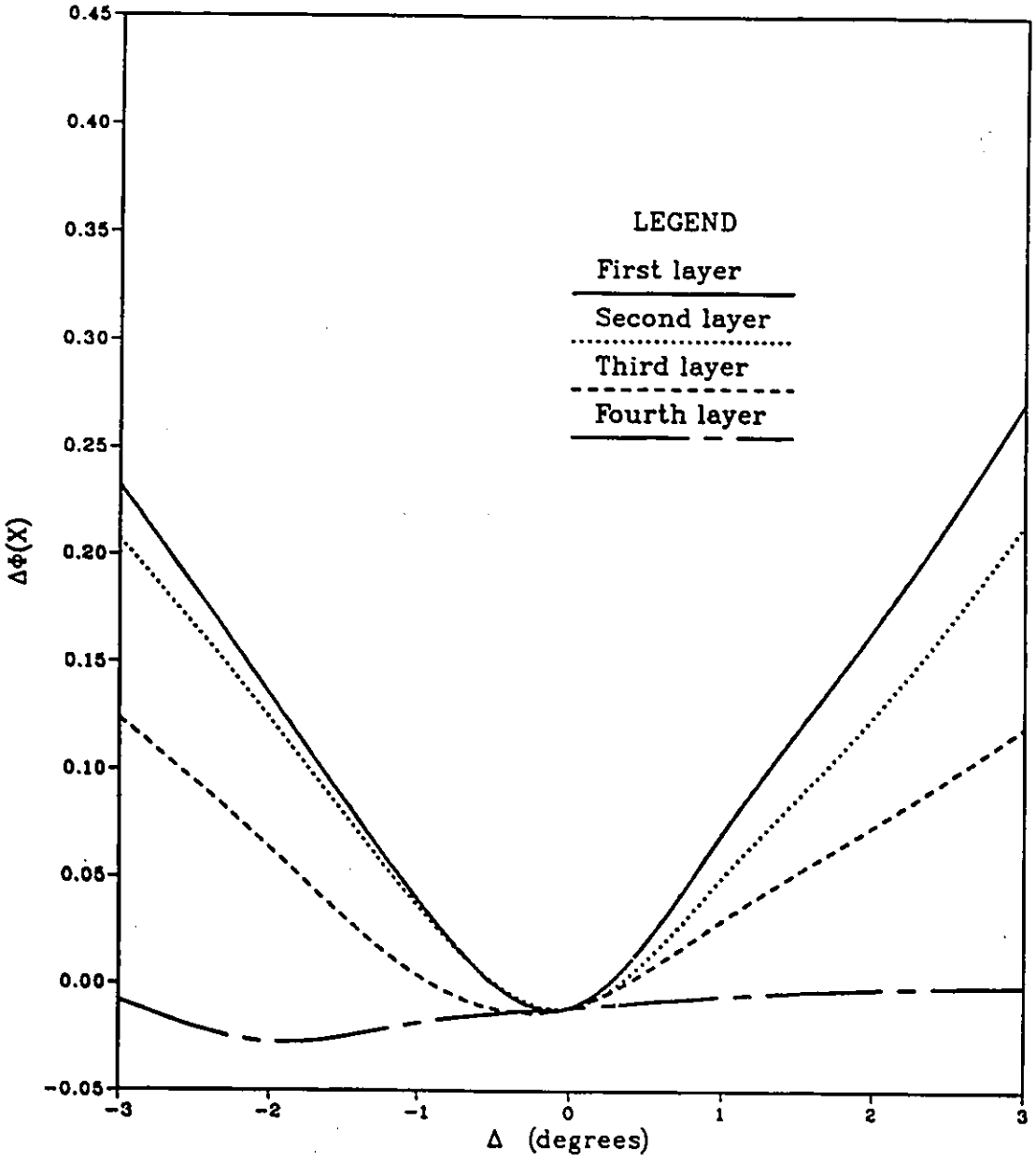

Figure 4-15 Maximum Tsai-Wu Function ($\Phi(X)$) Versus Small Variations in Wind Angle for a 4 Layer, Unequal Thickness Vessel α_i= (50/47/55/87), t_i=(3.3mm,3.6mm,2.0mm,2.2mm) b/a=1.35, p=265 MPa

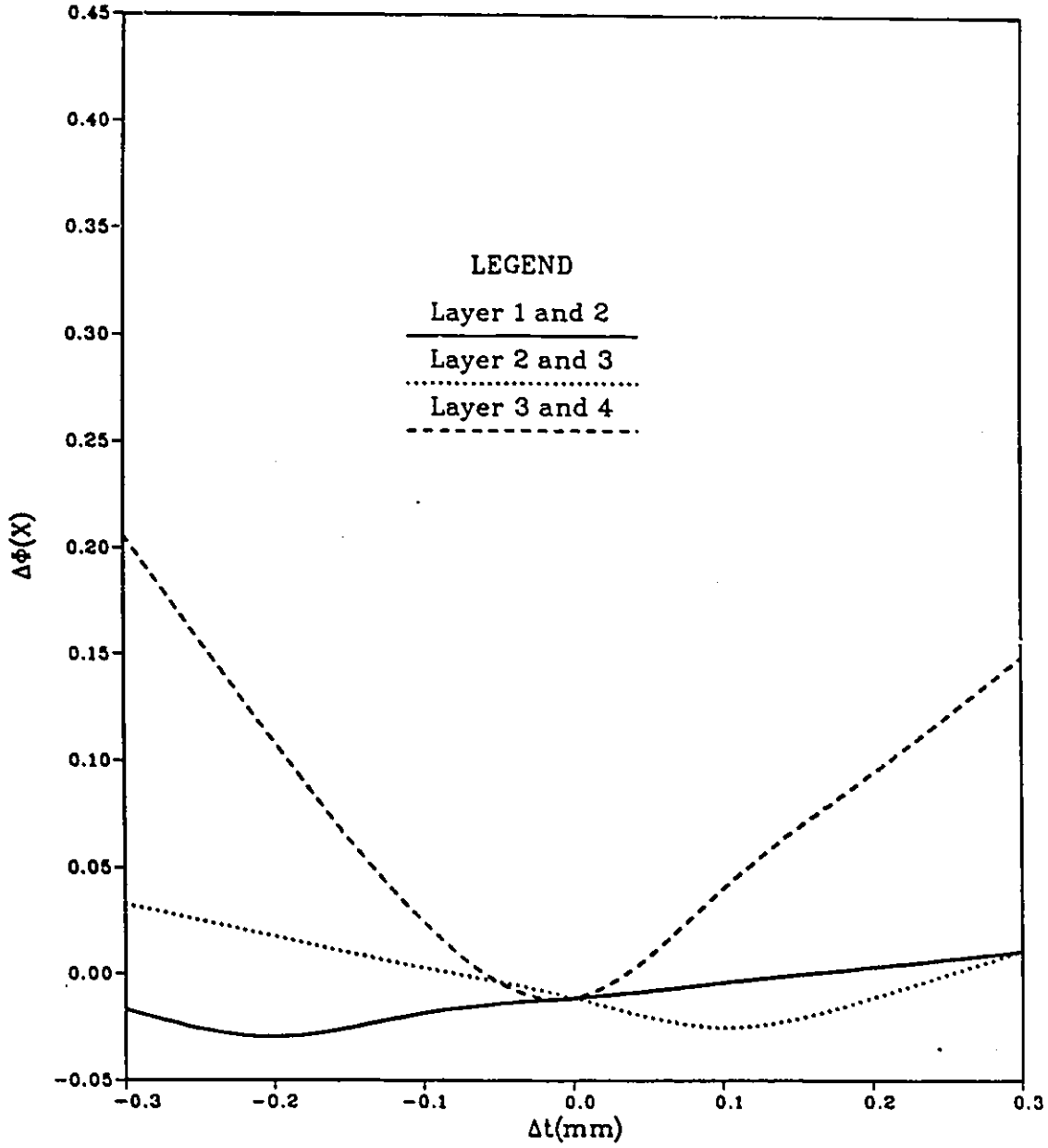

Figure 4-16 Maximum Tsai-Wu Function ($\Phi(X)$) Versus Small Variations in Thickness for a 4 Layer, Unequal Thickness Vessel α_i= (50/47/55/87), t_i=(3.3mm,3.6mm,2.0mm,2.2mm) b/a=1.35, p=265 MPa

Chapter 5

VESSEL MANUFACTURING AND TESTING

5.1 General Goals

The general goals for this study were the modelling, optimization, fabrication and testing of a fibre composite pressure vessel. The emphasis was on modelling and optimization, as the fabrication and in particular, testing and development aspects are extremely involved and time-consuming.

As time constraints were a mitigating factor in this undertaking, it was not possible to produce a complete set of test vessels to conclusively determine the extent of the optimized winding parameters on the vessel performance. A proof-of-concept approach for vessel testing was chosen, in light of these considerations. The method of design and manufacture of a filament wound test pressure vessel is now detailed.

Due to the unavailability of suitable experimental results in the literature, it

was deemed necessary to manufacture the test vessel using the facilities at the university. At the beginning of this study, the manufacturing equipment used for filament winding was in need of upgrading and extensive maintenance and modifications, as recommended by D. Lindstrom [5], the original designer of the entire filament winding system. In addition to this, the control system software previously used was now obsolete; it was then necessary to develop and implement new control software.

5.2 Filament Winder Upgrade

5.2.1 General

The filament winding apparatus had been used extensively at the university for a number of projects, for several years and was in need of repair. All modifications to the winding machine were performed by the author, throughout the duration of this study. Extensive assistance, especially with regards to software development, was provided by a colleague, Etienne Bernard.

The original winder was a five-axis helical filament winder. Stepper motors coupled to low friction linear drives provided the linear motions of the axes. The filament winder is shown in Figure 5-1. The winder was originally controlled by two eight-bit Z-80 microprocessors. An Apple II microcomputer acted as the host computer to direct the simultaneous motions of the stepper motors

The two Z-80 microprocessors were replaced by much faster 16-bit controllers, manufactured by Compumotor Co. The Apple II microcomputer was also changed to a 32-bit microcomputer. The five Compumotor PC21 controller cards were dedicated to each of the axes of the winder. Communications between the microcomputer and the PC21 controller cards required a suitable software; an interactive, user-friendly routine, coded in C-language was developed for this purpose.

The operator is able to control axis motion by uploading a pre-arranged set of commands to the PC21 controllers, or by manually inputting the individual commands relating to distance, velocity, acceleration and direction for each of the five axes.

To determine the numerous motor parameters for the filament winding of the vessels, a FORTRAN-based routine (called "WPARAM", Appendix C) was written. The user inputs the vessel parameters and some winding parameters (fibre feed rate, mandrel drive gear, etc.) to obtain the set of necessary position, speed and acceleration motor commands to later be uploaded to the PC21 cards.

5.2.2 Maintenance

For any type of industrial machinery, periodic maintenance is of the utmost importance, if productivity and trouble-free operation is to be expected. For machines that operate for extremely long production runs, with harmful vapours and thermosetting epoxy resins, this point cannot be more emphasized.

A major overhaul of the machine was necessary. Firstly, the excess resin that had accumulated everywhere on the machine was painstakingly removed. The stepper motor for the mandrel axis was replaced with a new one and refitted to the machine. The motor for the Z-axis was installed. All belts and pulleys were adjusted and/or replaced. Finally, all worn bearings or ones exposed to the resin were replaced.

Accuracy tests were performed for each axis. Positional accuracy was within ± one thousand of an inch (± 0.025 mm) for the four lead-screw axes. The mandrel axis exhibited less accuracy, which also varied with the gear ratio selected. This was due to the noticeable backlash in the gear-reduction mechanism. A direct drive system for the mandrel axis was proposed and will be implemented in the near future, but for the time being, the original configuration was used.

5.2.3 Electrical

In order to reduce the reliability problems that were not uncommon, it was decided that the entire electrical system for the winding machine should be redone, as problems relating to the original connections were suspect.

The motor winding connections from the current switching translators, the line voltage supply to the translators, controllers and all the accessories were rewired according to specifications and re-routed through watertight cable conduit. Connections to the stepper motors were done using 14-gauge wire, due to the high-

current requirements. The wire was also braided along its length to reduced the induced field caused by high-current switching.

The instrumentation of the many accessories needed during the filament winding process (i.e. power indicators, thermocouple, heater bath etc.) were re-wired so that all needed accessories could be controlled directly from the control panel housing of the translator and controller cabinet.

5.3 Design Improvements

Certain design modifications were needed for the general improvement of the filament winding process; these were the payout eye system, the fibre tensioning device and pulley system and the resin impregnation system.

The payout eye enables the fibre to be delivered to the mandrel without breakage or twisting. The motion of the payout eye (Figure 1-7) is such that it can rotate full circle so that no fibre damage from twisting occurs. Design considerations for the new system were high overall stiffness of the structure, ease of adjustment, small end effector dimensions, ease of replacement of nylon wheel and smooth operation of the unit. The payout eye installed on the machine is shown in Figure 5-2.

Maintaining proper tension during winding and avoiding fibre breakage or fraying is of utmost importance for an accurate and repeatable winding process. The

tensioning system and its associated pulleys were modified, again to reduce fibre damage. Flat nylon rollers rotating on stainless steel shafts were used in place of the original stainless pulleys. The flat rollers worked smoothly and fibre damage was reduced.

The motivation behind modifications to the resin impregnation system was twofold. Firstly, fibre damage was occurring at the impregnation stage and secondly, the excess resin carried on the fibre was far too high. To solve both these problems, a different method of resin impregnation which incorporated a light alloy wheel rotating in the resin bath was used to deposit the resin on the fibre tow. A doctor blade was adjusted to remove the proper amount of resin on the wheel, thereby controlling the amount of resin absorbed by the fibre. This resulted in less fibre damage and less excess resin. Figure 5-3 shows the impregnation assembly.

5.3.1 Pressure Testing

The burst testing apparatus at the university consisted of a 70 MPa hydraulic cylinder mounted in an Instron test frame (Figure 5-4) and a containment facility (Figure 5-5). For the pressure testing of vessels, the existing burst testing apparatus [5] was also in need of some modifications. A new air bleeding system was developed to more effectively remove trapped air from the high-pressure lines.

The containment facility houses the specimen during pressure testing. Improved lighting was installed inside the chamber and a specimen mounting jig was constructed to more easily hold the vessel inside the apparatus.

5.3.2 Data Acquisition System

As several strain gauges were to be simultaneously monitored during the pressurization cycle, a data-acquisition system was necessary to accomplish this task. A Hewlett-Packard Data Acquisition system was used in order to take readings from up to forty individual strain gauges. An interactive computer program, where the user can select many different options (i.e., type of gauges, gauge factors, type of bridge etc.) was developed so that the system could be used by an unfamiliar user (Appendix D).

5.4 Selection of Design Parameters for Test Pressure Vessel

A single fibre composite vessel was fabricated. In order to best choose the design for the pressure vessel, certain selection criteria were considered. For a practical design, the ability to manufacture the vessel (or "manufacturability") was also an important factor that applied to the final selection of the pressure vessel.

From the cases considered in the analysis of Chapter 4, it was clear that a design using layers of unequal thickness and the maximum number of individual layers was be optimal. Consequently, a four-layered vessel with unequal thickness layers was chosen.

Referring to Figure 4-9, which shows composite efficiency versus laminate thickness, the peak efficiency for all cases was in the region of b/a=1.25, yet for maximum first ply failure pressure, a b/a ratio of 1.75 was suggested (Figure 4-1). A four-layered vessel, with b/a=1.35 was a reasonable compromise design in that it was between the two design points, had a high FPF pressure (265 MPa, Table 4-3) yet could be manufactured in a reasonable length of time.

The end of the payout eye, although designed for compactness, is quite large when compared to the diameter of the vessel, for this case. Consequently, radial pins were necessary to ensure that no fibre slippage occurs on the ends of the vessel. These radial pins also imposed limits on the maximum possible wind angle (where the wind angle is measured from the meridian of the cylindrical section), which was near 70 degrees. This limit is caused by the tendency of the pins to fray the fibres as the pins were crossed. At the other extreme, there was a limit of 10-15 degrees for low wind angles, depending on the cylinder length. This limit was caused by the fibre tension becoming too low at the point when the mandrel must reverse direction. These problems were more pronounced for smaller diameter vessels.

There are some advantages to a small diameter vessel. Vessels that have large L/d ratios (where L is the axial length and d is the inner diameter) tend to be less

influenced by so-called "end effects", where bending and other stresses tend to contribute to the state of stress at points near the centre of the vessel. The L/d for the vessel in this study was approximately 10, which was well within the range specified by Rizzo and Vicario [26]

Wind angle combinations for the 4-layer equal thickness vessel of b/a=1.35 were 47/56/40/77; for the unequal thickness vessel, they were 50/47/55/87. Since wind angles above 70 degrees were difficult to wind, the 77 degree outer layer resulted in a vessel design that was not feasible. The unequal thickness vessel had an outer layer with a wind angle of 87 degrees. Since this was essentially equivalent to a hoop wind (90 degrees) which was easily done by filament winding, this design was much more easily manufactured and consequently selected for the test vessel. A sketch of the vessel wall configuration, with metallic liner, is shown in Figure 5-6.

As first-ply-failure was assumed for this analysis, it should be described what type of behaviour was expected beyond that point, for the particular vessel being designed and tested. Jones has given an algorithm describing the calculation method (Appendix B). The typical laminate load-deformation behaviour is given in Figure 5-7

The first layer to experience failure in this case is the inside layer (Appendix E). After this has occurred, by arbitrarily setting the mechanical properties of the failed layer to zero (i.e. removing the layer, as in Jones' approach), it was noticed that all three other plies in the laminate immediately failed (Appendix F), due to the extra load that must be borne by these remaining layers.

It was also of importance to have an estimate of the magnitude of the changes in strain readings from the strain gauges, if in fact the entire vessel did not fail. In other words, was first ply failure of the inner layer a detectable event?.

The increase in strain at the outer layers due to FPF, for the ε_z, ε_θ and $\gamma_{\theta z}$ strain terms (load axes) are

$$\Delta\varepsilon_z = 6116 \times 10^{-6}, \qquad \Delta\varepsilon_\theta = 15060 \times 10^{-6}$$

$$\text{and} \qquad \Delta\gamma_{\theta z} = -4174 \times 10^{-6}$$

Which were all easily detectable values. This effectively demonstrated the optimization of the individual layers in the vessel.

5.5 Manufacturing of Pressure Vessels

The general method of manufacture of the selected multiple layer fibre composite vessel consisted of three phases:

(1) Mandrel preparation

(2) Fibre layup

(3) Curing cycle

The first phase involved the selection of a suitable mandrel. For this study, an T6061 thin-walled aluminum alloy tube was selected, with machined aluminum ends welded to the tube. The mandrel also acted as the vessel liner. Radial stainless steel pins were used at each end of the vessel, to prevent fibre slippage. A stainless steel filler pin and coupling were affixed to the end of the vessel, for burst testing. Drawings for these components are shown in Appendix G.

Once assembled, the mandrel was ready for winding. The vessel was wet wound (where the dry fibre strand was impregnated with resin as the fibre was wound onto the mandrel) at specific wind angles. In helical filament winding of closed-end pressure vessels, the ends are filament wound at the same time as the cylindrical portion. There is a specific path that the fibre strand follows over the cylinder and end domes. A single path is shown in Figure 5-8.

Following the mixture of the resin and hardener, the single fibre was passed through the series of pulleys and affixed to the shaft of the mandrel. The resin mixture (Table 5-1) was then poured into the heated resin bath, which was kept at a temperature of 50°C. Finally, the host microcomputer was connected to the winding machine and the machine was ready to receive commands for winding.

The fibre layup involved the placement of fibres along a specific path, at a single wind angle. This path was repeated and incremented, until coverage over the entire vessel was accomplished. To wind an entire layer at a single wind angle, a reversal of the rotating mandrel was required. Another layer was wound at the

opposite angle to complete the ± ply or laminae. This procedure was repeated as necessary, for a given set of ± laminae oriented at their respective wind angles to construct the laminate. The radial pins prevented the fibre strand from slipping off the path when the direction of rotation was reversed.

The ends were reinforced by hoop wraps, normal to the longitudinal axis of the mandrel to prevent premature failure from occurring there, where bending effects are most pronounced [28].

The wet composite was consolidated with wraps of perforated heat shrink tape and an absorbent cloth as detailed in Table 5-3. Upon curing, the heat shrink tape squeezed any excess resin into the cloth sandwiched between the two shrink tape layers. This technique provided a smooth surface for later application of strain gauges along the length of the specimen.

Finally, the vessel was installed on a jig which slowly rotates the vessel in the curing oven for one hour at 100°C. To prevent any potential leaks between the aluminum shell and welded ends, a low modulus, high elongation polyurethane liner was centrifugally cast inside the tube's interior. The details of the liner are in Table 5-2. The manufactured vessel with consolidation tape is shown in Figure 5-9. The completed vessel, with end fittings attached is shown in Figure 5-10.

5.6 Testing of Pressure Vessel

The manufactured vessel was burst test at the high-pressure testing facilities at the National Research Council in Ottawa. The vessel was pre-filled with water, then the air was evacuated. Strain gauges were mounted along the outside surface of the cylindrical section of the vessel, shown in Figure 5-11. Strains were monitored with a portable switch-and- balance unit.

The high-pressure couplings were installed between the pump and the vessel and the vessel was placed in a steel container, filled with water. The vessel, with attached fittings is shown in Figure 5-12. Pressurization was done in steps, to provide sufficient time to obtain strain readings.

During pressurization, audible cracks were heard at 7400, 9400, 14600 and 17000 psi. Complete failure of the vessel occurred at 20500 psi. Burst was caused by the sudden failure of the end caps, with the vessel failing catastrophically.

The recorded strains during pressurization are compared to the predicted strains in Figure 5-13. These values were tabulated for pressures up until the first audible crack was heard. Reasonable agreement between experimental and predicted values were found for the axial strains, but the hoop strains for the experimental values seem to indicate residual strains present in the hoop direction.

MATERIAL	DESCRIPTION
Resin (1)	Shell Epon 825 Epoxy
Hardener (1)	Pacific Anchor Chemicals Ancamine 1482
Fiber	Hysal Grafil E/XAS 12K

(1) Resin to hardener ratio was 100:19, (by wt.) heated to 50° C for wet winding, and cured for 1 hour at 100° C

Table 5-1 Material Details

COMPONENT	AMOUNT (GRAMS)
Component A (1)	50
Component B (1)	26

Preheat resin and hardener at 40° C for 1 hour prior to mixing. Mix components by hand for 1-2 minutes. Pour immediately into the specimen and start rotation.

Mount heat gun from the upper frame of the payout eye assembly directed at the cylinder. Keep the cylinder at a temperature that is warm to the touch (about 50° C) for about 4 hours.

(1) SF2012 from H B Fuller (Canada) Ltd.

Table 5-2 Polyurethane Liner Mixture

MATERIAL	DESCRIPTION
inner releasing shrink film	Airtech International
sandwich absorbent cloth	Airtech International
over high shrink film	Airtech International

Table 5-3 Laminate Consolidation Tape

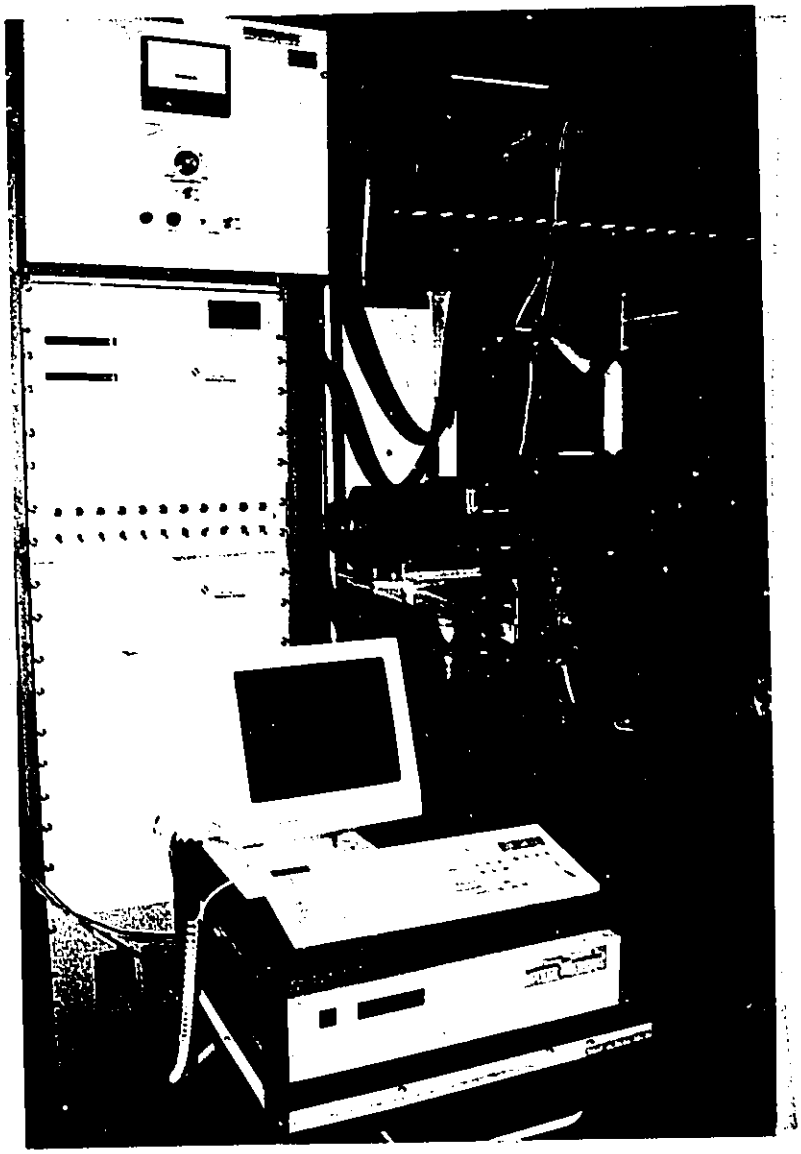

Figure 5-1 Upgraded Five-Axis Computer Controlled Filament Winder

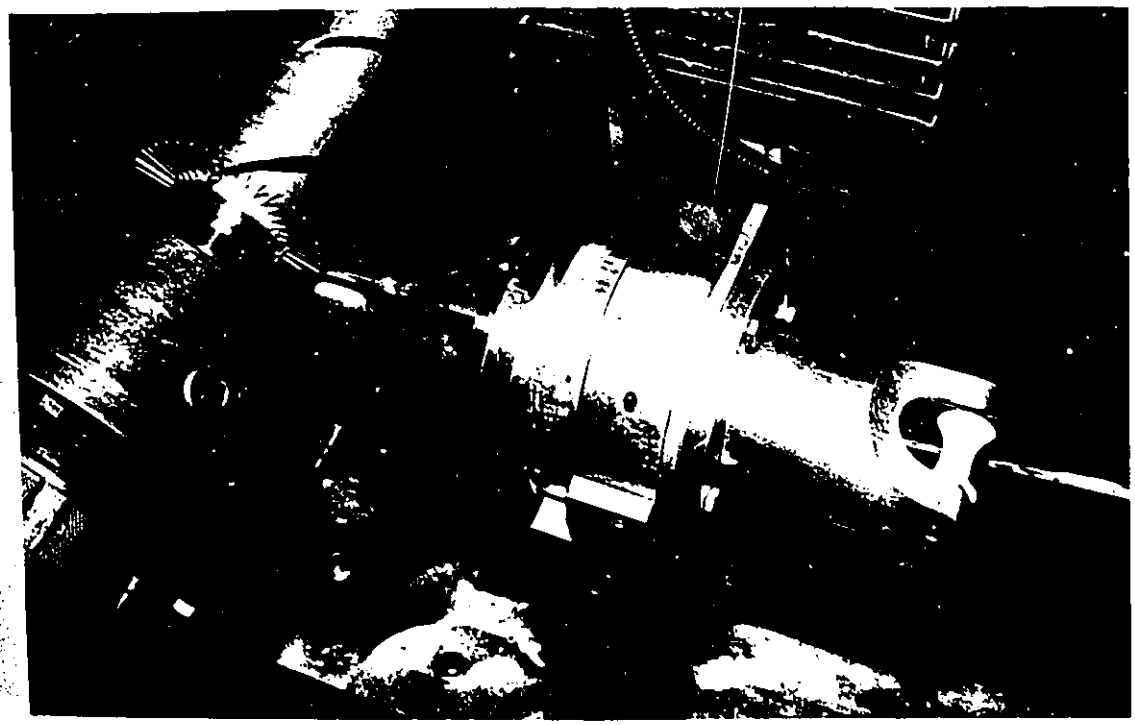

Figure 5-2 Payout Eye Assembly

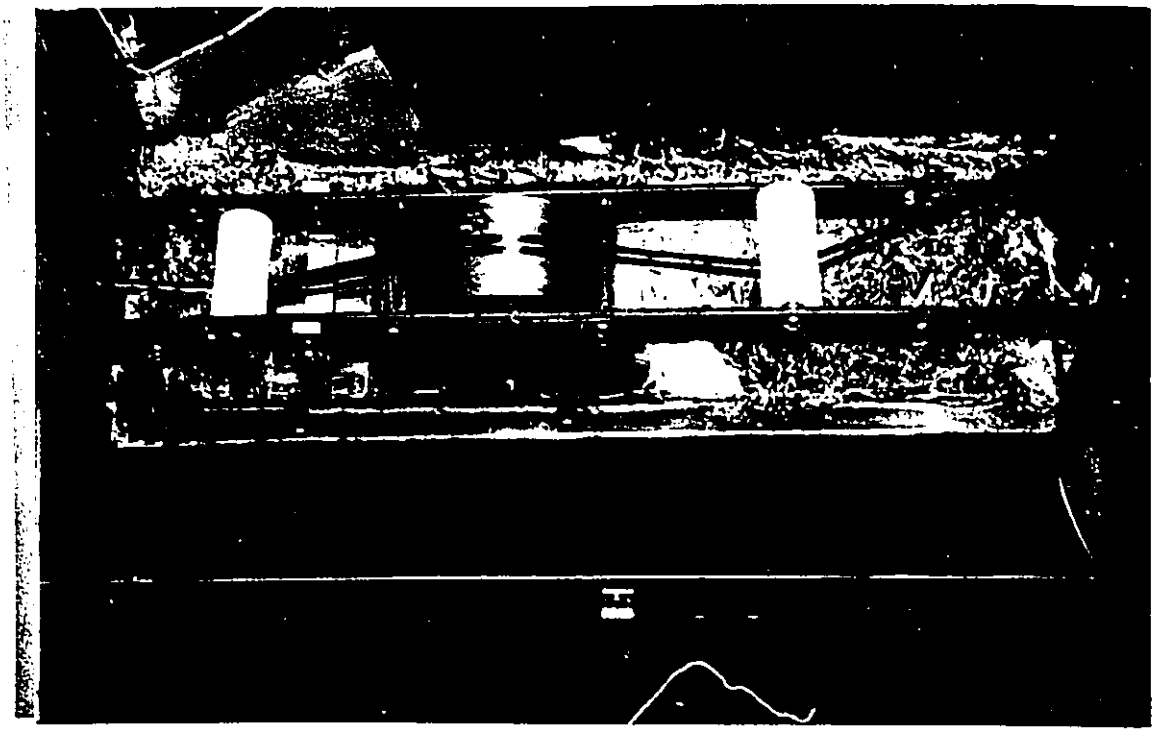

Figure 5-3 Impregnation Assembly

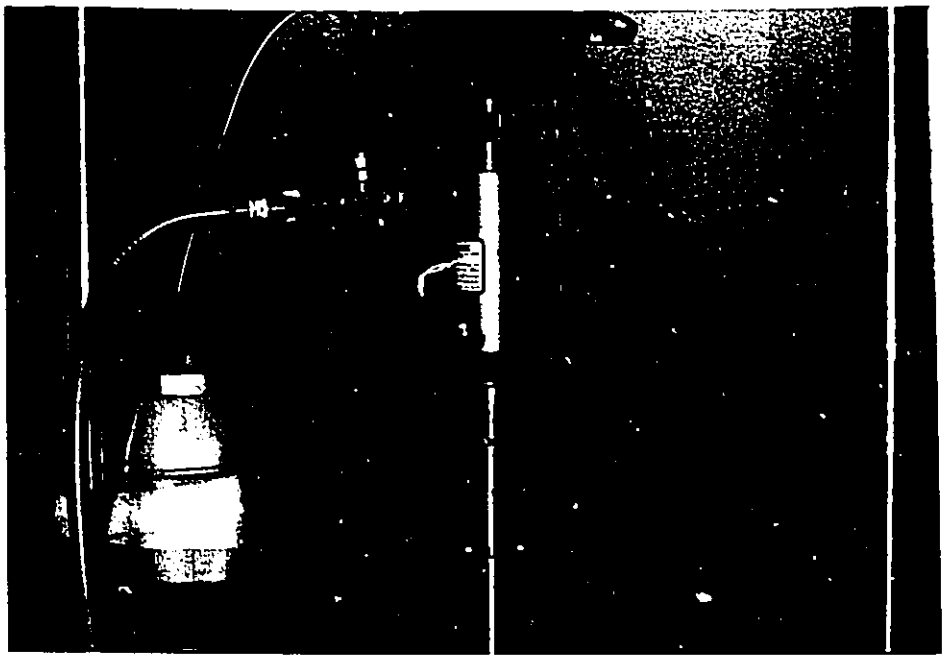

Figure 5-4 Revised Pressurization System

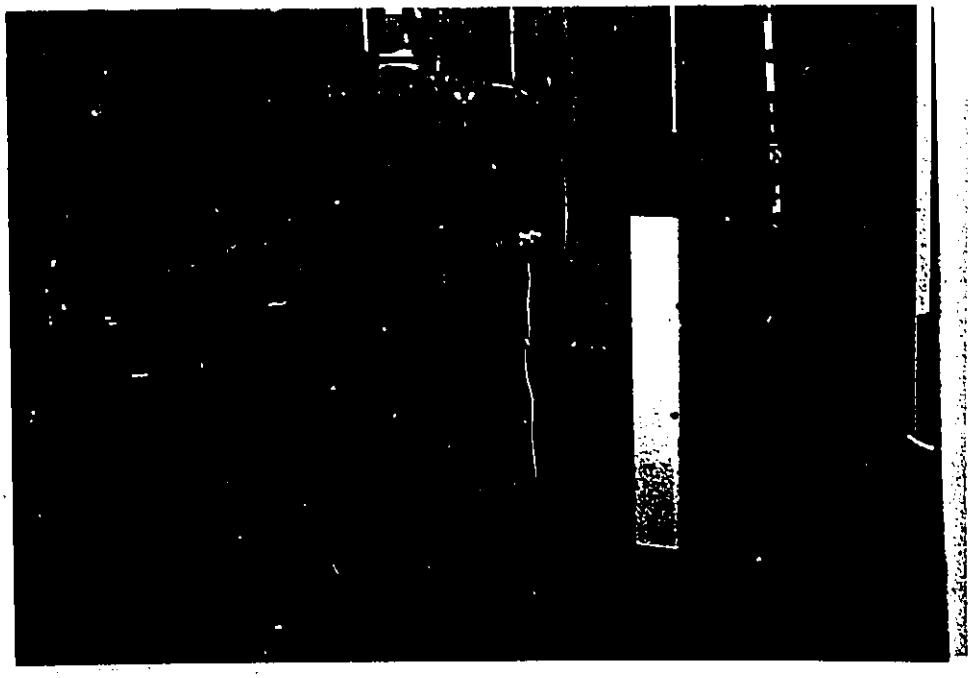

Figure 5-5 Containment Facility

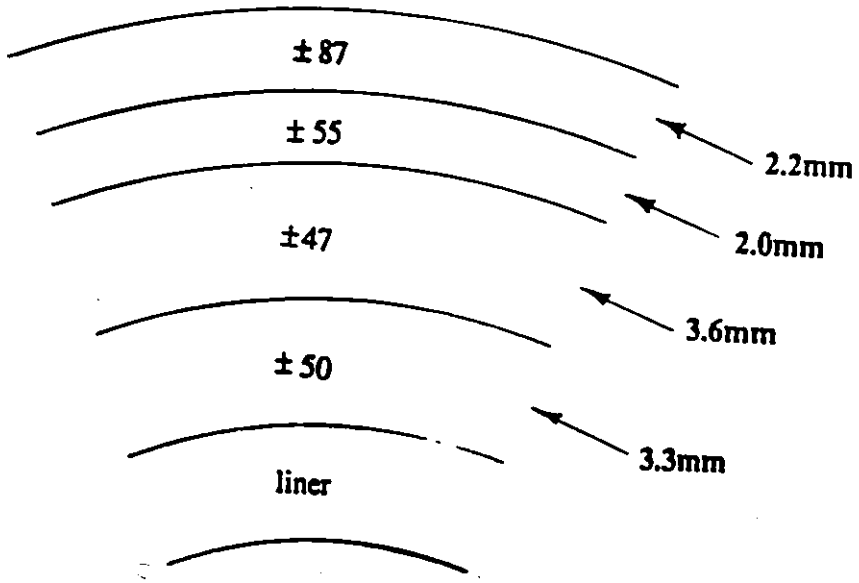

Figure 5-6 Laminate Configuration for Design Vessel

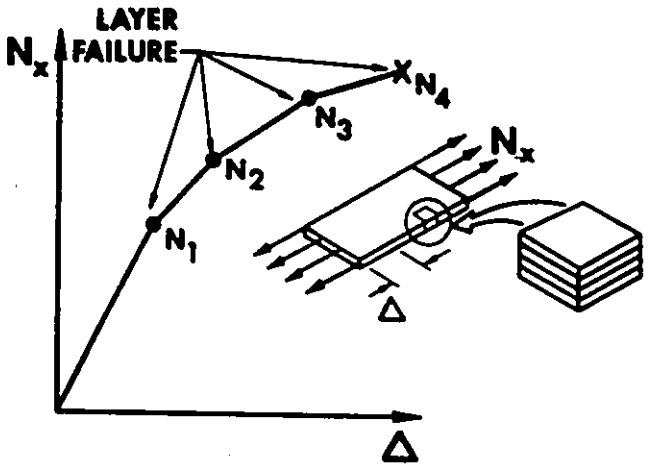

Figure 5-7 Laminate Load-Deformation Behavior (From [30])

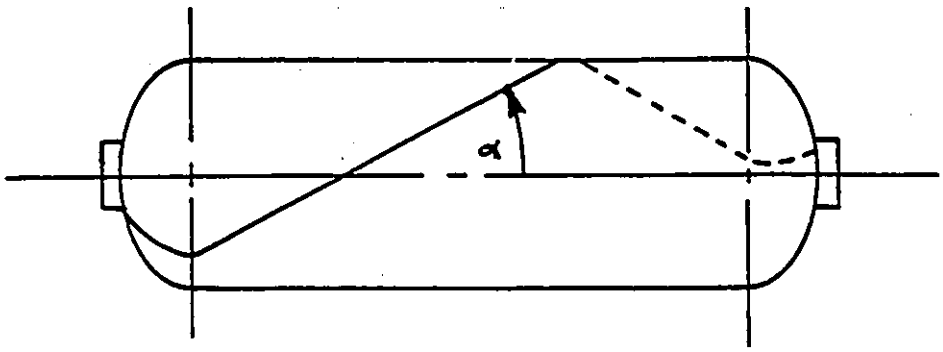

Figure 5-8 Path for a Single Fibre on Vessel

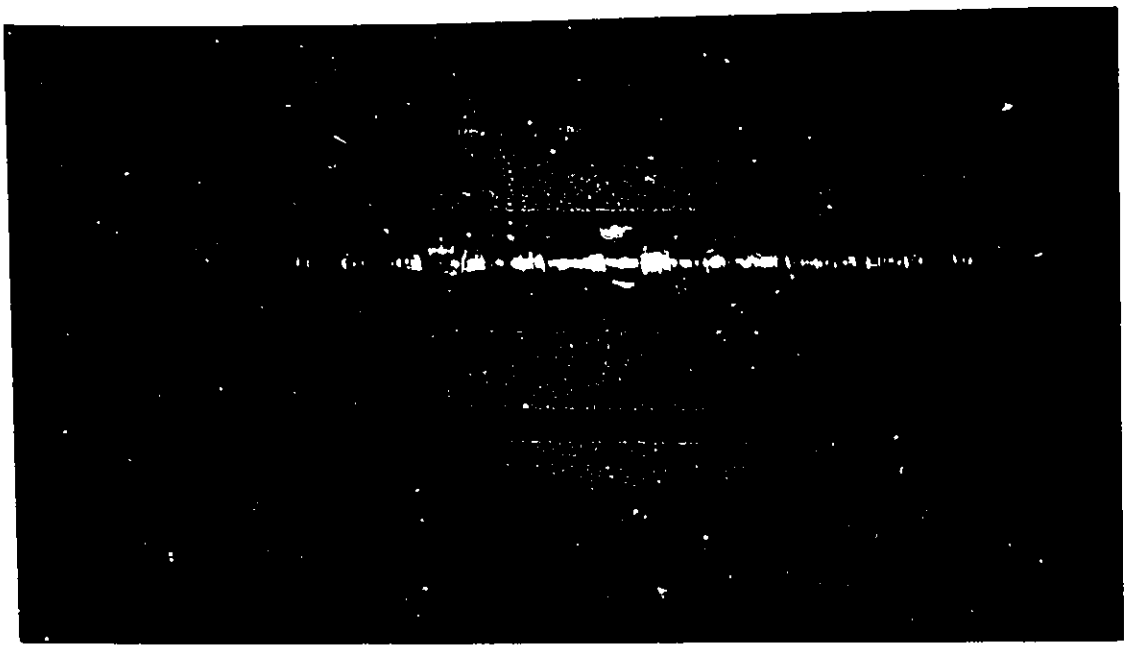

Figure 5-9 265 Mpa Vessel With Consolidation Tape

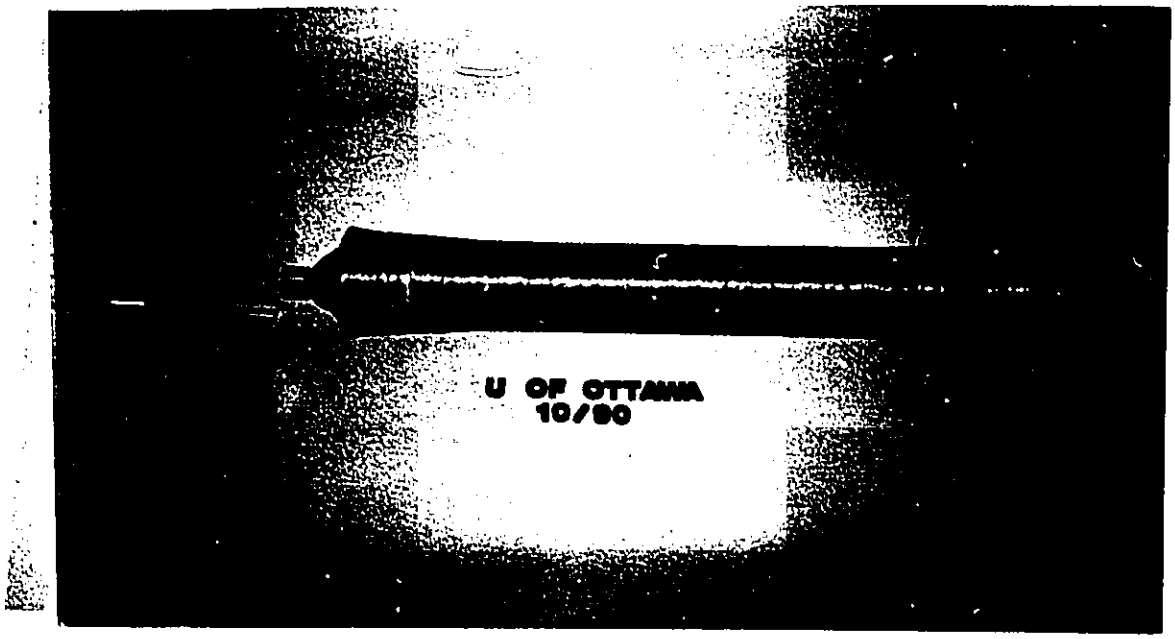

Figure 5-10 Completed 265 Mpa Vessel With End Fittings

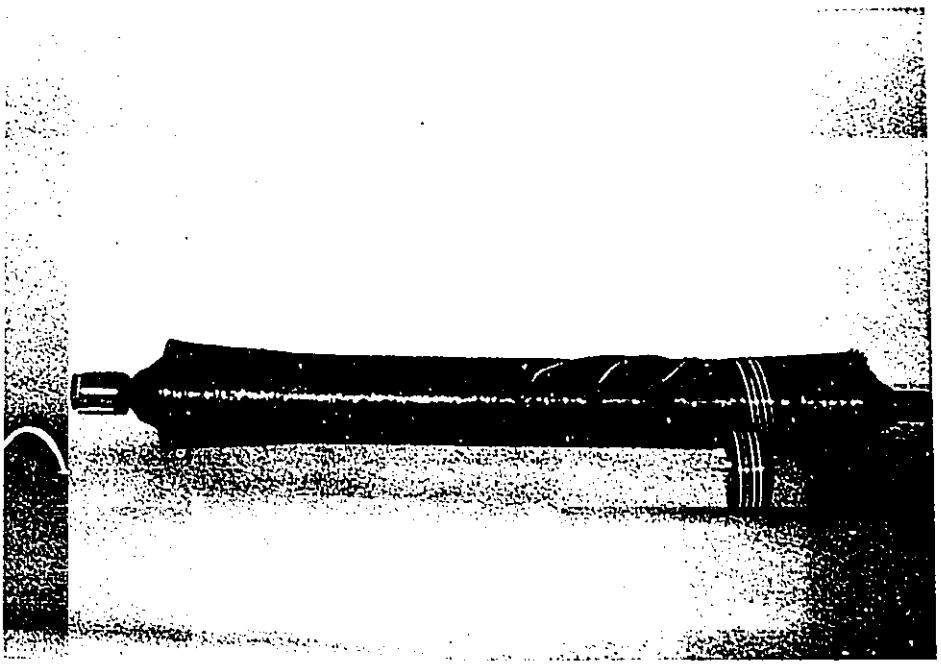

Figure 5-11 Completed Vessel with Strain Gauges

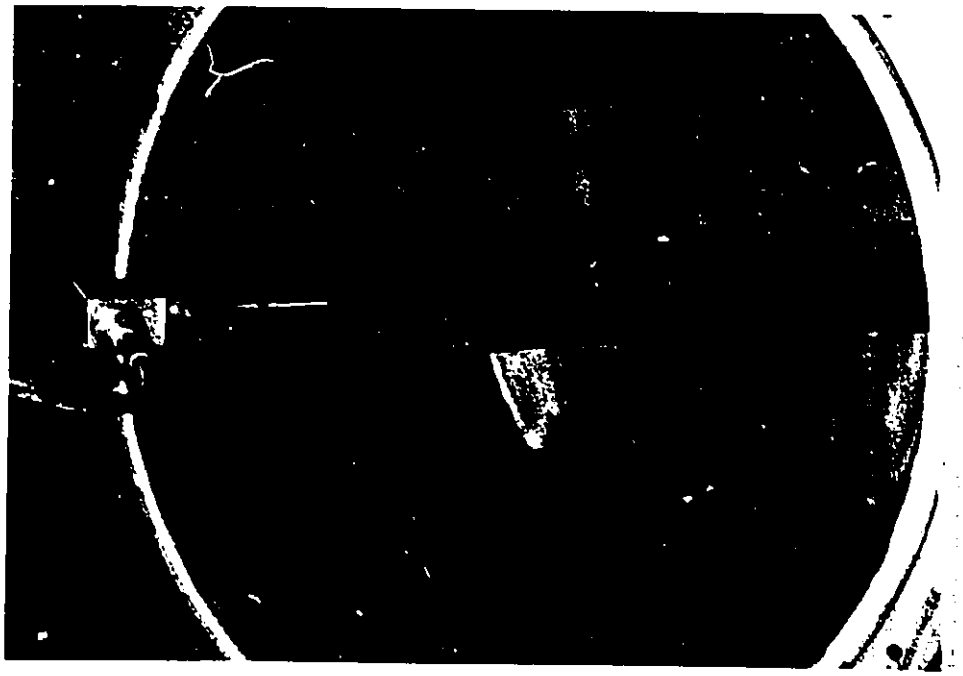

Figure 5-12 Vessel in Water Test Container

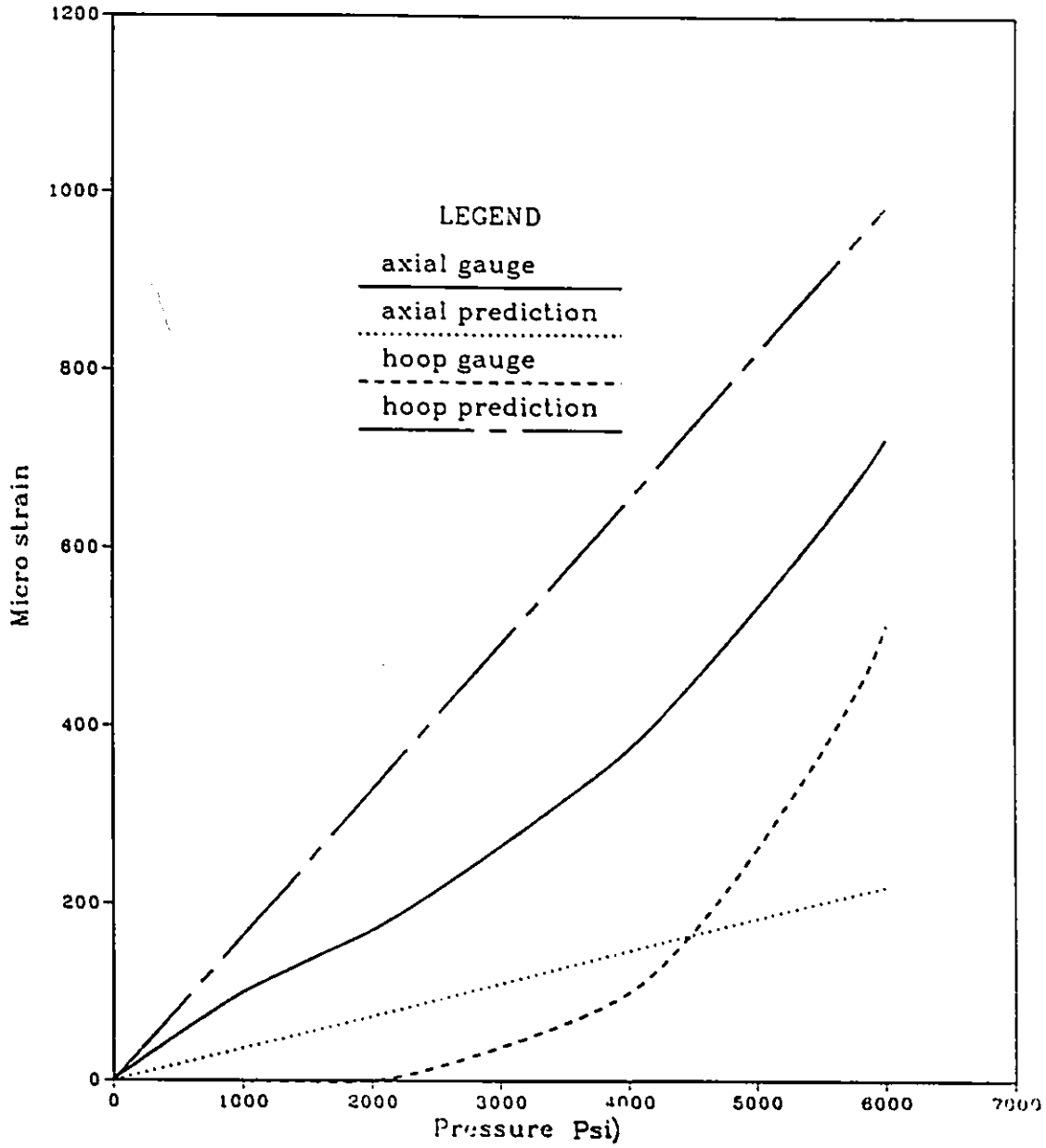

Figure 5-13 Predicted Vs. Experimental Strains

Chapter 6

CONCLUSIONS AND RECOMMENDATIONS

6.1 Conclusions

The majors goal of this study was to devise a mathematical model that would provide optimum parameter selection for a cylindrical, multiple layered, multiple-angle fibre composite pressure vessel. A Hooke & Jeeves direct search technique was used to select optimum design parameters of individual layer wind angles and thickness at the same time. Different failure theories were considered and Tsai-Wu theory was chosen as the most appropriate. Optimization was performed for vessels with equal and unequal thickness layers for different total thickness vessels and compared on the basis of FPF pressure and efficiency.

For this study, a number of conclusions can be presented. The ability of the pressure vessel to resist the internal pressure without failure increased with increasing

total wall thickness (as judged by FPF) although generally above b/a ratios of 1.75, no increase in ability was noted. The FPF pressure increased with increasing b/a in a fairly linear fashion for thinner laminates (b/a<1.50); beyond this, the FPF pressure continued to increase, but at a decreasing rate, until reaching a limit at roughly b/a>1.75.

It has also been shown that for b/a ratios greater than 1.25, an improved design of a fibre composite pressure vessel can be accomplished by increasing the number of individual equal thickness layers in the vessel wall. Additional improvement in the design can be obtained for vessels with b/a ratios greater than 1.50 by allowing the thickness of each individual layer to vary.

Peak efficiency generally occurred at the same b/a ratio, b/a=1.25, for all laminate configurations. This implies that the efficiency is mostly affected by the type of fibre/matrix combination selected and that improvements in efficiency are limited by the type of composite material selected.

In terms of vessel efficiency, a slight improvement was noticed by increasing the number of individual layers and allowing their thicknesses to vary.

The sensitivity of the designs were shown for 2 layer equal thickness vessels and a 4 layer unequal thickness optimum design. The 2 layer design was seen to be fairly insensitive to small changes in wind angle for many combinations of wind angles. For the 4 layer unequal thickness vessel, the sensitivity of the optimum design was seen to be moderately sensitive to small changes in wind angle and thickness.

Testing of the vessel showed that high burst pressures (130 Mpa) could be attained. Reasonable agreement betweeen actual and predicted strains was also seen for the initial stages of deformation.

6.2 Recommendations

To provide more insight into the behaviour of composite laminates, a more extensive testing program should be implemented. Apart from manufacturing and testing several vessels, there should be improvements or more work done in the following areas:

- The effect of hybrid laminates could be investigated.

- Non-destructive testing techniques, such as acoustic emissions or ultrasonics could be used to monitor damage during the pressurization cycle. FPF could be better estimated using such an approach.

- Strain gauges could be placed inside the laminate during the layup, to be able to monitor interlaminar strains.

- Other search routines could be considered, especially for cases where several parameters are being optimized. The Hooke & Jeeves approach works quite well for searches with a small number of variables. For searches of more than

four or five variables, a more sophisticated search routine should perhaps be used, one where a univariate optimization is performed in each of the search directions, to lessen the chances of locating too many local optimum.

- A preliminary grid search could be performed, if large computing capabilities were available, to provide a better estimate of the location of a global minimum.

- A LPF (last-ply-failure) theory approach could be investigated and/or developed to predict a more realistic burst pressure for vessels.

- A geodesic winding pattern should be used to wind along the vessel ends, to provide reinforcement in this critical area. An optimized shape for the vessel ends should also be investigated.

REFERENCES

1. M. Munro, D. Lindstrom and M. Tenace, "Advanced Concepts for the Development of a Method of Design and Manufacture of Composite Material Containers for Ultra-High Pressure Applications," DND/DSS Contract No.06SB.W7708-6-7249 (1989).

2. M. Munro and D. Lindstrom, "Development of a Method of Design and Manufacture of Composite Material Containers for Ultra-High Pressure Applications," Annual Report (1986) DND/DSS Contract No.8S283-00175 (Classified).

3. M. Munro and D. Lindstrom, "Development of a Method of Design and Manufacture of Composite Material Containers for Ultra-High Pressure Applications," Annual Report (1985) DND/DSS Contract No.8SB83-00175 (Classified).

4. M. Munro and D. Lindstrom, "Development of a Method of Design and Manufacture of Composite Material Containers for Ultra-High Pressure Applications," Annual Report (1984) DND/DSS Contract No.8SB83-00175

(Classified).

5. D. Lindstrom, "Series Solution for a Cylindrical Composite Shell Subject to Axisymmetric Loadings," Ph.d Thesis, University of Ottawa, 1990.

6. A.K. Roy and S.W. Tsai, "Design of Thick Composite Cylinders," Composites Design, 3rd Edition, Think Composites, Dayton, Ohio (1987).

7. Yong-Qiu Jiang, "Optimum Design of Laminated Circular Cylindrical Shells with Fiber Reinforced Composite Materials," 5th International Conference on Composite Materials, ICCM-V, San Diego, Ca. (July-Aug. 1985).

8. F.P. Gerstle, Jr. and M. Moss, "Thick-Walled Spherical Pressure Vessels," Composites in Pressure Vessels and Piping, S.V. Kulkarni and C.H. Zweben eds., ASME, PVP-PB-021, 1977.

9. T.R. Guess, "Thick-Walled Kevlar 49/Epoxy Pressure Vessels," 29th National Sampe Symposium and Exibition, (April 1984), p.1007-1021.

10. H. Saatchi, "Development of Advanced Composite Pressure Vessels," ASM Conference, (Dec. 1985), p.285

11. R.L Grover and S. Ayler, "Development of Thick-Walled Composite Pressure Vessels For Ultra-High Internal Presssures, AIAA Paper 81-0584, 1981.

12. V.T. Tomashevskii et al., "Optimization of Structures of Reinforced Cylindrical Shells Made of Composites," Mekhanika Kompozitnykh Materialov, No.5 (Sept. 1987), p.853.

13. T.R. Tauchert, "Optimum Design of a Reinforced Pressure Vessel," J. Composite Materials, Vol.15 (Sept. 1981), p.390.

14. R.E. Sherrer, "Filament-Wound Cylinders with Axial-Symmetric Loads," J. Composite Materials, Vol.1 (1967), p.344.

15. A.S. Tooth, W.M. Banks and P.M. Wilson, "A Study of the Multi-Layered GRP Composite Cylindrical Vessel," 7th International Conference on Offshore Mechanics and Arctic Engineering, Houston, Texas (Feb 7-12, 1988).

16. P.M.J.W. Martin, "Optimal Design of Filament Wound Composite Pressure Vessels," 7th International Conference on Offshore Mechanics and Arctic Engineering, Houston, Texas (Feb.7-12, 1988).

17. M.N. Nahas, "Survey of Failure and Post-Failure Theories of Laminated Fiber-Reinforced Composites," J. Composites Technology & Research, Vol.8, No.4 (Winter 1986), p.138.

18. V.D. Azzi and S.W. Tsai, "Anisotropic Strength of Composites," Experimental Mechanics (Sept. 1965).

18. O. Hoffman, "The Brittle Strength of Orthotropic Materials," J. Composite Materials, Vol.1 (1967), p.200.

19. S.W. Tsai and E.M. Wu, "A General Theory of Strength for Anisotropic Materials," J. Composite Materials, Vol.5 (Jan.1971),p.58.

20. E.M. Wu, "Phenomenological Anisotropic Failure Criterion," Composite Materials, Vol.2, Academic Press, New York, 1974.

21. R. Burk, "Standard Failure Criteria Needed for Advanced Composites," Astronautics and Aeronautics, Vol. 21, June 1983.

22. W. Murray, "Numerical Methods for Unconstrained Optmization," Academic Press, London and New York (1972).

23. S.S. Rao, "Optimization Theory and Applications," 2nd edition, (1977)

24. M.B. Munro, A. Miyase, R.C. Flanagan, D. Lindstrom, D. Bouchard, C. Aleong, J. Wong, "Advanced Materials and Manufacturing Studies for Fiber Composite Flywheels," Technical Report No.VOME-FP-8304-1, National Research Council of Canada, Contract No. OSU80-00043 1983).

25. M.B. Munro and A. Miyase, "Basic Material Studies for Fiber Composite Flywheels," Report No. UOME-FP-8302-1, NRC/DSS Contract No.OSU80-00043. Department of Mechanical Engineering, University of Ottawa (1983).

26. M. Munro and S. Lee, "Modelling of In-Plane Shear Modulus of Advanced Composite Materials for Aerospace Applications," submitted for publication.

27. C.C. Chamis, "Simplified Composite Micromechanics Equations for Hygral, Thermal and Mechanical Properties," SAMPE Quarterly (April 1984).

28. R.R. Rizzo and A.A. Vicario, "A Finite Element Analysis of Laminated Anisotropic Tubes," J. Composite Materials, Vol. 4 (July 1970), p.344.

29. M.Munro, "Review of Manufacturing of Fiber Composite Components By Filament Winding," Polymer Composites, (Oct. 1988) Vol.9, No.5.

30. R.M. Jones, "Mechanics of Composite Materials," Scripta Book Co., (1975).

31. G. Lewis, "Filament-Wound Spherical Pressure Vessels: A State-of-the-Art Review," J. Composite Technology & Research, Vol.9 (Summer 1987), p.33-39.

32. G. Lewis, "Theories of Failure of Filament Wound Case Composite Materials," SAMPE Quarterly, Vol.17 (July 1986), p.59-64.

33. T.R. Guess and C.B. Haizlip, Jr., "End-Grip Configuration For Axial Loading of Composite Tubes," Experimental Mechanics (January 1980).

34. R.f. Lark, "Recent Advances in Lightweight, Filament-Wound Composite

Pressure Vessel Technology," Composites in Pressure Vessels and Piping, ASME,PVP-PB-021 (1977).

35. S.W. Tsai, "A Survey of Macroscopic Failure Criteria For Composite Materials," J. of Reinforced Plastics and Composites, Vol.3 (Jan.1984).

36. R.C. Flanagan, M. Munro, J. Wong and A. Miyase, "Rotor Design Assessment and R & D Program Definition," Report No. UOME-FP-8301-1, NRC/DSS Contract No. 8SB83-00175 (1983).

37. R.C. Flanagan, J. Wong, M. Munro and A. Miyase, "High Energy Density Fibre Composite Rotor Design and Analysis," Report No. UOME-FP-8301-1, NRC/DSS Contract No. 0SU80-00043, Dept. of Mech. Eng., University of Ottawa (1983).

38. R.C. Flanagan, P. Miller, M. Munro et al., "Design and Development of High-Speed Spin Test Facility and Rotor Dynamic Testing," Report No. UOME-FP-8305-1, NRC/DSS Contract No. 0SU80-00043, Dept. of Mech. Eng., University of Ottawa (1983).

39. S.W. Tsai and V.D. Azzi, "Strength of Laminated Composite," AIAA Journal (Feb. 1966), Vol.4, No.2.

40. A. Fahim, M. Munro and H. Sarrazin, "High Power to Weight Robots Utilizing

High Performace Composite Materials," DREP/RRMC Proceedings on Military Robotic Applications, Victoria, B.C., (Aug. 1987).

Appendix A

Program Listings

```
C*************************************************************
C
C       program name: GHJM.FOR  (GENERAL LAMINATE, 2D, FMAX)
C       date written: 7/03/90
C           updated: 28/08/90
C       program type: MAIN
C     calls data file: PLY.DAT
C     WHERE    NVAR=NUMBER OF WIND ANGLES + NUMBER OF THICKNESS ANGLES
C          FOR EXAMPLE, IF   NVAR=5
C                    THEN  NWA=3
C                    AND   NTA=2
C              X(1,2,3)=WIND ANGLE VARIABLES
C              X(4,5)=THICKNESS ANGLE VARIABLES
C
C   subroutine file(s): SUBHJ.OBJ
C
C   description: COMPUTES OPTIMUM THICKNESS DISTRIBUTION AND WIND ANGLES
C             FOR AN ANGLE-PLIED LAMINATE (2 OR MORE PLIES).
C             THIS ROUTINE COMPUTES THE OPTIMUM USING MINMAX CRITERION
C             WHERE ICRIT=
C
C                    1 = MAX. STRAIN
C                    2 = MAX. STRESS
C                    3 = TSAI-HILL
C                    4 = HOFFMAN
C                    5 = TSAI-WU
C
C
C   CAN USE A RANDOM GENERATOR FOR START VALUES WHICH
C   LOOPS J TIMES
C
C    PRINTOUT = 3
C    TERMINAL = 6
C    FILE     = 10
C
C*************************************************************
      IMPLICIT DOUBLE PRECISION(A-H,O-Z)
      COMMON /VESPAR/PIN
      DIMENSION EPSI(20),EPS(20),X(0:50),Q(20),QQ(20),W(20)
       OPEN(UNIT=3, FILE='PRN')
       OPEN(UNIT=6, FILE='CON')
       OPEN(UNIT=10, FILE='GHJ.RES')
       OPEN(UNIT=7, FILE='PLY.DAT')

      READ(7,707) NVAR
707    FORMAT(I5)
808    FORMAT(F12.7)
      READ(7,808) (X(I), I=1,7)
      READ(7,808) BA
      READ(7,707) LUN
      READ(7,707) IPRINT
      READ(7,808) (EPSI(I), I=1,7)
      READ(7,808) EPSY
      READ(7,707) ITMAX
      READ(7,707) NKAT
      READ(7,808) ALPHA
      READ(7,808) BETA
      READ(7,707) IFLAG
      READ(7,707) ILOOP
```

```
      READ(7,707) ISEED
      READ(7,707) ICRIT
      WRITE(6,364)
C
364    FORMAT(1X,'INPUT PRESSURE (IN MPA):')
C      PIN=200.0
      READ(6,*) PIN
      PIN=PIN*1E06

       DO 876 J=1,ILOOP
        IF(IFLAG.EQ.0) GOTO 123
         USEED=USTART(ISEED)
         DO 5 I=1,NVAR
           X(I)=UNI()*90.0
5         CONTINUE
         ISSED=ISEED+1
123    QD=0.0
      DO 375 I=1,NVAR
         EPS(I)=EPSI(I)
375    CONTINUE
      WRITE(LUN,423)
423    FORMAT(/,1X,70('*'))
      WRITE(LUN,421) BA
421    FORMAT(/,1X,'B/A =',F5.3)

      CALL HOOKE(X,EPS,NVAR,BA,ITMAX,NKAT,EPSY,ALPHA,BETA,
     $       QD,Q,QQ,W,IPRINT,LUN,ICRIT)
876    CONTINUE
      STOP
      END
C*****************************************************************

       SUBROUTINE OBJECT(X,NVAR,BA,ICRIT,FUNC)
      IMPLICIT DOUBLE PRECISION (A-H,O-Z)
      COMMON /VESPAR/PIN
      DIMENSION MT(50),THETA(50),R(0:50),Q(6,6,50)
      DIMENSION B(50,50),RHS(50),AL(50),GA1(50),GA2(50)
      DIMENSION ANS(50),X(0:50)
C
      CF=1.0/57.2957795131
      PIN=200.0E06
      POUT=0.0
      TORQ=0.0
      FZ=0.0

      R(0)=0.03175
C
      NLAYER=NVAR+1
      NWA=(NVAR+1)/2
      NTA=NWA-1
      TLAM=R(0)*(BA-1.0)
C
      RANGE=DBLE(TLAM/NTA)
      R(NLAYER)=R(0)+TLAM

C  SET FIBRE TYPE
      DO 60 LN=1,NLAYER
        MT(LN)=1
60     CONTINUE

      DO 46 I=1,NTA
        R(2*I)=R(0)+RANGE*(DSIN(X(NWA+I)*CF)*DSIN(X(NWA+I)*CF)
```

```
     $    +I-1)
          R(2*I-1)=(R(2*I)+R(2*I-2))/2.0
46        CONTINUE
          R(NLAYER-1)=(R(NLAYER)+R(NLAYER-2))/2.0

          DO 57 K=1,NWA
           THETA(2*K-1)=X(K)*CF
           THETA(2*K)=-THETA(2*K-1)
57        CONTINUE

          CALL QUE(NLAYER,MT,THETA,Q)
          CALL COEF(NLAYER,Q,R,AL,GA1,GA2,PIN,POUT,FZ,TORQ,B,RHS)
            NEQH=2*NLAYER+2
            NEQV=NEQH
          CALL GAUSJO(NEQH,NEQV,B,RHS,ANS,NEQ)
          CALL DEFORM(NLAYER,NEQ,ANS,AL,GA1,GA2,R,Q,THETA,
        $ ICRIT,FUNC)
          RETURN
          END
C*************************************************************

          SUBROUTINE DEFORM(NLAYER,NEQ,ANS,AL,GA1,GA2,R,Q,THETA,
        $ ICRIT,FUNC)
          IMPLICIT DOUBLE PRECISION(A-H,O-Z)
          COMMON /VESPAR/PIN
          DIMENSION ANS(50),AL(50),GA1(50),GA2(50),R(0:50),RR(3)
          DIMENSION STRESS(6,6),STRAIN(6,6),Q(6,6,50),THETA(50)
          DIMENSION EPS(6,6,20),EPSR(6,6,20),SIG(6,6,20),SIGR(6,6,20)
          DIMENSION THILL(6,20),HOFF(6,20),TWU(6,20)

C         STRAIN AND STRENGTH DATA FOR XAS

          E1T=0.0133
          E2T=0.0048
          E2C=0.0235
          E3T=E2T
          E3C=E2C
          ESH=0.00832

          X=1960.0E06
          YT=38.6E06
          YC=200.0E06
          ZT=YT
          ZC=YC
          SH=42.2E06

          CF1=57.2957795131

          DO 30 LN=1,NLAYER
          AI=ANS(2*LN-1)
          BI=ANS(2*LN)

C         I=1 IS INNER; I=2 IS MID; I=3 IS OUTER FOR THE LAMINA
          RR(1)=R(LN-1)
          RR(2)=(R(LN-1)+R(LN))/2.0D0
          RR(3)=R(LN)

C         CALCULATE INNER, MID, AND OUTER STRAINS,STRESSES, DISPLACEMENTS

          DO 20  I=1,3

C         STRAINS
```

```
      STRAIN(I,6)=ANS(NEQ)*RR(I)
      STRAIN(I,1)=ANS(NEQ-1)
        A1=AI*RR(I)**(AL(LN)-1.0D0)
        A2=BI*RR(I)**(-AL(LN)-1.0D0)
        A3=GA2(LN)*STRAIN(I,6)
      STRAIN(I,2)=A1+A2+GA1(LN)*STRAIN(I,1)+A3
      STRAIN(I,3)=AL(LN)*A1-AL(LN)*A2+GA1(LN)*STRAIN(I,1)+2.0D0*A3
      STRAIN(I,4)=0.0D0
      STRAIN(I,5)=0.0D0

C  STRESSES
      DO  10  J=1,6
        STRESS(I,J)=0.0D0
      DO 10   K=1,6
10        STRESS(I,J)=STRESS(I,J)+Q(J,K,LN)*STRAIN(I,K)

20    CONTINUE

C  ROTATE TO MATERIAL DIRECTIONS

      DO 80 I=1,3,2

      S=DSIN(THETA(LN))
      C=DCOS(THETA(LN))
      S2=S*S
      C2=C*C

      EPS(I,1,LN)=C2*(STRAIN(I,1))+S2*(STRAIN(I,2))+
     $   C*S*(STRAIN(I,6))
      EPS(I,2,LN)=S2*(STRAIN(I,1))+C2*(STRAIN(I,2))-
     $   C*S*(STRAIN(I,6))
      EPS(I,3,LN)=-2.0*C*S*(STRAIN(I,1))+2.0*C*S*
     $  (STRAIN(I,2))+(C2-S2)*(STRAIN(I,6))
      EPS(I,4,LN)=STRAIN(I,3)

      SIG(I,1,LN)=C2*(STRESS(I,1))+S2*(STRESS(I,2))+
     $   2.0*C*S*(STRESS(I,6))
      SIG(I,2,LN)=S2*(STRESS(I,1))+C2*(STRESS(I,2))-
     $   2.0*C*S*(STRESS(I,6))
      SIG(I,3,LN)=-C*S*(STRESS(I,1))+C*S*
     $  (STRESS(I,2))+(C2-S2)*(STRESS(I,6))
      SIG(I,4,LN)=STRESS(I,3)

C    CALCULATE STRAIN AND STRESS RATIOS

      EPSR(I,1,LN)=ABS(EPS(I,1,LN)/E1T)

       IF(EPS(I,2,LN).GT.0)THEN
        EPSR(I,2,LN)=EPS(I,2,LN)/E2T
       ELSE
        EPSR(I,2,LN)=EPS(I,2,LN)/(-E2C)
       END IF

       IF(EPS(I,4,LN).GT.0)THEN
        EPSR(I,4,LN)=EPS(I,4,LN)/E3T
       ELSE
        EPSR(I,4,LN)=EPS(I,4,LN)/(-E3C)
       END IF

      EPSR(I,3,LN)=ABS(EPS(I,3,LN)/ESH)

      SIGR(I,1,LN)=ABS(SIG(I,1,LN)/X)
```

```
      IF(SIG(I,2,LN).GT.0)THEN
        SIGR(I,2,LN)=SIG(I,2,LN)/YT
        Y=YT
      ELSE
        SIGR(I,2,LN)=SIG(I,2,LN)/(-YC)
        Y=-YC
      END IF

      IF(SIG(I,4,LN).GT.0)THEN
        SIGR(I,4,LN)=SIG(I,4,LN)/ZT
        Z=ZT
      ELSE
        SIGR(I,4,LN)=SIG(I,4,LN)/(-ZC)
        Z=-ZC
      END IF

      SIGR(I,3,LN)=ABS(SIG(I,3,LN)/SH)

C     CONSTANTS FOR FAILURE THEORIES

      A1=1.0/(X*X)
      A2=1.0/(Y*Y)
      A3=1.0/(SH*SH)

      B1=0.5*(2.0/(YT*YC)-A1)
      B2=0.5*(A1)
      B3=B2
      B4=1.0/YT-1.0/YC
      B5=B4
      B6=A3

      F11=A1
      F22=1.0/(YT*YC)
      F12=-0.5*SQRT(F11*F22)
      F13=-0.5*F22
      F66=A3
      F1=0.0
      F2=B4
C  SET RADIAL STRESS=0 FOR 2D
      SIG(I,4,LN)=0.0
      EPS(I,4,LN)=0.0

      THILL(I,LN)=A1*SIG(I,1,LN)*( SIG(I,1,LN)-SIG(I,2,LN) )
     $ + A2*SIG(I,2,LN)**2 + A3*SIG(I,3,LN)**2

      HOFF(I,LN)=B1*( SIG(I,2,LN)-SIG(I,4,LN) )**2
     $ + B2*( SIG(I,4,LN)-SIG(I,1,LN) )**2
     $ + B3*( SIG(I,1,LN)-SIG(I,2,LN) )**2
     $ + B4*SIG(I,2,LN) + B5*SIG(I,4,LN) + B6*SIG(I,3,LN)**2

      TWU(I,LN)=F11*SIG(I,1,LN)**2
     $ + F22*( SIG(I,4,LN)**2+SIG(I,2,LN)**2 )
     $ + 2.0*F12*SIG(I,1,LN)*( SIG(I,4,LN)+SIG(I,2,LN) )
     $ + 2.0*F13*SIG(I,4,LN)*SIG(I,2,LN)
     $ + F2*( SIG(I,4,LN)+SIG(I,2,LN) ) + F66*SIG(I,3,LN)**2

80    CONTINUE
30    CONTINUE


      FUNC=-1000.0
      FMAX=-1000.0
```

```
      FMIN=1000.0

      GO TO (100,200,300,400,500),ICRIT

100    DO 13 I=1,3,2
       DO 12 J=1,3
         DO 11 LN=1,NLAYER
         IF(EPSR(I,J,LN).GT.FMAX) FMAX=EPSR(I,J,LN)
C         IF(EPSR(I,J,LN).LT.FMIN) FMIN=EPSR(I,J,LN)
         FUNC=FMAX
11        CONTINUE
12      CONTINUE
13    CONTINUE
         GOTO 999

200    DO 23 I=1,3,2
         DO 22 J=1,3
         DO 21 LN=1,NLAYER
         IF(SIGR(I,J,LN).GT.FMAX) FMAX=SIGR(I,J,LN)
C         IF(SIGR(I,J,LN).LT.FMIN) FMIN=SIGR(I,J,LN)
         FUNC=FMAX
21        CONTINUE
22       CONTINUE
23     CONTINUE
         GOTO 999

300    DO 32 I=1,3,2
         DO 31 LN=1,NLAYER
         IF(THILL(I,LN).GT.FMAX) FMAX=THILL(I,LN)
C         IF(THILL(I,LN).LT.FMIN) FMIN=THILL(I,LN)
         FUNC=FMAX
31        CONTINUE
32      CONTINUE
         GOTO 999

400    DO 42 I=1,3,2
         DO 41 LN=1,NLAYER
         IF(HOFF(I,LN).GT.FMAX) FMAX=HOFF(I,LN)
C         IF(HOFF(I,LN).LT.FMIN) FMIN=HOFF(I,LN)
         FUNC=FMAX
41        CONTINUE
42      CONTINUE
         GOTO 999


500     DO 52 I=1,3,2
         DO 51 LN=1,NLAYER
         IF(TWU(I,LN).GT.FMAX) FMAX=TWU(I,LN)
C         IF(TWU(I,LN).LT.FMIN) FMIN=TWU(I,LN)
         FUNC=FMAX
51        CONTINUE
52      CONTINUE
         GOTO 999

999    RETURN
      END
C**********************
C
C    SUBHJ.FOR
C    UPDATED 29-08-90
C*****************************************************************
```

```
      SUBROUTINE HOOKE(X,EPS,NVAR,BA,ITMAX,NKAT,EPSY,ALPHA,BETA,
     $        QD,Q,QQ,W,IPRINT,LUN,ICRIT)
      IMPLICIT DOUBLE PRECISION(A-H,O-Z)
      COMMON /VESPAR/PIN
      DIMENSION X(0:50),EPS(NVAR),Q(NVAR),QQ(NVAR),W(NVAR)
      CHARACTER NAME(5)*11
C
      NAME(1)='MAX. STRAIN'
      NAME(2)='MAX. STRESS'
      NAME(3)='  TSAI-HILL'
      NAME(4)='  HOFFMAN '
      NAME(5)='  TSAI-WU '


      WRITE(LUN,200) NAME(ICRIT)
200    FORMAT(15X,'HJ PATTERN SEARCH—',A11,' CRITERION')
      WRITE(LUN,210)ITMAX,NKAT,EPSY,ALPHA,BETA
210    FORMAT(/,2X,'SEARCH PARAMETERS:',/,2X,'ITMAX=',I5,
     $ 4X,'NKAT=',I5,4X,'EPSY=',F10.8,4X,'ALPHA=',F5.2,
     $ 4X,'BETA=',F5.2)
      WRITE(LUN,215)
215    FORMAT(/,2X,'INITIAL X VALUES:',15X,'EPS VALUES:')
      DO 26 I=1,NVAR
      WRITE(LUN,220)X(I),EPS(I)
220    FORMAT(2X,F7.2,25X,F7.2)
26     CONTINUE
      KFLAG=0
      KAT=0
      KK1=0
C
      DO 11 I=1,NVAR
        Q(I)=X(I)
        W(I)=-1000.0
11     CONTINUE
C
C START OF ROUTINE
C
001    KCOUNT=0
      WBEST=W(NVAR)
      CALL OBJECT(X,NVAR,BA,ICRIT,FUNC)
      KK1=KK1+1
      BO=FUNC
      IF(KK1.EQ.1) QD=FUNC
      IF(KK1.EQ 1) GOTO 101
      IF(BO.GT.QD)THEN
        KFLAG=1
      ELSE
        QD=BO
      END IF
C
C FIND PATTERN
C
101    DO 12 I=1,NVAR
        QQ(I)=X(I)
        TEMP=X(I)
        X(I)=TEMP+EPS(I)
      CALL OBJECT(X,NVAR,BA,ICRIT,FUNC)
        KK1=KK1+1
        W(I)=FUNC
        IF(W(I).LT.QD) GOTO 404
        X(I)=TEMP-EPS(I)
      CALL OBJECT(X,NVAR,BA,ICRIT,FUNC)
```

```
      KK1=KK1+1
      W(I)=FUNC
      IF(W(I).LT.QD) GOTO 404
      X(I)=TEMP
      IF(I.EQ.1) GOTO 202
      W(I)=W(I-1)
      GOTO 303
202     W(I)=BO
303     CONTINUE
      KCOUNT=KCOUNT+1
      GOTO 505
404     QD=W(I)
      QQ(I)=X(I)
505     CONTINUE
12    CONTINUE
     IF(IPRINT)60,65,60
60    WRITE(LUN,100) KK1
100   FORMAT(//,2X,'NUMBER OF FUNCTION EVALUATIONS =',I8)
C
     WRITE(LUN,110)
110   FORMAT(1X,'END OF EACH PATTERN SEARCH')
     WRITE(LUN,115)QD
115   FORMAT(1X,'OBJECTIVE FUNCTION=',5X,F16.9)
     WRITE(LUN,117)
117   FORMAT(1X,'X VALUES:')
     DO 27 I=1,NVAR
     WRITE(LUN,120)I,X(I)
120   FORMAT(1X,'X(',I2,')=',F10.5)
27    CONTINUE
C
C
65    IF(KK1.GT.ITMAX) GOTO 999
     IF(KAT.GE.NKAT) GOTO 999
     IF(ABS(W(NVAR)-WBEST).LE.EPSY) GOTO 999
C
C   IF ALL AXES FAIL REDUCE STEP SIZE
C
      IF(KCOUNT.GE.NVAR)GOTO 002
      DO 13 I=1,NVAR
        X(I)=X(I)+ALPHA*(X(I)-Q(I))
13     CONTINUE
      DO 17 I=1,NVAR
        Q(I)=QQ(I)
17     CONTINUE
      GOTO 001
002     KAT=KAT+1
      IF(KFLAG.EQ.1) GOTO 003
      GOTO 004
003     KFLAG=0
      DO 14 I=1,NVAR
        X(I)=Q(I)
14     CONTINUE
004     DO 15 I=1,NVAR
          EPS(I)=EPS(I)*BETA
15     CONTINUE
      IF(IPRINT) 85,001,85
85     WRITE(LUN,130) KAT
130     FORMAT(/,2X,' STEP SIZE REDUCED ',I2,' TIMES')
      GOTO 001
C
C      DO 37 I=1,NVAR
999     WRITE(LUN,135)
```

```
135     FORMAT(/,1X,'FINAL EPS VALUES:',15X,'FINAL X VALUES:')
        DO 16 I=1,NVAR
        WRITE(LUN,140) I,EPS(I),I,X(I)
140     FORMAT(1X,'EPS(',I2,')=',F10.5,14X,
     $  'X(',I2,')=',F12.8)
16      CONTINUE
        WRITE(LUN,160) QD
160     FORMAT(/,1X,'THE MINIMUM FUNCTION VALUE IS:',2X,F16.9)
        WRITE(LUN,180) KK1
180     FORMAT(/,1X,'NUMBER OF FUNCTION EVALUATIONS=',I8)
        RETURN
        END
C
      SUBROUTINE QUE(NLAYER,MT,THETA,Q)

      IMPLICIT DOUBLE PRECISION (A-H,O-Z)
      DIMENSION MT(50),THETA(50),Q(6,6,50),E(3,3),C(6,6),S(6,6)

      DO 100  LN=1,NLAYER
         MAT=MT(LN)
         CALL DATAFI(MAT,E,UA,UB,UC)
         CALL COMPLI(E,UA,UB,UC,S,ST)
         CALL STIFF(S,ST,C)
         CALL ROTSTF(THETA,LN,C,Q)
100    CONTINUE

      RETURN
      END

C  ***************************************************

C  DATA BASE FOR MATERIALS
      SUBROUTINE DATAFI(MAT,E,UA,UB,UC)

      IMPLICIT DOUBLE PRECISION(A-H,O-Z)
      DIMENSION E(3,3)

      DO 10  I=1,3
      DO 10  J=1,3
10          E(I,J)=0.0D0

       GO TO (100,200,300,400),MAT

C  DATA FOR XAS/EPOXY AT 65% VOLUME FRACTION
C
100       E(1,1)=147.0E9
         E(2,2)=8.5E9
         E(3,3)=8.499E9
C
         E(1,2)=2.4E9
         E(1,3)=2.399E9
         E(2,3)=2.63E9
C
         UA=.3E0
         UB=.299E0
         UC=.628E0
        GOTO 999

C*****DATA FOR T6-6061 ALUMINUM*****************
200       E(1,1)=68.95E9
         E(2,2)=68.949E9
         E(3,3)=68.948E9
```

```
C
        E(1,2)=26.52E9
        E(1,3)=26.519E9
        E(2,3)=26.518E9
C
        UA=.3E0
        UB=.299E0
        UC=.298E0
      GOTO 999

C**** DATA FOR KEVLAR 49
300       E(1,1)=24.2E9
        E(2,2)=10.3E9
        E(3,3)=10.3E9
C
        E(1,2)=2.56E9
        E(1,3)=2.56E9
        E(2,3)=24.1E9
C
        UA=.25
        UB=.25
        UC=.25
      GOTO 999

C*** DATA FOR ELASTOMERIC LINER
400       E(1,1)=866.0
        E(2,2)=867.0
        E(3,3)=865.0
C
        E(1,2)=333.0
        E(1,3)=332.0
        E(2,3)=331.0
C
        UA=0.30
        UB=0.29
        UC=0.28
      GOTO 999
999    RETURN
      END

C  **************************************************

C
      SUBROUTINE COMPLI(E,UA,UB,UC,S,ST)
C
C  CALCULATE LAMINA UNIDIRECTIONAL COMPLIANCES
C
      IMPLICIT DOUBLE PRECISION(A-H,O-Z)
      DIMENSION E(3,3),S(6,6)

      DO 1   I=1,6
      DO 1   J=1,6
1           S(I,J)=0.0D0

            S(1,1)=1.0D0/E(1,1)
            S(2,2)=1.0D0/E(2,2)
            S(3,3)=1.0D0/E(3,3)
            S(1,2)=-UA/E(1,1)
            S(1,3)=-UB/E(1,1)
            S(2,3)=-UC/E(2,2)
            S(4,4)=1.0D0/E(2,3)
            S(5,5)=1.0D0/E(1,3)
```

```
      S(6,6)=1.0D0/E(1,2)
      ST=S(1,1)*S(2,2)*S(3,3)-S(1,1)*(S(2,3)**2)
     $     -S(2,2)*(S(1,3)**2)
     $     -S(3,3)*(S(1,2)**2)+2.0D0*S(1,2)*S(2,3)*S(1,3)
      DO 10 I=1,6
      DO 10 J=1,6
      S(J,I)=S(i,J)
10    CONTINUE
C
      RETURN
      END
C ***************************************************************
C
      SUBROUTINE STIFF(S,ST,C)
      IMPLICIT DOUBLE PRECISION (A-H,O-Z)
      DIMENSION C(6,6),S(6,6)
C
C     CALCULATE UNIDIRECTIONAL STIFFNESSES
C
      DO 1   I=1,6
      DO 1   J=1,6
1     C(I,J)=0.0D0
C
      C(1,1)=(S(2,2)*S(3,3)-S(2,3)**2)/ST
      C(2,2)=(S(3,3)*S(1,1)-S(1,3)**2)/ST
      C(3,3)=(S(1,1)*S(2,2)-S(1,2)**2)/ST
      C(1,2)=(S(1,3)*S(2,3)-S(1,2)*S(3,3))/ST
      C(1,3)=(S(1,2)*S(2,3)-S(1,3)*S(2,2) )/ST
      C(2,3)=(S(1,2)*S(1,3)-S(2,3)*S(1,1))/ST
      C(4,4)=1.0D0/S(4,4)
      C(5,5)=1.0D0/S(5,5)
      C(6,6)=1.0D0/S(6,6)
      DO 5   I=1,6
      DO 5   J=1,6

C10       FORMAT(D20.7)
      C(J,I)=C(I,J)
C       WRITE(3,10)C(I,J)
5     CONTINUE
      RETURN
      END
C
C     ***************************************************************
C
      SUBROUTINE ROTSTF(THETA,L,C,Q)
      IMPLICIT DOUBLE PRECISION (A-H,O-Z)
      DIMENSION THETA(50),C(6,6),Q(6,6,50)
      DOUBLE PRECISION MT,MT2,MT4,NT,NT2,NT4
C
C     CALCULATE ROTATED STIFFNESSES FOR EACH LAYER
C
      DO 1   I=1,6
      DO 1   J=1,6
1     Q(I,J,L)=0.0D0
C
      MT=DCOS(THETA(L))
      NT=DSIN(THETA(L))
      MT2=(DCOS(THETA(L)))**2
      NT2=(DSIN(THETA(L)))**2
      MT4=(DCOS(THETA(L)))**4
      NT4=(DSIN(THETA(L)))**4
    Q(1,1,L)=C(1,1)*MT4+2.0D0*MT2*NT2*(C(1,2)
```

```
     $              +2.0D0*C(6,6))+NT4*C(2,2)
       Q(1,2,L)=MT2*NT2*(C(1,1)+C(2,2)-4.0D0*C(6,6))
     $              +(MT4+NT4)*C(1,2)
       Q(1,3,L)=MT2*C(1,3)+NT2*C(2,3)
       Q(2,2,L)=NT4*C(1,1)+2.0D0*MT2*NT2*(C(1,2)
     $              +2.0D0*C(6,6))+MT4*C(2,2)
       Q(1,6,L)=MT*NT*(MT2*C(1,1)-NT2*C(2,2)
     $              -(MT2-NT2)*(C(1,2)+2.0D0*C(6,6)))
       Q(2,3,L)=NT2*C(1,3)+MT2*C(2,3)
       Q(3,3,L)=C(3,3)
       Q(4,4,L)=MT2*C(4,4)+NT2*C(5,5)
       Q(4,5,L)=-MT*NT*(C(4,4)-C(5,5))
       Q(5,5,L)=MT2*C(5,5)+NT2*C(4,4)
       Q(6,6,L)=MT2*NT2*(C(1,1)+C(2,2)-2.0D0*C(1,2))
     $              +((MT2-NT2)**2)*C(6,6)
       Q(2,6,L)=MT*NT*(NT2*C(1,1)-MT2*C(2,2)
     $              +(MT2-NT2)*(C(1,2)+2.0D0*C(6,6)))
C
       Q(3,6,L)=-NT*MT*(C(2,3)-C(1,3))

C
C            q(1,6,I)=0.0d0
C            q(2,6,I)=0.0d0
C            q(3,6,I)=0.0d0
C            q(4,5,I)=0.0d0
C            q(4,4,I)=1.0d3
C            q(5,5,I)=1.0d3
C            q(6,6,I)=1.0d3




C      QIJ IS SYMMETRIC
       DO 10 I=1,6
       DO 10 J=1,6
            Q(J,I,L)=Q(I,J,L)
CC             WRITE(4,9)I,J,L,Q(I,J,L)
CC9      FORMAT('Q(',I3,',',I3,',',I3,')=',D20.12)
10     CONTINUE
       RETURN
       END
C
C
C      **************************************************




C  THIS SUBROUTINE GENERATES THE MATRIX COEFFICIENTS FOR THE EXACT
C  SOLUTION TO THE THICK MONCLINIC CYLINDER SUBJECT TO AXISYMMETRIC
C  LOADINGS.

       SUBROUTINE COEF(NLAYER,Q,R,AL,GA1,GA2,PIN,POUT,FZ,TORQ,B,RHS)
       IMPLICIT DOUBLE PRECISION (A-H,O-Z)
```

```
      DIMENSION B(50,50),R(0:50),AL(50),GA1(50),GA2(50),Q(6,6,50)
      DIMENSION RHS(50)

      CALL MATRIX(NLAYER,Q,R,AL,GA1,GA2,B)

      CALL LOAD(PIN,POUT,FZ,TORQ,R,NLAYER,RHS)

      RETURN
      END


C     ***************************************************
C     THIS SUBROUTINE CALCULATES THE MATRIX B.
C
      SUBROUTINE MATRIX(NLAYER,Q,R,AL,GA1,GA2,B)
      IMPLICIT DOUBLE PRECISION (A-H,O-Z)
      DIMENSION B(50,50),R(0:50),AL(50),GA1(50),GA2(50),Q(6,6,50)
C
      N=NLAYER
      DO 5   I=1,2*N+2
      DO 5   J=1,2*N+2
           B(I,J)=0.0D0
5     CONTINUE
C
      DO 10  I=1,N
           AL(I)=(Q(2,2,I)/Q(3,3,I))**.5
           B1=(Q(1,2,I)-Q(1,3,I))/Q(3,3,I)
           B2=(Q(2,6,I)-2.0D0*Q(3,6,I))/Q(3,3,I)
           GA1(I)=B1/(1.0D0-AL(I)**2)
           GA2(I)=B2/(4.0D0-AL(I)**2)
10    CONTINUE
C
      B(1,1)=(Q(2,3,1)+AL(1)*Q(3,3,1))*R(0)**(AL(1)-1.0D0)
      B(1,2)=(Q(2,3,1)-AL(1)*Q(3,3,1))*R(0)**(-AL(1)-1.0D0)
      B(1,2*N+1)=Q(1,3,1)+GA1(1)*(Q(2,3,1)+Q(3,3,1))
      B(1,2*N+2)=(Q(3,6,1)+GA2(1)*(Q(2,3,1)+2.0D0*Q(3,3,1)))*R(0)
C
      DO 20  I=1,N-1
           B(2*I,2*I-1)=R(I)**AL(I)
           B(2*I,2*I)=R(I)**(-AL(I))
           B(2*I,2*I+1)=-R(I)**AL(I+1)
           B(2*I,2*I+2)=-R(I)**(-AL(I+1))
           B(2*I+1,2*I-1)=AL(I)*R(I)**AL(I)
           B(2*I+1,2*I)=-AL(I)*R(I)**(-AL(I))
           B(2*I+1,2*I+1)=-AL(I+1)*R(I)**AL(I+1)
           B(2*I+1,2*I+2)=AL(I+1)*R(I)**(-AL(I+1))
           B(2*I,2*N+1)=(GA1(I)-GA1(I+1))*R(I)
           B(2*I,2*N+2)=(GA2(I)-GA2(I+1))*R(I)**2
           B(2*I+1,2*N+1)=(GA1(I)-GA1(I+1))*R(I)
           B(2*I+1,2*N+2)=2.0D0*(GA2(I)-GA2(I+1))*R(I)**2
20    CONTINUE
C
      B(2*N,2*N-1)=(Q(2,3,N)+AL(N)*Q(3,3,N))*R(N)**(AL(N)-1.0D0)
      B(2*N,2*N)=(Q(2,3,N)-AL(N)*Q(3,3,N))*R(N)**(-AL(N)-1.0D0)
      B(2*N,2*N+1)=Q(1,3,N)+GA1(N)*(Q(2,3,N)+Q(3,3,N))
      B(2*N,2*N+2)=(Q(3,6,N)+GA2(N)*(Q(2,3,N)+2.0D0*Q(3,3,N)))*R(N)
C
      DO 30  I=1,N
           F1=Q(1,2,I)+AL(I)*Q(1,3,I)
           F2=Q(1,2,I)-AL(I)*Q(1,3,I)
           F3=Q(1,1,I)+GA1(I)*(Q(1,2,I)+Q(1,3,I))
           F5=GA2(I)*(Q(1,2,I)+2.0D0*Q(1,3,I))+Q(1,6,I)
```

```
C
          AL1=AL(I)+1.0D0
          AL2=-AL(I)+1.0D0
C
      B(2*N+1,2*I-1)=F1*(R(I)**AL1-R(I-1)**AL1)/AL1
      B(2*N+1,2*I)=F2*(R(I)**AL2-R(I-1)**AL2)/AL2
      B(2*N+1,2*N+1)=B(2*N+1,2*N+1)+F3*(R(I)**2-R(I-1)**2)/2.0D0
      B(2*N+1,2*N+2)=B(2*N+1,2*N+2)+F5*(R(I)**3-R(I-1)**3)/3.0D0


          AL3=AL(I)+2.0D0
          AL4=-AL(I)+2.0D0

          H1=Q(2,6,I)+AL(I)*Q(3,6,I)
          H2=Q(2,6,I)-AL(I)*Q(3,6,I)
          H3=Q(1,6,I)+GA1(I)*(Q(2,6,I)+Q(3,6,I))
          H5=GA2(I)*(Q(2,6,I)+2.0D0*Q(3,6,I))+Q(6,6,I)
      B(2*N+2,2*I-1)=H1*(R(I)**AL3-R(I-1)**AL3)/AL3
      B(2*N+2,2*I)=H2*(R(I)**AL4-R(I-1)**AL4)/AL4
      B(2*N+2,2*N+1)=B(2*N+2,2*N+1)+H3*(R(I)**3-R(I-1)**3)/3.0D0
      B(2*N+2,2*N+2)=B(2*N+2,2*N+2)+H5*(R(I)**4-R(I-1)**4)/4.0D0
30    CONTINUE


              DO 100  I=1,2*N+2
              DO 100  J=1,2*N+2
CC                  WRITE(3,90)I,J,B(I,J)
CC90     FORMAT('B(',I1,',',I2,')= ',D20.7)
 100              CONTINUE



      RETURN
      END
C     ***********************************************************
C
      SUBROUTINE LOAD(PIN,POUT,FZ,TORQ,R,NLAYER,RHS)
      IMPLICIT DOUBLE PRECISION (A-H,O-Z)
      DIMENSION RHS(50),R(0:50)
C     RIGHT HAND SIDE OF EQUATIONS
C
      N=2*NLAYER+2
      CF=DBLE(3.1415927*2.0)
      RC=(R(0)+R(NLAYER))/2.0D0
      DO 10  I=1,N
           RHS(I)=0.0D0
10    CONTINUE
           RHS(1)=-PIN
           RHS(N-2)=-POUT
           RHS(N-1)=-(POUT*R(NLAYER)**2-PIN*R(0)**2)/2.0D0
     $              +FZ/CF
C          rhs(n-1)=fz/cf
C          rhs(n-1)=0.0d0
          RHS(N)=TORQ/(CF*RC)
      DO 20  I=1,N
CC          WRITE(3,30)I,RHS(I)
CC30         FORMAT(' RHS(',I3,')=  ',D20.10)
20    CONTINUE
      RETURN
      END
C
```

```
C  THIS SUBROUTINE FINDS THE SOLUTION OF A SET OF SIMULTANEOUS LINEAR
C  EQUATIONS USING THE GAUSS-JORDON ELIMATION METHOD. THE SOLUTION USES
C  RECURSION TO IMPROVE ACCURACY WHEN THE SET OF EQUATIONS IS ILL-
C  CONDITIONED. THE EQUATION SET IS
C              B . X = RHS
C              =   -   --
C  THE MATRIX OF COEFFICIENTS IS OF RANK ( NEQV X NEQH )
C  WHERE NEQV IS THE NUMBER OF COLUMNS AND NEQH IS THE NUMBER OF ROWS.

C  NOTE THAT THIS ROUTINE IS A MODIFIED VERSION OF THAT APPEARING IN
C  "LINEAR EQUATIONS" BY                    , PUBLISHED BY




      SUBROUTINE GAUSJO(NEQH,NEQV,B,RHS,ANS,NEQ)
      IMPLICIT DOUBLE PRECISION(A-H,O-Z)
      DIMENSION  X(50),B(50,50),RHS(50),UL(50,50)
      DIMENSION LR(50),ANS(50)
C

      NEQH0=NEQH
      NEQV0=NEQV

      CALL SHIFT(RHS,B,NEQ,NEQH0,NEQV0,LR)
      CALL DECOMP(NEQ,B,UL)
      CALL SOLVE(NEQ,UL,RHS,X)
      CALL IMPRUV(NEQ,B,UL,RHS,X)
      CALL VECTOR(NEQ,NEQV,LR,X,ANS)


      RETURN
      END
C     **********************************************************
C
      SUBROUTINE SHIFT(RHS,B,NEQ,NEQH0,NEQV0,LR)
      IMPLICIT DOUBLE PRECISION (A-H,O-Z)
      DIMENSION RHS(50),B(50,50),LR(50)
C      ROTATE ZERO COLUMNS OUT
C
C  FILL IN B MATRIX TO SQUARE
      MM=MAX0(NEQH0,NEQV0)+1
      DO 2   I=NEQV0+1,MM
           RHS(I)=0.0D0
      DO 2   J=1,MM
           LR(J)=0.0D0
2          B(I,J)=0.0D0

      DO 3   I=1,MM
      DO 3   J=NEQH0+1,MM
3          B(I,J)=0.0D0



C
```

```
C  FIND ZERO EQUATIONS

      DO 7   I=1,NEQH0
           IC=0
           DO 6   J=1,NEQV0
                IF(B(I,J).NE.0.0D0)IC=IC+1
6          CONTINUE
           IF(IC.NE.0)LR(I)=0
           IF(IC.EQ.0)LR(I)=1
7     CONTINUE

C  ROTATE ZERO ROWS OUT
5     IT=0
      IH=0
C
      DO 130  I=1,NEQH0
           IF(I.GT.NEQH0-IH)GOTO 130
           IC=0
           DO 110  J=1,NEQV0
                IF(B(I,J).NE.0.0D0)IC=IC+1
110          CONTINUE
                IF(IC.NE.0) GOTO 130
           DO 120  K=I,NEQH0-IH
                DO 115  J=1,NEQV0
                     IF(K.GT.NEQH0-IH)GOTO 120
                     B(K,J)=B(K+1,J)
115               CONTINUE
                IF(K.GE.NEQH0-IH)GOTO 120
                RHS(K)=RHS(K+1)
120          CONTINUE
           IH=IH+1
130   CONTINUE
           NEQH0=NEQH0-IH


C  ROTATE ZERO COLUMNS OUT

      DO 30   J=1,NEQV0
           IF(J.GT.NEQV0-IT)GOTO 30
           IC=0
           DO 10   I=1,NEQH0
                IF(B(I,J).NE.0.0D0)IC=IC+1
10         CONTINUE
           IF(IC.NE.0)GOTO 30
           DO 20  K=J,NEQV0-IT
           DO 20  I=1,NEQH0
                IF(K.GT.NEQV0-IT)GOTO 20
                B(I,K)=B(I,K+1)
20         CONTINUE
           IT=IT+1
30    CONTINUE
           NEQV0=NEQV0-IT
35    CONTINUE

C
C     CHECK MATRIX
C
      IF(IT.EQ.0.AND.IH.EQ.0)GOTO 140
      GOTO 5
140    CONTINUE
C
      NEQ=MIN0(NEQH0,NEQV0)
```

```
C
      DO 40 I=1,NEQ
      DO 40 J=1,NEQ
CC       WRITE(*,420)I,J,B(I,J),I,RHS(I)
CC420    FORMAT('BS(',I3,',',I3,')=',D20.7,' RH(',I3,')=  ',D20.7)
40     CONTINUE



      RETURN
      END
C
C     ***************************************************
C
      SUBROUTINE DECOMP(NEQ,B,UL)
      IMPLICIT DOUBLE PRECISION (A-H,O-Z)
      DIMENSION IPS(50),UL(50,50),SCALES(50),B(50,50)
      COMMON IPS
      N=NEQ
C
C     INITIALIZE IPS,UL AND SCALES
      DO 5   I=1,N
           IPS(I)=I
           ROWNRM=0.0D0
           DO 2   J=1,N
                UL(I,J)=B(I,J)
                IF(ROWNRM-DABS(UL(I,J))) 1,2,2
1     ROWNRM=DABS(UL(I,J))
2     CONTINUE
      IF(ROWNRM) 3,4,3
3     SCALES(I)=1.0D0/ROWNRM
      GOTO 5
4     CALL SING(1)
      SCALES(I)=0.0D0
5     CONTINUE
C
C     GAUSSIAN ELIMINATION WITH PARTIAL PIVOTING
C
      NM1=N-1
      DO 17  K=1,NM1
           BIG=0.0D0
           DO 11  I=K,N
                IP=IPS(I)
                SIZE=DABS(UL(IP,K))*SCALES(IP)
                IF(SIZE-BIG) 11,11,10
10                   BIG=SIZE
                     IDXPIV=I
11         CONTINUE
           IF(BIG)13,12,13
12              CALL SING(2)
                GOTO 17
13         IF(IDXPIV-K) 14,15,14
14              J=IPS(K)
                IPS(K)=IPS(IDXPIV)
                IPS(IDXPIV)=J
15         KP=IPS(K)
           PIVOT=UL(KP,K)
           KP1=K+1
           DO 16  I=KP1,N
                IP=IPS(I)
                EM=-UL(IP,K)/PIVOT
```

```
                UL(IP,K)=-EM
                DO 16  J=KP1,N
                    UL(IP,J)=UL(IP,J)+EM*UL(KP,J)
16          CONTINUE
17     CONTINUE
       KP=IPS(N)
       IF(UL(KP,N)) 19,18,19
18     CALL SING(2)
19     RETURN
       END
C
C      ********************************************************
C
C
       SUBROUTINE SOLVE(NEQ,UL,RHS,X)
       IMPLICIT DOUBLE PRECISION (A-H,O-Z)
       DIMENSION RHS(50),X(50),UL(50,50),IPS(50)
       COMMON IPS
       N=NEQ
       NP1=N+1
C
       IP=IPS(1)
       X(1)=RHS(IP)
       DO 2   I=2,N
            IP=IPS(I)
            IM1=I-1
            SUM=0.0D0
            DO 1   J=1,IM1
1                SUM=SUM+UL(IP,J)*X(J)
2      X(I)=RHS(IP)-SUM
C
       IP=IPS(N)
       X(N)=X(N)/UL(IP,N)
       DO 4   IBACK=2,N
            I=NP1-IBACK
            IP=IPS(I)
            IP1=I+1
            SUM=0.0D0
            DO 3   J=IP1,N
3                SUM=SUM+UL(IP,J)*X(J)
4      X(I)=(X(I)-SUM)/UL(IP,I)
       RETURN
       END
C
C      ********************************************************
C
       SUBROUTINE IMPRUV(NEQ,B,UL,RHS,X)
       IMPLICIT DOUBLE PRECISION(A-H,O-Z)
       DIMENSION X(50),RHS(50),DX(50),RS(50),B(50,50),UL(50,50)
       N=NEQ
       EPS=1.0D-19
       ITMAX=50
15     XNORM=0.0D0
       DO 1   I=1,N
1           XNORM=DMAX1(XNORM,DABS(X(I)))
       IF(XNORM) 3,2,3
2           DIGITS=-DLOG10(EPS)
            GOTO 11
C
3      DO 9   ITER=1,ITMAX
            DO 5   I=1,N
                DSUM=0.0D0
```

```
                DO 4   J=1,N
                    BIJ=B(I,J)
                    XJ=X(J)
4                    DSUM=DSUM+XJ*BIJ
                    DSUM=RHS(I)-DSUM
5           RS(I)=DSUM
      CALL SOLVE(N,UL,RS,DX)
      DXNORM=0.0D0
           DO 6   I=1,N
                T=X(I)
                X(I)=X(I)+DX(I)
                DXNORM=DMAX1(DXNORM,DABS(X(I)-T))
6           CONTINUE
      IF(N.LT.5)GOTO 12
      IF(N.GE.5.AND.DABS(X(3)).GT.1.0D10)GOTO 10
12          IF(ITER-1) 8,7,8
7                DIGITS=-DLOG10(DMAX1(DXNORM/XNORM,EPS))
                CN=1.0D0/EPS*10.0D0**(-DIGITS)
C                 PRINT *,'CONDITION IS ',CN
8           IF(DXNORM-EPS*XNORM) 11,11,9
9     CONTINUE
C     ITERATION DID NOT CONVERGE
C      NEQ=NEQ-1
      CALL SING(3)
11     CONTINUE
10     RETURN
      END
C
C     ***************************************************
C
      SUBROUTINE SING(IWHY)
11     FORMAT('MATRIX WITH ZERO ROW IN DECOMPOSE')
12     FORMAT('SINGULAR MATRIX IN DECOMPOSE. ZERO DIVIDE IN SOLVE')
13     FORMAT('NO CONVERGENCE IN IMPROVE. MATRIX IS NEARLY SINGULAR')
      GOTO (1,2,3),IWHY
1      WRITE(6,11)
      GOTO 10
2      WRITE(6,12)
      GOTO 10
3      CONTINUE
C3      WRITE(6,13)
10     RETURN
      END
C
C     ***************************************************
C
C
      SUBROUTINE VECTOR(NEQ,NEQV,LR,X,ANS)
C
C     SUBROUTINE REINSERTS ZEROS INTO SOLUTION AND STORES AND DISPLAY
C     RESULTS IN A MEANINGFUL USER FORM
C
      IMPLICIT DOUBLE PRECISION(A-H,O-Z)
      DIMENSION ANS(50),X(50)
      DIMENSION LR(50)

      I=1
      DO 20   J=1,NEQV
           IF(LR(J).EQ.0.AND.I.LE.NEQ) THEN
              ANS(J)=X(I)
              I=I+1
           ELSE IF(LR(J).EQ.1.AND.J.LE.NEQV) THEN
```

```
            ANS(J)=0.0D0
          ENDIF
20     CONTINUE

C

C       DO 30  I=1,NEQV
CC30      PRINT*,'ANS(',I,')= ',ANS(I)



      RETURN
      END
C     ***************************************************
C
      SUBROUTINE SOLCHK(B,X,RHS,NEQ)
      IMPLICIT DOUBLE PRECISION(A-H,O-Z)
      DIMENSION X(50),RHS(50),RCHK(50),B(50,50)
      N=NEQ
      DO 10  I=1,N
      RCHK(I)=0.0D0
      DO 20  J=1,N
           RCHK(I)=RCHK(I)+B(I,J)*X(J)
20    CONTINUE
           RCHK(I)=DABS(RHS(I)-RCHK(I))
          PRINT*,'RCHK = ',RCHK(I)
10    CONTINUE
      RETURN
      END

C*******************************
C
C
C
      DOUBLE PRECISION FUNCTION UNI()
      PARAMETER(
     *   CSAVE=362436./16777216. ,
     *   CD=7654321./16777216.,
     *   CM=16777213./16777216. )
C                        2**24=16777216
      DOUBLE PRECISION U(17),S,T,USTART,C,UNIB
      INTEGER I,J,II,JJ,K,KK,I1,J1,K1,L1,M1,ISEED
C
      SAVE U,I,J,K,C
C     Load data array in case user forgets to initialize.
C     This array is the result of calling UNI 100000 times
C       with ISEED=305 and K=64.
      DATA U/
     *0.8668672834238,  0.3697986366357,  0.8008968294805,
     *0.4173889774680,  0.8254561579836,  0.9640965269077,
     *0.4508667414265,  0.6451309529668,  0.1645456024730,
     *0.2787901807898,  0.06761531340295, 0.9663226330820,
     *0.01963343943798, 0.02947398211399, 0.1636231515294,
     *0.3976343250467,  0.2631008574685/
      DATA I,J,K,C/17,5,24,CSAVE/
C
C  Basic generator is Fibonacci
C
      UNI = U(I)-U(J)
      IF(UNI.LT.0.0)UNI = UNI+1.0
      U(I) = UNI
      I = I-1
```

```
      IF(I.EQ.0)I = 17
      J = J-1
      IF(J.EQ.0)J = 17
C
C     Second generator is congruential
C
      C = C-CD
      IF(C.LT.0.0) C=C+CM
C
C     Combination generator
C
      UNI = UNI-C
      IF(UNI.LT.0.0)UNI = UNI+1.0
      RETURN
C
      ENTRY USTART(ISEED)
C
C         Set up ...
C         Convert ISEED to four smallish positive integers.
C
       I1 = MOD(ABS(ISEED),177)+1
       J1 = MOD(ABS(ISEED),167)+1
       K1 = MOD(ABS(ISEED),157)+1
       L1 = MOD(ABS(ISEED),147)+1
C
C            Generate random bit pattern in array based on given seed.
C
       DO 2 II = 1,17
        S = 0.0
        T = 0.5
C           Do for each of the bits of mantissa of word
C           Loop  over K bits, where K is defaulted to 24 but can
C             be changed by user call to UNIB(K)
        DO 3 JJ = 1,K
              M1 = MOD(MOD(I1*J1,179)*K1,179)
              I1 = J1
              J1 = K1
              K1 = M1
              L1 = MOD(53*L1+1,169)
              IF(MOD(L1*M1,64).GE.32)S=S+T
    3         T = .5*T
    2  U(II) = S
       USTART = FLOAT(ISEED)
       RETURN
C
       ENTRY UNIB(KK)
        IF(KK.LE.24)THEN
           K=24
        ELSE
           K=KK
        ENDIF
        UNIB=FLOAT(K)
        RETURN
        END
```

```
C*************************************************************
C
C       program name: GPLY.FOR (2-D)
C       date written: 7/03/90
C           updated: 26/07/90
C       program type: MAIN
C     calls data file: PLY.DAT
C     WHERE    NVAR=NUMBER OF WIND ANGLES + NUMBER OF THICKNESS ANGLES
C           FOR EXAMPLE, IF   NVAR=5
C                     THEN  NWA=3
C                     AND   NTA=2
C              X(1,2,3)=WIND ANGLE VARIABLES
C              X(4,5)=THICKNESS ANGLE VARIABLES
C
C   subroutine file(s): SUBPLY.OBJ
C
C   description: COMPUTES SELECTED PARAMETERS FOR A VARIABLY DISTRIBUTED
C              ANGLE-PLIED LAMINATE
C                 WHERE ICRIT=
C
C                     1 = MAX. STRAIN
C                     2 = MAX. STRESS
C                     3 = TSAI-HILL
C                     4 = HOFFMAN
C                     5 = TSAI-WU
C
C    PRINTOUT = 3
C    TERMINAL = 6
C    FILE     = 10
C
C*************************************************************
      IMPLICIT DOUBLE PRECISION(A-H,O-Z)
      COMMON /VESPAR/PIN
      DIMENSION R(0:50),THETA(50),MT(50),X(0:50)
      OPEN(UNIT=6, FILE='CON')
      OPEN(UNIT=3, FILE='PRN')
      OPEN(UNIT=7, FILE='PLY.DAT')
      OPEN(UNIT=10,FILE='GPLY.RES')
      CF=1.0/57.2957795131

      WRITE(6,364)
364    FORMAT(1X,'INPUT PRESSURE (IN MPA):')
      READ(6,*) PIN
C      PIN=200.0
      PIN=PIN*1E06

      READ(7,707) NVAR
      READ(7,808) (X(I), I=1,7)
      READ(7,808) BA
      READ(7,707) LUN
707    FORMAT(I5)
808    FORMAT(F16.9)

      R(0)=0.03175
      POUT=0.0
      TORQ=0.0
      FZ=0.0

      NLAYER=NVAR+1
      NWA=(NVAR+1)/2
      NTA=NWA-1
      TLAM=R(0)*(BA-1.0)
```

```
      WRITE(LUN,423)
423    FORMAT(/,1X,70("))
      WRITE(LUN,421)BA
421    FORMAT(1X,'B/A =',F5.3)

      RANGE=DBLE(TLAM/NTA)
       R(NLAYER)=R(0)+TLAM

      DO 46 I=1,NTA
       R(2*I)=R(0)+RANGE*(DSIN(X(NWA+I)*CF)*DSIN(X(NWA+I)*CF)
     $   +I-1)
       R(2*I-1)=(R(2*I)+R(2*I-2))/2.0
46     CONTINUE
       R(NLAYER-1)=(R(NLAYER)+R(NLAYER-2))/2.0

C     SET FIBRE TYPE
       DO 86 LN=1,NLAYER
        MT(LN)=1
86     CONTINUE

       DO 57 K=1,NWA
       THETA(2*K-1)=X(K)*CF
       THETA(2*K)=-THETA(2*K-1)
        THICKN=R(2*K)-R(2*K-2)
        WRITE(LUN,288)K,THICKN
288      FORMAT(1X,'THICKNESS FOR LAYER',I2,'=',F12.9,' m')
57     CONTINUE

      CALL EXACT(R,NLAYER,THETA,MT,POUT,TORQ,FZ,LUN)
87       CONTINUE
        STOP
        END

C*****************************************************************

      SUBROUTINE DEFORM(NLAYER,NEQ,ANS,AL,GA1,GA2,R,Q,THETA,LUN)
      IMPLICIT DOUBLE PRECISION(A-H,O-Z)
      COMMON /VESPAR/PIN
      DIMENSION ANS(50),AL(50),GA1(50),GA2(50),R(0:50),RR(3)
      DIMENSION STRESS(6,6),STRAIN(6,6),Q(6,6,50),THETA(50)
      DIMENSION EPS(6,6,20),EPSR(6,6,20),SIG(6,6,20),SIGR(6,6,20)
      DIMENSION THILL(6,20),HOFF(6,20),TWU(6,20)

C     STRAIN AND STRENGTH DATA FOR XAS

       E1T=0.0133
       E2T=0.0048
       E2C=0.0235
       E3T=E2T
       E3C=E2C
       ESH=0.00832

       X=1960.0E06
       YT=38.6E06
       YC=200.0E06
       ZT=YT
       ZC=YC
       SH=42.2E06

      CF1=57.2957795131

      WRITE(LUN,543)
```

```
      WRITE(LUN,544)
543   FORMAT(/,10X,'STRAINS AND STRESSES - MATERIAL DIRECTIONS')
544   FORMAT(/,2X,'STRAIN -1-',5X,'STRAIN -2-',5X,'STRAIN -3-',
     $ 5X,'STRAIN -6-',7X,'HELIX')

      DO 30 LN=1,NLAYER
      AI=ANS(2*LN-1)
      BI=ANS(2*LN)

C     I=1 IS INNER; I=2 IS MID; I=3 IS OUTER FOR THE LAMINA
      RR(1)=R(LN-1)
      RR(2)=(R(LN-1)+R(LN))/2.0D0
      RR(3)=R(LN)

C     CALCULATE INNER, MID, AND OUTER STRAINS,STRESSES, DISPLACEMENTS

      DO 20   I=1,3

C     STRAINS
         STRAIN(I,6)=ANS(NEQ)*RR(I)
         STRAIN(I,1)=ANS(NEQ-1)
            A1=AI*RR(I)**(AL(LN)-1.0D0)
            A2=BI*RR(I)**(-AL(LN)-1.0D0)
            A3=GA2(LN)*STRAIN(I,6)
         STRAIN(I,2)=A1+A2+GA1(LN)*STRAIN(I,1)+A3
         STRAIN(I,3)=AL(LN)*A1-AL(LN)*A2+GA1(LN)*STRAIN(I,1)+2.0D0*A3
         STRAIN(I,4)=0.0D0
         STRAIN(I,5)=0.0D0

C     STRESSES
         DO  10  J=1,6
            STRESS(I,J)=0.0D0
         DO 10   K=1,6
10          STRESS(I,J)=STRESS(I,J)+Q(J,K,LN)*STRAIN(I,K)

20       CONTINUE

C     ROTATE TO MATERIAL DIRECTIONS

      DO 80 I=1,3,2

      S=DSIN(THETA(LN))
      C=DCOS(THETA(LN))
      S2=S*S
      C2=C*C

      EPS(I,1,LN)=C2*(STRAIN(I,1))+S2*(STRAIN(I,2))+
     $  C*S*(STRAIN(I,6))
      EPS(I,2,LN)=S2*(STRAIN(I,1))+C2*(STRAIN(I,2))-
     $  C*S*(STRAIN(I,6))
      EPS(I,3,LN)=-2.0*C*S*(STRAIN(I,1))+2.0*C*S*
     $ (STRAIN(I,2))+(C2-S2)*(STRAIN(I,6))
      EPS(I,4,LN)=STRAIN(I,3)

      SIG(I,1,LN)=C2*(STRESS(I,1))+S2*(STRESS(I,2))+
     $  2.0*C*S*(STRESS(I,6))
      SIG(I,2,LN)=S2*(STRESS(I,1))+C2*(STRESS(I,2))-
     $  2.0*C*S*(STRESS(I,6))
      SIG(I,3,LN)=-C*S*(STRESS(I,1))+C*S*
     $ (STRESS(I,2))+(C2-S2)*(STRESS(I,6))
      SIG(I,4,LN)=STRESS(I,3)
```

```
C     CALCULATE STRAIN AND STRESS RATIOS

      EPSR(I,1,LN)=ABS(EPS(I,1,LN)/E1T)

      IF(EPS(I,2,LN).GT.0)THEN
        EPSR(I,2,LN)=EPS(I,2,LN)/E2T
      ELSE
        EPSR(I,2,LN)=EPS(I,2,LN)/(-E2C)
      END IF

      IF(EPS(I,4,LN).GT.0)THEN
        EPSR(I,4,LN)=EPS(I,4,LN)/E3T
      ELSE
        EPSR(I,4,LN)=EPS(I,4,LN)/(-E3C)
      END IF

      EPSR(I,3,LN)=ABS(EPS(I,3,LN)/ESH)

      SIGR(I,1,LN)=ABS(SIG(I,1,LN)/X)
       IF(SIG(I,2,LN).GT.0)THEN
         SIGR(I,2,LN)=SIG(I,2,LN)/YT
         Y=YT
       ELSE
         SIGR(I,2,LN)=SIG(I,2,LN)/(-YC)
         Y=-YC
       END IF

       IF(SIG(I,4,LN).GT.0)THEN
         SIGR(I,4,LN)=SIG(I,4,LN)/ZT
         Z=ZT
       ELSE
         SIGR(I,4,LN)=SIG(I,4,LN)/(-ZC)
         Z=-ZC
       END IF

       SIGR(I,3,LN)=ABS(SIG(I,3,LN)/SH)

C     CONSTANTS FOR FAILURE THEORIES

      A1=1.0/(X*X)
      A2=1.0/(Y*Y)
      A3=1.0/(SH*SH)

      B1=0.5*(2.0/(YT*YC)-A1)
      B2=0.5*(A1)
      B3=B2
      B4=1.0/YT-1.0/YC
      B5=B4
      B6=A3

      F11=A1
      F22=1.0/(YT*YC)
      F12=-0.5*SQRT(F11*F22)
      F13=-0.5*F22
      F66=A3
      F1=0.0
      F2=B4

C     SET RADIAL STRESS=0
       EPS(I,4,LN)=0.0
       SIG(I,4,LN)=0.0
```

```
      THILL(I,LN)=A1*SIG(I,1,LN)*( SIG(I,1,LN)-SIG(I,2,LN) )
     $ + A2*SIG(I,2,LN)**2 + A3*SIG(I,3,LN)**2

      HOFF(I,LN)=B1*( SIG(I,2,LN)-SIG(I,4,LN) )**2
     $ + B2*( SIG(I,4,LN)-SIG(I,1,LN) )**2
     $ + B3*( SIG(I,1,LN)-SIG(I,2,LN) )**2
     $ + B4*SIG(I,2,LN) + B5*SIG(I,4,LN) + B6*SIG(I,3,LN)**2

      TWU(I,LN)=F11*SIG(I,1,LN)**2
     $ + F22*( SIG(I,4,LN)**2+SIG(I,2,LN)**2 )
     $ + 2.0*F12*SIG(I,1,LN)*( SIG(I,4,LN)+SIG(I,2,LN) )
     $ + 2.0*F13*SIG(I,4,LN)*SIG(I,2,LN)
     $ + F2*( SIG(I,4,LN)+SIG(I,2,LN) ) + F66*SIG(I,3,LN)**2

C  PRINTOUT RESULTS

      WRITE(LUN,821) EPS(I,1,LN),EPS(I,2,LN),EPS(I,4,LN),
     $  EPS(I,3,LN),THETA(LN)*CF1
821    FORMAT(1X,5(1PE10.3,5X))

80     CONTINUE
30     CONTINUE

      WRITE(LUN,836)
836    FORMAT(/,2X,'STRESS -1-',5X,'STRESS -2-',5X,'STRESS -3-',
     $  5X,'STRESS -6-')

      DO 37 LN=1,NLAYER
       DO 28 I=1,3,2

       WRITE(LUN,822) SIG(I,1,LN),SIG(I,2,LN),SIG(I,4,LN),
     $   SIG(I,3,LN)
822     FORMAT(1X,4(1PE10.3,5X))
28     CONTINUE
37     CONTINUE

      WRITE(LUN,629)
629    FORMAT(//,10X,'STRAIN AND STRESS RATIOS - MATERIAL DIRECTIONS')
      WRITE(LUN,385)
385    FORMAT(/,2X,' e/E -1- ',6X,' e/E -2- ',6X,' e/E -3- ',
     $  6X,' e/E -6- ')

      DO 70 LN=1,NLAYER
      DO 60 I=1,3,2

      WRITE(LUN,832) EPSR(I,1,LN),EPSR(I,2,LN),EPSR(I,4,LN),
     $  EPSR(I,3,LN)
832    FORMAT(1X,4(1PE10.3,5X))
60     CONTINUE
70     CONTINUE

      WRITE(LUN,945)
945    FORMAT(/,2X,' s/S -1- ',6X,' s/S -2- ',6X,' s/S -3- ',
     $  6X,' s/S -6- ')
      DO 77 LN=1,NLAYER
       DO 66 I=1,3,2

      WRITE(LUN,549) SIGR(I,1,LN),SIGR(I,2,LN),SIGR(I,4,LN),
     $  SIGR(I,3,LN)
549    FORMAT(1X,4(1PE10.3,5X))
66     CONTINUE
77     CONTINUE
```

```
      WRITE(LUN,578)
578    FORMAT(//,10X,'ENERGY METHODS')
      WRITE(LUN,239)
239    FORMAT(/,3X,'TSAI-HILL',7X,'HOFFMAN',8X,'TSAI-WU')

       DO 82 LN=1,NLAYER
        DO 83 I=1,3,2

       WRITE(LUN,957) THILL(I,LN),HOFF(I,LN),TWU(I,LN)
957     FORMAT(1X,3(F10.4,5X))
83      CONTINUE
82      CONTINUE

      RETURN
      END
```

Hooke & Jeeves Search Path

```
B/A = 1.250
        HJ PATTERN SEARCH--- TSAI-WU CRITERION

SEARCH PARAMETERS:
ITMAX= 500   NKAT=  4   EPSY=0.00001000   ALPHA= 1.00   BETA= 0.50

INITIAL X VALUES:          EPS VALUES:
  80.00                    4.00
  85.00                    4.00


 NUMBER OF FUNCTION EVALUATIONS =     5
END OF EACH PATTERN SEARCH
OBJECTIVE FUNCTION=        16.901574970
X VALUES:
X( 1)= 76.00000
X( 2)= 81.00000


 NUMBER OF FUNCTION EVALUATIONS =    10
END OF EACH PATTERN SEARCH
OBJECTIVE FUNCTION=        12.447318629
X VALUES:
X( 1)= 68.00000
X( 2)= 73.00000


 NUMBER OF FUNCTION EVALUATIONS =    15
END OF EACH PATTERN SEARCH
OBJECTIVE FUNCTION=         2.576609498
X VALUES:
X( 1)= 56.00000
X( 2)= 61.00000


 NUMBER OF FUNCTION EVALUATIONS =    20
END OF EACH PATTERN SEARCH
OBJECTIVE FUNCTION=         2.576609498
X VALUES:
X( 1)= 44.00000
X( 2)= 49.00000

  STEP SIZE REDUCED  1 TIMES


 NUMBER OF FUNCTION EVALUATIONS =    25
END OF EACH PATTERN SEARCH
OBJECTIVE FUNCTION=         1.439338881
X VALUES:
X( 1)= 54.00000
X( 2)= 59.00000


 NUMBER OF FUNCTION EVALUATIONS =    30
END OF EACH PATTERN SEARCH
OBJECTIVE FUNCTION=         1.071763546
```

```
X VALUES:
X( 1)= 52.00000
X( 2)= 57.00000

 STEP SIZE REDUCED  2 TIMES


 NUMBER OF FUNCTION EVALUATIONS =     34
END OF EACH PATTERN SEARCH
OBJECTIVE FUNCTION=        1.060718939
X VALUES:
X( 1)= 52.00000
X( 2)= 58.00000


 NUMBER OF FUNCTION EVALUATIONS =     39
END OF EACH PATTERN SEARCH
OBJECTIVE FUNCTION=        1.060718939
X VALUES:
X( 1)= 50.00000
X( 2)= 57.00000

 STEP SIZE REDUCED  3 TIMES


 NUMBER OF FUNCTION EVALUATIONS =     44
END OF EACH PATTERN SEARCH
OBJECTIVE FUNCTION=        1.050861133
X VALUES:
X( 1)= 51.50000
X( 2)= 58.00000


 NUMBER OF FUNCTION EVALUATIONS =     48
END OF EACH PATTERN SEARCH
OBJECTIVE FUNCTION=        1.045236918
X VALUES:
X( 1)= 51.00000
X( 2)= 58.50000


 NUMBER OF FUNCTION EVALUATIONS =     53
END OF EACH PATTERN SEARCH
OBJECTIVE FUNCTION=        1.040577990
X VALUES:
X( 1)= 50.50000
X( 2)= 59.00000

 STEP SIZE REDUCED  4 TIMES


 NUMBER OF FUNCTION EVALUATIONS =     58
END OF EACH PATTERN SEARCH
OBJECTIVE FUNCTION=        1.040577990
X VALUES:
X( 1)= 51.00000
X( 2)= 58.50000

FINAL EPS VALUES:          FINAL X VALUES:
EPS( 1)= 0.25000           X( 1)= 51.00000000
EPS( 2)= 0.25000           X( 2)= 58.50000000
```

THE MINIMUM FUNCTION VALUE IS: 1.040577990

NUMBER OF FUNCTION EVALUATIONS= 58

Appendix B

Jones' Algorithm

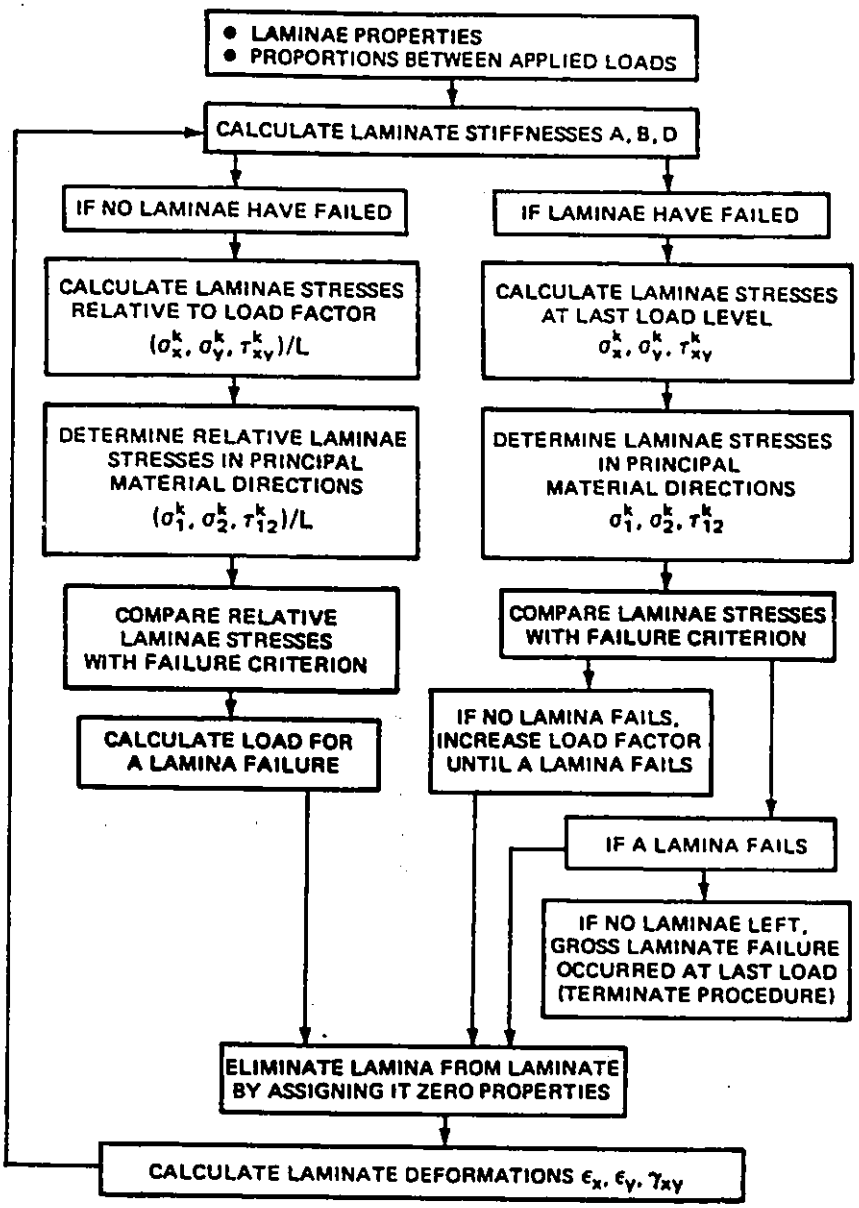
• LAMINAE PROPERTIES
• PROPORTIONS BETWEEN APPLIED LOADS
CALCULATE LAMINATE STIFFNESSES A, B, D
IF NO LAMINAE HAVE FAILED
IF LAMINAE HAVE FAILED
CALCULATE LAMINAE STRESSES RELATIVE TO LOAD FACTOR
$(\sigma_x^k, \sigma_y^k, \tau_{xy}^k)/L$
CALCULATE LAMINAE STRESSES AT LAST LOAD LEVEL
$\sigma_x^k, \sigma_y^k, \tau_{xy}^k$
DETERMINE RELATIVE LAMINAE STRESSES IN PRINCIPAL MATERIAL DIRECTIONS
$(\sigma_1^k, \sigma_2^k, \tau_{12}^k)/L$
DETERMINE LAMINAE STRESSES IN PRINCIPAL MATERIAL DIRECTIONS
$\sigma_1^k, \sigma_2^k, \tau_{12}^k$
COMPARE RELATIVE LAMINAE STRESSES WITH FAILURE CRITERION
COMPARE LAMINAE STRESSES WITH FAILURE CRITERION
CALCULATE LOAD FOR A LAMINA FAILURE
IF NO LAMINA FAILS, INCREASE LOAD FACTOR UNTIL A LAMINA FAILS
IF A LAMINA FAILS
IF NO LAMINAE LEFT, GROSS LAMINATE FAILURE OCCURRED AT LAST LOAD (TERMINATE PROCEDURE)
ELIMINATE LAMINA FROM LAMINATE BY ASSIGNING IT ZERO PROPERTIES
CALCULATE LAMINATE DEFORMATIONS $\epsilon_x, \epsilon_y, \gamma_{xy}$

Appendix C

WPARAM listing

```
C*****************************************************************
C   WPARAM.FOR
C
C   PROGRAMMER: M.TENACE 10/90
C
C
C******* THIS PROGRAM CALCULATES THE WIND PARAMETERS FOR   C              GIVEN PRESSURE VESSEL
C
C       DESCRIPTION OF VARIABLES
C
C
C     HELIX :  HELIX ANGLE (DEGREES)
C     B : OUTER RADIUS (INCHES)
C     A : BOSS RADIUS (INCHES)
C     EDGE : Y DISTANCE FROM END OF VESSEL TO RADIAL PINS
C     Y,MRES :MOTOR RESOLUTION=400 PULSES/REV FOR HALF STEP MODE
C                  =200 FOR FULL STEP MODE
C     RSF : ROTATION CONVERSION FACTOR FOR EYE = 1250 PULSES/DEGREE
C     YADV : Y ADVANCE OF SCREW = 6 ROTATIONS OF SCREW/INCH
C     MAM : MANDREL MOTOR ACCELERATION
C     FR : FIBRE FEED RATE (INCHES/SEC)
C     LC : PIN-TO-PIN Y DISTANCE ALONG VESSEL
C     LP : RADIAL LENGTH OF PINS
C     XC : X DISTANCE FROM END OF PINS TO PAYOUT EYE
C     GRM : GEAR REDUCTION FOR MANDREL (SEE TABLE)
C          54 LO: 1872/56640       315 HI: 5265/28800
C          90 LO: 5200/100990      500 HI: 14625/51300
C         140 LO: 6864/86730       775 HI: 19305/44100
C         224 LO: 8736/70800      1200 HI: 24570/36000
C
C
C
C     GRY : GEAR REDUCTION FOR Y AXIS : 13/20
C
C
C
C*****************************************************************
      IMPLICIT REAL (A-Z)
      INTEGER LUN

      PARAMETER (PI=3.141592654)
      OPEN(UNIT=3, FILE='PRINTER')
      OPEN(UNIT=6, FILE='TERMINAL')
C
C  INPUT INITIAL PARAMETERS
C

      LUN=6

      LO54=1872./56640.
      HI315=5265./28800.
      LO90=5200./100890.
      HI500=14625./51300.
      LO140=6864./86730.
      HI775=19305./44100.
      LO224=8736./70800.
      HI1200=24570./36000.

      HELIX=55.0
      B=(2.50/2.0)+(0.129)+(0.1417)+(0.0866/2.)
```

```
      LC=27.5313
      EDGE=0.750
      YRES=400.0
      MRES=400.0
      RSF=1250.0
      YADV=6.0
      LP=0.875
      XC=0.375+0.4063
      FR=2.00
      GRM=LO54
      GRY=13./20.
      MAM=8.
      CON=PI/180.
C
C   START OF COMPUTATIONS
C
      THETA=ACOS(B/(B+LP+XC))
      ARC=THETA*B
      YOFF=ARC/TAN(HELIX*CON)
      PTL=SQRT(ARC*ARC+YOFF*YOFF)
      TL=SQRT((LP+XC)**2+PTL*PTL)
C      YX=(XC*PTL/(XC+LP))*COS(HELIX*CON)
C

C      YD0V=-(YX-EDGE)
C      YD0M=YD0V*YRES*YADV/GRY
C
C  FIRST MOVE
C

      YD1V=YOFF+EDGE
      YD1M=YD1V*YRES*YADV/GRY

      MD1V=YOFF*TAN(HELIX*CON)/(2.*PI)
      MD1M=-MD1V*MRES/GRM

      RD1V=-(90.0-HELIX)
      RD1M=RD1V*RSF

      RD2V=180.0-HELIX
      RD2M=RD2V*RSF
C
C SECOND MOVE
C
      YD2V=LC-2.0*EDGE
      YD2M=YD2V*YRES*YADV/GRY

      MD2V=YD2V*TAN(HELIX*CON)/(2.*PI*B)
      MD2M=-MD2V*MRES/GRM
C
C  THIRD MOVE
C
      YD3V=-(YOFF-EDGE)
      YD3M=YD3V*YRES*YADV/GRY

      MD3V=(1.00-MD1V)/2.
      MD3M=-MD3V*MRES/GRM

C      RD2V=-HELIX
C      RD2M=RD2V*RSF

      MSM=FR/(2*PI*B*GRM)
```

```
      YSM=FR/TAN(HELIX*CON)*6.0/GRY

      YAM=(YSM-0.5)/(MSM-0.5)*MAM


      WRITE(LUN,100)
100    FORMAT(/,'INPUT :  B(in.)    LP(in.)    XC(in.)   HELIX(deg)
     $  FEED RATE(in/sec)')

      WRITE(LUN,200)B,LP,XC,HELIX,FR
200    FORMAT(3X,5(F10.3,3X))

      WRITE(LUN,300)
300    FORMAT(/,'OUTPUT: THETA(rot.)  YOFF(in)  PTL(in.)  TL(in.)')

      WRITE(LUN,400)THETA/(2*PI),YOFF,PTL,TL
400    FORMAT(3X,5(F10.3,2X))

      WRITE(LUN,500)
500    FORMAT(/,'      YD1V(in)     YD2V      YD3V      MD1V(rev)
     $  MD2V       MD3V')

      WRITE(LUN,600)YD1V,YD2V,YD3V,MD1V,MD2V,MD3V
600    FORMAT(3X,6(F10.3,2X))


      WRITE(LUN,650)
650    FORMAT(/,'      YSM(rps)     MSM(rps)  YAM(rpss) MAM(rpss)')

      WRITE(LUN,700)YSM,MSM,YAM,MAM
700    FORMAT(3X,4(F10.3,2X))

      WRITE(LUN,800)
800    FORMAT(/,'PULSES: YD1M    YD2M    YD3M     MD1M    MD2M
     $MD3M')

      WRITE(LUN,900)YD1M,YD2M,YD3M,MD1M,MD2M,MD3M
900    FORMAT(3X,6F9.0,3X)

      STOP
      END
```

Appendix D

Data Acquisition Program

```
10    ! This program computes the strains of up to 12 rosette gages.
20    ! Each card can moniter 3 rosettes, up to a maximum of 4 cards.
30    ! Optionally, 36 single strain gages can be monitored.
40    !
50    ASSIGN @1 TO "INITR"
60    OPTION BASE 1
70    INTEGER Chnum,Pincr,Pressure,Ncard,Port(4),Ns
80    SHORT S_ratio(4,10),U_ratio(4,10),Strn(4,10)
90    COM Scn,Dvm,Svm,Error,Err$,Ercnt$
100   CALL Init(3497)
110   PRINTER IS 0
120   GOTO Input
130 Input:INPUT "Input number of hp strain gage cards (press -CONT- when done)>"
,Ncard
140   FOR N=1 TO Ncard
150     INPUT "Card # < > is in slot # < >",N,Ns
160     Port(N)=Ns
170   NEXT N
180   INPUT "Input initial and increment pressure (in psi)",Pressure,Pincr
190   Initial=0
200   GOTO Bridge_meas
210 Pause:Initial=1
220   DISP "Pressure is";Pressure;"psi...press -CONT- for measurement"
230   PRINT "Pressure is";Pressure;"psi"
240   PAUSE
250   GOTO Bridge_meas
260   ! This routine measures the strained & unstrained bridge voltage ratios
270 Bridge_meas:FOR I=1 TO Ncard
280     FOR J=1 TO 9
290       Chnum=Port(I)*20+J
300       CALL Brmeas(<Chnum),Bridge,Excitation,Ratio)
310       IF Initial=0 THEN
320         U_ratio(I,J)=Ratio
330         MAT PRINT @1;U_ratio
340       ELSE
350         S_ratio(I,J)=Ratio
360       END IF
370     NEXT J
380   NEXT I
390   IF Initial=0 THEN Pause
400   GOTO Strain_comp
410   ! This routine computes the strains
420 Strain_comp:FOR I=1 TO Ncard
430     FOR J=1 TO 9
440       Chnum=Port(I)*20+J
450       A=S_ratio(I,J)
460       B=U_ratio(I,J)
470       Strn(I,J)=FNStrain(1,2.1,1,A,B)
480     NEXT J
490   NEXT I
500   Pressure=Pressure+Pincr
510   GOTO Print
520   ! This routine prints out the strains
530 Print:FOR I=1 TO Ncard
540     FOR J=1 TO 3! No. of rosettes per card
550    PRINT "e";3*(I-1)+J;"(0)=";Strn(I,3*(J-1)+1),"  e";3*(I-1)+J;"(45)=";Strn
(I,3*(J-1)+2);"      e";3*(I-1)+J;"(90)=";Strn(I,3*(J-1)+3)
560     NEXT J
570   NEXT I
580   GOTO Pause
590   END
600   !
610   ! SUBROUTINES
```

```
620   !
630   SUB Brmeas(Channel,Bridge,Excitation,Ratio)
640   ! 87-02-9 C. PILETTE
650     Exc_chn=Channel
660     COM Scn,Dvm,Svm,Error,Err$
670     GOTO Ok !   IF Channel MOD 20<10 THEN Ok
680     Error=2
690     GOTO Abort
700 Ok: OUTPUT Dvm USING "#"
710     STATUS Dvm DIV 100;A,A,A,Here1
720     Here2=4*(Scn<>0)
730     IF Dvm=Scn THEN Chk
740     OUTPUT Scn USING "#"
750     STATUS Scn DIV 100;A,A,A,Here2
760 Chk:Error=2*((Channel<0) OR (Channel>999))+16*(NOT BIT(Here2,2) OR NOT BIT(H
ere1,2) AND (Dvm=Scn))+32*(NOT BIT(Here1,2) AND (Dvm<>Scn))
770     IF Error THEN Abort
780 Read:OUTPUT Scn;"VT4AC";INT(Exc_chn)
790     IF Dvm=Scn THEN OUTPUT Dvm;"VR1VR5VN1VA1VF1VD5VC0VS0VW0VT3"
800     IF Dvm<>Scn THEN OUTPUT Dvm;"HR2R11STI6STGT3"
810     ENTER Dvm;Excitation
820     IF Channel<>Exc_chn THEN Done
830     Bridge=Excitation
840     IF ABS(Bridge)<=.119 THEN Skip
850   ! PRINT
860   ! PRINT "WARNING!  CHANNEL #";INT(Channel)
870   ! PRINT "IMBALANCE NOT READ ON 0.1V RANGE"
880 Skip:Exc_chn=Channel DIV 10*10+10
890     GOTO Read
900 Done:IF (ABS(Excitation)>.1) AND (ABS(Excitation)<5.4) THEN Skip2
910   ! PRINT
920   ! PRINT "WARNING!  BRIDGE EXCITATION FOR"
930   ! PRINT "CHANNEL #";INT(Channel);" IS";ABS(Excitation);"VOLTS"
940   ! PRINT "LIMITS ARE 0.01 TO 5.4 VOLTS"
950 Skip2:IF Excitation<.5 THEN Ovld
960     Ratio=Bridge/Excitation
970     SUBEXIT
980 Abort:Err$="Brmeas"
990     CALL Warn
1000    Bridge=9E19
1010    Excitation=9E19
1020 Ovld:Ratio=9E19
1030  SUBEND
1040  DEF FNStrain(Gages,Gf,Poisson,S_ratio,U_ratio)
1050  ! 87-02-09 C.PILETTE
1060    IF (Gages<>1) AND (Gages<>2) AND (Gages<>4) THEN Error1
1070    IF Gf=0 THEN Error2
1080    Dif=S_ratio-U_ratio
1090    IF (Dif<-1) OR (Dif>1) THEN Error3
1100    IF Gages<>1 THEN Jmp1
1110    Strain=-(4*Dif)/(Gf*(1+2*Dif))
1120    GOTO Format
1130 Jmp1:IF (Poisson<0) OR (Poisson>.5) AND (Poisson<>1) THEN Error4
1140    IF Gages<>2 THEN Jmp2
1150    Strain=-(4*Dif)/(Gf*(1+Poisson-2*Dif*(Poisson-1)))
1160    GOTO Format
1170 Jmp2:Strain=-(2*Dif)/(Gf*(1+Poisson))
1180 Format:Strain=INT(Strain*1000000+.5*SGN(Strain))
1190    RETURN Strain
1200 Error1:PRINT
1210    PRINT "WARNING!  INVALID NO. OF ACTIVE GAGES: PASS PARAMETER Gages=";Gag
```

```
1220    GOTO Error
1230 Error2:PRINT
1240    PRINT "WARNING!  GAGE FACTOR (Gf)=0"
1250    GOTO Error
1260 Error3:    ! PRINT
1270    ! PRINT "WARNING!  BRIDGE OUTPUT TO EXCITATION VOLTAGE RATIO OUT OF RANGE;
1280    ! PRINT "STRAINED=";S_ratio;"  UNSTRAINED=";U_ratio
1290    GOTO Error
1300 Error4:PRINT
1310    PRINT "WARNING! INVALID POISSON RATIO:  PASS PARAMETER Poisson=";Poisson
1320 Error:    ! PRINT "STRAIN NOT COMPUTED"
1330    RETURN 999999
1340  FNEND
1350  SUB Init(Dvmeter)                                    ! 9835/45  REV. A  6/23/80
1360    COM Scn,Dvm,Svm,Error,Err$,Ercnt$
1370    DIM Message$[24]
1380    INTEGER Address
1390    Error=0
1400    IF (Dvmeter<>3456) AND (Dvmeter<>3497) THEN Abort
1410 ! INITIALIZE  DEVICE ADDRESSES
1420    Computer=721          !  SYSTEM COMPUTER
1430    Scn=709               !  3497A SCANNER ADDRESS
1440    Dvm=722               !  3456A DIGITAL VOLTMETER ADDRESS
1450    Svm=724               !  3437A SYSTEM VOLTMETER ADDRESS
1460    Bus=Scn DIV 100
1470    Initdvm=Dvm
1480    IF Dvmeter=3497 THEN Dvm=Scn
1490    Ercnt$=RPT$("0",15)
1500 ! VERIFY THAT INTERFACE IS HP-IB
1510    READ IO Bus,5;Signature !  SIGNATURE OF 98034A HP-IB INTERFACE
1520    IF BIT(Signature,"XX00XXXX") THEN Message$="PRESENT"
1530    IF NOT BIT(Signature,"XX00XXXX") THEN Message$="HP-IB"
1540    IF BIT(Signature,"XX11XXXX") THEN Hpib
1550    OUTPUT 16 USING "@,/,10X,K,K,K,2/,21X,K";"CAUTION:   INTERFACE  #";Bus
;"  IS   NOT   "&Message$;"ABNORMAL TERMINATION OF PROGRAM."
1560    BEEP
1570    STOP
1580 Hpib:ABORTIO Bus                !  INITIALIZES INTERFACE AND BUS
1590    RESET Bus                  !  SENDS DEVICE CLEAR (DCL)
1600 ! CHECK FOR EQUIPMENT ON BUS AT ALL ADDRESSES AND PRINT DEVICE NAMES
1610    OUTPUT 16 USING "@,/,25X,K,DD,K,/";" EQUIPMENT PRESENT ON BUS #"&CHR$(
132);Bus;CHR$(128)
1620    FOR Address=0 TO 30
1630      OUTPUT Bus,Address USING "#"     ! ADDRESS DEVICE TO LISTEN
1640      STATUS Bus;A,A,A,Onbus           ! SEE IF IT LISTENED
1650      IF NOT BIT(Onbus,2) THEN Nxt     ! BIT 2 TRUE IF DEVICE PRESENT
1660      Message$="        Device Unknown"
1670      IF Address=Computer MOD 100 THEN Message$="       System Computer"
1680      IF Address=Scn MOD 100 THEN Message$="3497A  Mainframe"
1690      IF Address=Initdvm MOD 100 THEN Message$="3456A  Digital Voltmeter"
1700      IF Address=Svm MOD 100 THEN Message$="3437A  System Voltmeter"
1710      IF (Dvm=Scn) AND (Address=Scn MOD 100) THEN Message$=Message$&", DVM"
1720      OUTPUT 16 USING Fmt;Message$;Address
1730 Nxt:NEXT Address
1740 Fmt:IMAGE  20X,24A," at address ",ZZ
1750    SUBEXIT
1760 Abort:Error=2
1770    Err$="Init"
1780    CALL Warn
1790  SUBEND
1800  DEF FNRcv(Channel)                                   ! 9835/45  REV. A  6/23/80
1810    COM Scn,Dvm,Svm,Error,Err$
1820    OUTPUT Dvm USING "#"       -
1830    STATUS Dvm DIV 100;A,A,A,Here1
1840    Here2=4*(Scn<>0)                 ! MAKE A DEVICE NOT THERE CLEAR BIT 2
1850    IF (Dvm=Scn) OR (Channel=-1) THEN Chk
1860    OUTPUT Scn USING "#"
1870    STATUS Scn DIV 100;A,A,A,Here2
1880 Chk:Error=2*(((Channel<0) OR (Channel>999)) AND (Channel<>-1))+16*(NOT BIT(
Here2,2) OR NOT BIT(Here1,2) AND (Dvm=Scn))+32*(NOT BIT(Here1,2) AND (Dvm<>Scn))
1890    IF Error THEN Abort
1900    IF Channel<>-1 THEN OUTPUT Scn;"AC";INT(Channel)
1910    IF Dvm=Scn THEN OUTPUT Dvm;"VR5VN1VA1VF1VD5VC0VS0VW0VT3"!3497 SETUP & TR
```

```
1920    IF Dvm<>Scn THEN OUTPUT Dvm;"H1ST16STGT3"                !3456 SETUP & TRG
1930    ENTER Dvm;Reading
1940    RETURN Reading
1950 Abort:Err$="Dcv"
1960    CALL Warn
1970    RETURN 9E19
1980  FNEND
1990  SUB Warn                                                   ! 9845  REV. A  6/23/80
2000    COM Scn,Dvm,Svm,Error,Err$,Ercnt$
2010    DIM Da$[14],Erm$(0:14)[55]
2020    INTEGER Max_warns,Flag,Index,Nerrs,Here
2030    Max_warns=2             ! MAXIMUM NUMBER OF WARNINGS ON EACH ERROR ( <=9 )
2040    Flag=0
2050    IF LEN(Ercnt$)<15 THEN Ercnt$=RPT$("0",15)     ! FILL Ercnt$ IF NECESSARY
2060    FOR Index=0 TO 14                                ! ANY ERRORS THAT NEED WARNINGS?
2070      IF BIT(Error,Index) AND (VAL(Ercnt$[Index+1,Index+1])<Max_warns) THEN
Flag=Flag+2^Index
2080    NEXT Index
2090    IF Flag=0 THEN Exit                                          ! NO...RETURN
2100    MAT READ Erm$                                               ! YES...DO SETUP
2110    Nerrs=0
2120    ON ERROR GOTO Nodate
2130    ON INT #Scn DIV 100 GOTO Nodate
2140    SET TIMEOUT Scn DIV 100;1000
2150    OUTPUT Scn USING "#"
2160    STATUS Scn DIV 100;Dummy,Dummy,Dummy,Here
2170    OFF ERROR
2180    IF NOT BIT(Here,2) THEN Nodate
2190    OUTPUT Scn;"TD"
2200    ENTER Scn;Da$
2210    IF Da$="01:01:00:00:00" THEN Nodate
2220    OUTPUT 0 USING "3(K)";RPT$("*",23);"  Date: "&Da$[1,2]&"/"&Da$[4,5]&"
  Time: "&Da$[7,14]&"  ";RPT$("*",23)
2230    GOTO Warnout
2240 Nodate:OUTPUT 0;RPT$("*",80)
2250 Warnout:OFF ERROR
2260    OUTPUT 0;"WARNING: SUBPROGRAM "&Err$&" WAS NOT EXECUTED"
2270    FOR Index=0 TO 14                              ! IDENTIFY THE INDIVIDUAL ERRORS
2280      IF NOT BIT(Flag,Index) THEN Next_indx
2290      Ercnt$[Index+1,Index+1]=VAL$(VAL(Ercnt$[Index+1,Index+1])+1)! INCREMEN
T
2300      Nerrs=Nerrs+1
2310      OUTPUT 0 USING "4(K)";"  ERROR CODE #";Index;": ";Erm$(Index)
2320      IF VAL(Ercnt$[Index+1,Index+1])=Max_warns THEN OUTPUT 0;"  This is the
 last warning for this error."
2330 Next_indx:NEXT Index
2340    IF Nerrs>1 THEN OUTPUT 0;"SEE THE "&Err$&" DOCUMENTATION TO INTERPRET TH
ESE ERRORS"
2350    IF Nerrs=1 THEN OUTPUT 0;"SEE THE "&Err$&" DOCUMENTATION TO INTERPRET TH
IS ERROR"
2360    OUTPUT 0;RPT$("*",80)
2370    DATA " Passed array is dimensioned improperly."! ERROR MESSAGES IN ORDER
2380    DATA " First pass parameter out of range."
2390    DATA " Second pass parameter out of range."
2400    DATA " Third pass parameter out of range."
2410    DATA " 3497A does not respond to bus commands."
2420    DATA " 3456A does not respond to bus commands."
2430    DATA " 3437A does not respond to bus commands."
2440    DATA " Voltage (resistance) to temp. conversion out of range."
2450    DATA " Thermocouple temp. to volt. conversion out of range."
2460    DATA " Axis endpoints equal_each other."
2470    DATA "Scaling value(=0 on a log axis."
2480    DATA "Datapoint(=0 on a log axis."
2490    DATA "Level crossing not found."
2500    DATA "User definable error."
2510    DATA "User definable error."
2520 Exit:SUBEND
```

Appendix E

Layer Stresses

B/A =1.350
THICKNESS FOR LAYER 1= 0.003303549 m
THICKNESS FOR LAYER 2= 0.003602812 m
THICKNESS FOR LAYER 3= 0.002000662 m
THICKNESS FOR LAYER 4= 0.002205478 m

STRAINS AND STRESSES - MATERIAL DIRECTIONS

STRAIN -1-	STRAIN -2-	STRAIN -3-	STRAIN -6-	HELIX
1.048E-02	7.849E-03	0.000E+00	1.548E-02	5.000E+01
9.224E-03	6.967E-03	0.000E+00	1.337E-02	5.000E+01
9.322E-03	6.869E-03	0.000E+00	-1.334E-02	-5.000E+01
8.310E-03	6.153E-03	0.000E+00	-1.163E-02	-5.000E+01
7.592E-03	6.871E-03	0.000E+00	1.181E-02	4.700E+01
6.773E-03	6.164E-03	0.000E+00	1.029E-02	4.700E+01
6.882E-03	6.054E-03	0.000E+00	-1.027E-02	-4.700E+01
6.221E-03	5.474E-03	0.000E+00	-9.033E-03	-4.700E+01
7.343E-03	4.352E-03	0.000E+00	8.556E-03	5.500E+01
6.950E-03	4.161E-03	0.000E+00	8.008E-03	5.500E+01
7.061E-03	4.050E-03	0.000E+00	-7.927E-03	-5.500E+01
6.718E-03	3.880E-03	0.000E+00	-7.444E-03	-5.500E+01
9.254E-03	1.344E-03	0.000E+00	9.533E-04	8.700E+01
8.776E-03	1.343E-03	0.000E+00	9.065E-04	8.700E+01
8.789E-03	1.330E-03	0.000E+00	-6.587E-04	-8.700E+01
8.404E-03	1.329E-03	0.000E+00	-6.151E-04	-8.700E+01

STRESS -1-	STRESS -2-	STRESS -3-	STRESS -6-
1.440E+09	-7.260E+07	0.000E+00	3.715E+07
1.277E+09	-5.013E+07	0.000E+00	3.209E+07
1.292E+09	-5.084E+07	0.000E+00	-3.201E+07
1.162E+09	-3.162E+07	0.000E+00	-2.792E+07
1.058E+09	-2.643E+07	0.000E+00	2.834E+07
9.526E+08	-1.244E+07	0.000E+00	2.469E+07
9.685E+08	-1.323E+07	0.000E+00	-2.465E+07
8.839E+08	-9.653E+05	0.000E+00	-2.166E+07
1.046E+09	-9.079E+06	0.000E+00	2.053E+07
9.971E+08	1.061E+06	0.000E+00	1.922E+07
1.013E+09	2.568E+05	0.000E+00	-1.903E+07
9.712E+08	9.794E+06	0.000E+00	-1.787E+07
1.337E+09	-8.541E+06	0.000E+00	2.288E+06
1.284E+09	1.305E+07	0.000E+00	2.176E+06
1.286E+09	1.296E+07	0.000E+00	-1.581E+06
1.245E+09	3.290E+07	0.000E+00	-1.476E+06

STRAIN AND STRESS RATIOS - MATERIAL DIRECTIONS

e/E -1-	e/E -2-	e/E -3-	e/E -6-
7.881E-01	1.635E+00	1.226E+00	1.860E+00
6.935E-01	1.452E+00	1.017E+00	1.607E+00
7.009E-01	1.431E+00	1.017E+00	1.603E+00
6.248E-01	1.282E+00	8.429E-01	1.398E+00
5.708E-01	1.431E+00	8.429E-01	1.419E+00
5.092E-01	1.284E+00	7.008E-01	1.236E+00
5.175E-01	1.261E+00	7.008E-01	1.235E+00
4.678E-01	1.140E+00	5.809E-01	1.086E+00
5.521E-01	9.066E-01	5.809E-01	1.028E+00
5.226E-01	8.669E-01	5.063E-01	9.625E-01
5.309E-01	8.437E-01	5.063E-01	9.528E-01
5.051E-01	8.083E-01	4.377E-01	8.947E-01
6.958E-01	2.800E-01	4.377E-01	1.146E-01
6.598E-01	2.798E-01	3.183E-01	1.089E-01
6.606E-01	2.771E-01	3.183E-01	7.917E-02
6.319E-01	2.768E-01	2.099E-01	7.393E-02

s/S -1-	s/S -2-	s/S -3-	s/S -6-
7.346E-01	3.630E-01	1.325E+00	6.902E-01
6.517E-01	2.507E-01	1.061E+00	7.604E-01
6.590E-01	2.542E-01	1.062E+00	7.584E-01
5.928E-01	1.581E-01	8.393E-01	6.616E-01
5.400E-01	1.021E-01	8.322E-01	6.716E-01
4.860E-01	6.218E-02	6.561E-01	5.850E-01
4.941E-01	6.614E-02	6.571E-01	5.842E-01
4.510E-01	4.826E-02	5.067E-01	5.137E-01
5.335E-01	4.540E-02	5.173E-01	4.866E-01
5.087E-01	2.748E-02	4.162E-01	4.555E-01
5.169E-01	6.652E-03	4.173E-01	4.509E-01
4.955E-01	2.537E-01	3.229E-01	4.283E-01
6.821E-01	4.270E-02	3.480E-01	5.421E-02
6.551E-01	3.382E-01	1.664E-01	3.155E-02
6.560E-01	3.357E-01	1.665E-01	3.746E-02
6.354E-01	8.522E-01	3.629E-17	3.498E-02

ENERGY METHODS

TSAI-HILL	HOFFMAN	TSAI-WU
1.4735	0.5066	1.0665
1.0825	0.2971	0.6523
1.0911	0.2984	0.6626
0.8237	0.2671	0.4709
0.7674	0.2879	0.4430
0.5855	0.3416	0.4073
0.5931	0.3348	0.4059
0.4675	0.4474	0.4522
0.5260	0.3448	0.3974
0.4667	0.4883	0.4824
0.4704	0.4756	0.4743
0.4867	0.6095	0.5867
0.4730	0.3020	0.3654
0.5418	0.7224	0.6294
0.5402	0.7201	0.6277
1.1205	1.2222	0.9949

B/A =1.230
THICKNESS FOR LAYER 1= 0.003614615 m
THICKNESS FOR LAYER 2= 0.002008199 m
THICKNESS FOR LAYER 3= 0.002208685 m

STRAINS AND STRESSES - MATERIAL DIRECTIONS

STRAIN -1-	STRAIN -2-	STRAIN -3-	STRAIN -6-	HELIX
1.351E-02	1.291E-02	0.000E+00	8.365E-03	4.700E+01
1.222E-02	1.179E-02	0.000E+00	5.957E-03	4.700E+01
1.221E-02	1.180E-02	0.000E+00	-5.959E-03	-4.700E+01
1.117E-02	1.091E-02	0.000E+00	-4.036E-03	-4.700E+01
1.174E-02	1.034E-02	0.000E+00	3.796E-03	5.500E+01
1.114E-02	1.005E-02	0.000E+00	2.956E-03	5.500E+01
1.112E-02	1.006E-02	0.000E+00	-2.966E-03	-5.500E+01
1.060E-02	9.804E-03	0.000E+00	-2.232E-03	-5.500E+01
1.138E-02	9.023E-03	0.000E+00	2.330E-04	8.700E+01
1.065E-02	9.021E-03	0.000E+00	1.563E-04	8.700E+01
1.065E-02	9.022E-03	0.000E+00	-1.864E-04	-8.700E+01
1.005E-02	9.021E-03	0.000E+00	-1.239E-04	-8.700E+01

STRESS -1-	STRESS -2-	STRESS -3-	STRESS -6-
1.900E+09	-2.159E+07	0.000E+00	2.008E+07
1.737E+09	5.079E+06	0.000E+00	1.430E+07
1.735E+09	5.176E+06	0.000E+00	-1.430E+07
1.607E+09	2.848E+07	0.000E+00	-9.687E+06
1.663E+09	2.440E+07	0.000E+00	9.111E+06
1.615E+09	4.116E+07	0.000E+00	7.094E+06
1.613E+09	4.126E+07	0.000E+00	-7.117E+06
1.549E+09	5.679E+07	0.000E+00	-5.356E+06
1.662E+09	5.114E+07	0.000E+00	5.593E+05
1.577E+09	7.822E+07	0.000E+00	3.750E+05
1.577E+09	7.823E+07	0.000E+00	-4.473E+05
1.508E+09	1.028E+08	0.000E+00	-2.974E+05

STRAIN AND STRESS RATIOS - MATERIAL DIRECTIONS

e/E -1-	e/E -2-	e/E -3-	e/E -6-
1.016E+00	2.690E+00	1.424E+00	1.005E+00
9.187E-01	2.456E+00	1.178E+00	7.160E-01
9.177E-01	2.459E+00	1.178E+00	7.162E-01
8.401E-01	2.272E+00	9.711E-01	4.851E-01
8.826E-01	2.154E+00	9.711E-01	4.563E-01
8.374E-01	2.093E+00	8.510E-01	3.553E-01
8.364E-01	2.096E+00	8.510E-01	3.564E-01
7.970E-01	2.042E+00	7.418E-01	2.682E-01
8.557E-01	1.880E+00	7.418E-01	2.801E-02
8.009E-01	1.879E+00	5.877E-01	1.878E-02
8.008E-01	1.880E+00	5.877E-01	2.240E-02
7.557E-01	1.879E+00	4.498E-01	1.489E-02

s/S -1-	s/S -2-	s/S -3-	s/S -6-
9.694E-01	1.080E-01	1.325E+00	4.757E-01
8.863E-01	1.316E-01	1.010E+00	3.388E-01
8.854E-01	1.341E-01	1.010E+00	3.389E-01
8.197E-01	7.377E-01	7.427E-01	2.296E-01
8.613E-01	6.320E-01	7.485E-01	2.159E-01
8.239E-01	1.066E+00	5.827E-01	1.681E-01
8.229E-01	1.069E+00	5.825E-01	1.687E-01
7.906E-01	1.471E+00	4.308E-01	1.269E-01
8.480E-01	1.325E+00	4.386E-01	1.325E-02
8.045E-01	2.026E+00	2.082E-01	8.887E-03
8.044E-01	2.027E+00	2.083E-01	1.060E-02

ENERGY METHODS

TSAI-HILL	HOFFMAN	TSAI-WU
1.1685	0.7858	1.0134
0.9154	1.0076	0.9587
0.9144	1.0080	0.9582
1.2570	1.4131	1.1534
1.1771	1.3648	1.1364
1.8266	1.7696	1.4010
1.8305	1.7712	1.4022
2.7815	2.2231	1.7351
2.4526	2.1052	1.6337
4.7213	3.0430	2.3589
4.7224	3.0433	2.3592
7.6502	4.0719	3.2116